ADVANCED MATERIALS
www.advmat.de

Progress and Opportunities in Soft Photonics and Biologically Inspired Optics

Mathias Kolle and Seungwoo Lee**

Optical components made fully or partially from reconfigurable, stimuli-responsive, soft solids or fluids—collectively referred to as soft photonics—are poised to form the platform for tunable optical devices with unprecedented functionality and performance characteristics. Currently, however, soft solid and fluid material systems still represent an underutilized class of materials in the optical engineers' toolbox. This is in part due to challenges in fabrication, integration, and structural control on the nano- and microscale associated with the application of soft components in optics. These challenges might be addressed with the help of a resourceful ally: nature. Organisms from many different phyla have evolved an impressive arsenal of light manipulation strategies that rely on the ability to generate and dynamically reconfigure hierarchically structured, complex optical material designs, often involving soft or fluid components. A comprehensive understanding of design concepts, structure formation principles, material integration, and control mechanisms employed in biological photonic systems will allow this study to challenge current paradigms in optical technology. This review provides an overview of recent developments in the fields of soft photonics and biologically inspired optics, emphasizes the ties between the two fields, and outlines future opportunities that result from advancements in soft and bioinspired photonics.

1. Introduction

Photonics, the science and technology concerned with the control of light, plays a significant role in our life. Enabling continuous advances in energy-efficient lighting,[1,2] photovoltaic energy harvesting,[3–6] biological/chemical sensing,[7] medical diagnostics/treatment,[8] information processing/transfer,[9] and optical computing,[10] photonics pervades our modern societies and the world economy. Much of the evolution of photonics into a major scientific and technological field over the last half-century is owed to the rapid advances in semiconductor processing in the context of computer chip manufacture. The industrial advent and rapid advancement of technologies such as photolithography, micromachining, electron beam (e-beam) lithography, and nanoimprinting have allowed researchers in the academic and industrial realms to conceive ever more complex and powerful strategies to form micro- and nanoscale structures for manipulating light.[11–22]

While great advances have been made this way, we will argue in this review that the time has come to widen our scope of materials and fabrication approaches used to create novel optical technology suited for addressing pressing challenges of the 21st century. In this review, we will discuss recent progress in establishing soft solids and fluids as versatile material classes for the realization of tunable and hierarchically ordered optical components, which would be difficult to achieve with conventional hard approaches. We will also illuminate light manipulation strategies inspired by understanding nature's approaches to control light. These approaches often rely on the integration of soft solids and fluids in complex, tunable, and hierarchically structured multifunctional micro- and nanoscale morphologies with optical performance characteristics not matched by artificial components to date.

1.1. Conventional "Hard" Approaches for Micro/Nanophotonics

Traditionally, the field of micro- and nanophotonics—broadly including diffraction gratings, photonic crystals (PhCs), plasmonics, metamaterials/metasurfaces, and their use in various optoelectronic devices—has relied primarily on the monolithic, top-down fabrication of micro- and nanostructures.[11–13,16–18] In particular, metallic and dielectric materials (e.g., noble metals and inorganic semiconductors) have been successfully formed into sophisticated micro- and nanostructures by taking advantage of recent advances in monolithic fabrication processes. These processes generally consist of a collection of individual steps, including 1) the definition of a mask by photolithography or e-beam lithography, 2) the physical/chemical deposition of the target materials, and 3) wet/dry etching. This way, blueprints of theoretically designed micro- and nanophotonic structures have been materialized in prototypes with deterministic structural fidelity, allowing researchers to experimentally exploit various exotic electromagnetic phenomena at the micro- and nanoscales.

Prof. M. Kolle
Department of Mechanical Engineering
Massachusetts Institute of Technology (MIT)
Cambridge, MA 02139, USA
E-mail: mkolle@mit.edu
Prof. S. Lee
SKKU Advanced Institute of Nanotechnology (SAINT)
Department of Nano Engineering and School of Chemical Engineering
Sungkyunkwan University (SKKU)
Suwon 16419, Republic of Korea
E-mail: seungwoo@skku.edu
The ORCID identification number(s) for the author(s) of this article can be found under https://doi.org/10.1002/adma.201702669.

DOI: 10.1002/adma.201702669

However, despite tremendous advances in conventional monolithic micro- and nanofabrication approaches over the last two decades, several limitations persist: 1) photonic elements formed from hard materials do generally not have the ability to reconfigure autonomously in response to changes in their surrounding environment. However, such homeostasis-like behavior could be useful in photonics applications, for instance, benefiting photovoltaic elements that reorient their light-harvesting elements to continuously optimize light collection efficiency as the sun passes through the sky.[23–25] 2) The 3D, heterogeneous, and functional integration of different components and material constituents in photonic systems remains challenging.[26] For instance, the seamless integration of meta-atoms; plasmonic nanostructures; light emitters, such as fluorophores, and quantum dots (QDs); photonic crystals; and diffraction gratings into complex functional photonic architectures is currently not easily achievable with monolithic fabrication processes.[27] 3) The minimum feature sizes that are realistically achievable with photolithography or electron beam lithography, especially with standard university laboratory equipment, are limited to tens of nanometers.[11–22] This limitation in feature size can represent obstacles for accessing the molecular and atomic-scale design space, with fine control of structures on the nanoscale being especially important for plasmonic elements and metamaterials.[28–36] These challenges, which result from limitations in current state-of-the-art hard manufacturing approaches and materials choices, severely restrict the pace of advancement in photonic technology.

1.2. Soft Components for Photonics: A Paradigm Shift in Materials' Choice and Processing Strategies

Recent advances and increased efforts in the field of "soft photonics" have enabled us to address or circumnavigate the limitations of conventional "hard photonics."[28–33,35–44] Using soft materials otherwise unachievable structural dimensions and compositions can be realized which have the capability to adapt and reconfigure dynamically, thereby enabling unprecedented photonic functionality.[28–51] The term "soft photonics" refers primarily to the realization of photonic systems from various individual components such as gratings, photonic crystals, plasmonic structures, microlenses, and metamaterials, which are formed fully or partially from a broad range of soft materials. These materials include fluids,[41,44–49] DNA assemblies,[28,31,33,42,50–63] hydrogels,[64–68] flexible and stretchable elastomers,[69–79] photo-reconfigurable polymers,[80–87] biological components,[88–90] and colloidal suspensions.[37,40,43,64–67,69,71,91–104] They are processed using suitable soft matter processing strategies, including self-assembly,[28,30–37,39,40,42,50–67,69,71,78,80,88–106] reaction–diffusion processes,[107,108] nanoimprinting/transfer printing,[15,19,26,27,109–114] fluidic extrusion,[92,93,102,115] directed assembly,[99,116–118] origami techniques,[119,120] shearing,[121,122] and other unconventional methods.[74–76,82–87,91,123–126] An important advantage of the use of soft materials in photonic components is their ability to dynamically respond in their configuration, shape, mechanical properties, and optical characteristics to a variety of physical or chemical stimuli, including mechanical forces,[25,46,47,69–78] light,[66,80–87,127] chemical triggers,[50,54,61] changes in temperature,[64–68,128] humidity,[129,130] or applied electric field.[92,93,113]

The use of DNA complementary binding,[28,31,33,42,50–63,127] directed colloidal self-assembly,[99,116–118] programed buckling of elastomers,[74,75] and reconfigurable microfluidic channels[44–49] and emulsion droplets[92,93,101,102] has enabled the realization of sophisticated adaptive, stimuli-responsive, and even autonomously reconfigurable micro- and nanophotonic structures. We anticipate that significant potential scientific, economic, and social benefits will arise from broadening our materials' palette to include soft solids and fluids in the effort to design the next generation of photonic systems that are mechanically compliant, dynamically conformal, sensitive to mechanical, chemical, or optical cues, and capable of homeostasis to ensure adequate function in a broad range of conditions. In this regard, nature's portfolio of light manipulation strategies provides a good perspective on the benefits that could be attainable through advancements in multimaterial integration involving

Mathias Kolle obtained his diploma in physics from the Saarland University, Germany, and the University of Lorraine (formerly Henri Poincaré University), France, in 2006. He then received his PhD from the Cavendish Laboratories, University of Cambridge, UK, in 2010. He worked as a postdoctoral researcher for Prof. Joanna Aizenberg at the School of Engineering and Applied Sciences of Harvard University, and joined the faculty of the Massachusetts Institute of Technology (MIT) as an Assistant Professor in 2013. His research focusses on translating unique biological optical sensing, communication, and energy-conversion mechanisms into bioinspired, adaptive, and tunable micro-optical materials and devices.

Seungwoo Lee obtained his B.S. in chemical engineering from Sogang University in 2005, and his Ph.D. in chemical and biomolecular engineering from Korea Advanced Institute of Science and Technology (KAIST) in 2011. He then completed his postdoctoral works at KAIST (with Bumki Min) and at Harvard University (with William M. Shih), focusing on soft metamaterials using elastomer, graphene, and DNA origami (2011–2014). Since 2014, he has held an assistant professor position at Sungkyunkwan University (SKKU) with an appointment in SKKU Advanced Institute of Nanotechnology (SAINT) & School of Chemical Engineering.

soft matter, combined with better control of material composition and morphology across relevant length scales.

1.3. Biological Inspiration for Photonics

Recent successes in utilizing soft materials for photonics promise compelling opportunities for advancing photonic system design; however, current synthetic soft photonic materials and devices rarely capture the range of structural complexity and dynamic behavior, which can be observed in nature's optical materials. Cephalopods—termed affectionately "kings of camouflage"—utilize a variety of intracellular optical features in their skin to dynamically control the spectral composition and brightness of reflected light, and to change micro- and macroscale skin texture, while also being able to deform their whole body to a great extent.[131–134] To date, synthetic soft optical materials do not measure up to the mind-boggling multifunctionality and optical performance of cephalopod skin. We need to refine our understanding of structure–composition–function relations in soft photonic architectures and conceive fabrication strategies that enable hierarchical integration of material morphologies with the required length scale bridging complexity. By continuing to take a careful look at nature's light manipulation strategies, we can learn valuable lessons about the control of morphology across scales, the integration of photonic components within multifunctional materials, the dynamic control of composition and morphology to enable reconfigurable and responsive optical materials, and valuable strategies to generate desired photonic elements on the small and the large scale. This is the foundation of the field of "biologically inspired optics," which is based on utilizing unparalleled and desirable biological light manipulation concepts in man-made, bioderived, and bioinspired synthetic optical systems. Insights into the design and functions of biological optical components have provided advanced starting points for the design of artificial photonic elements.[135–142] We anticipate great synergies between the fields of biologically inspired optics and soft photonics, and expect that currently ongoing and future research efforts will advance rapidly to form photonic materials and devices that, for instance, match or exceed the amazing optical and mechanical properties of cephalopod skin. Bioinspired, soft photonic materials will greatly enrich the optical engineer's toolbox and form the foundation for optical technology that is needed to address significant 21st century challenges in healthcare, bioengineering, energy capture and conversion, sensing, and communication and data processing.

1.4. Scope of This Review

Several recent reviews have captured the status of progress in self-assembly-based soft photonics, focusing primarily on 3D photonic crystals and photonic glasses.[37,39,40,43] Insightful and comprehensive reviews have also assessed progress in biological optics and bioinspired photonics.[135–138,140–146] In this review, we aim to elucidate advances in both fields with emphasis on fruitful synergies and overlaps. We believe that substantial overlap in interest and significant potential for cross-fertilization exists between the two fields; more and more, efforts in bioinspired optics are focused on emulating biological, stimuli-responsive, reconfigurable materials that rely on the integration of soft with hard components in photonic morphologies. In this review, we aim to provide a comprehensive overview of the state-of-the-art in soft and bioinspired photonics. We focus on design concepts, materials, formation processes, and dynamic behavior. In addition, we have emphasized specific biological light manipulation concepts that merit consideration in the design of novel soft and bioinspired photonic elements. We have stressed to which extend these biological strategies have already been captured in man-made optical materials. We identify success stories in the fields of soft and bioinspired photonics, and outline future challenges. Particularly, by stressing current achievements and putting them in perspective with natural material analogs, we aim to depict a vision for possible future directions of research in soft and bioinspired photonics.

2. Soft Materials in Micro- and Nanophotonics

In this section, we elucidate key concepts and important parameters for efficient control of light–matter interaction using soft materials and specify why these materials are valuable for photonic engineering.

2.1. Controlling Light–Matter Interaction in Soft Materials

In general, light–matter interaction can be fully rationalized by Maxwell's equations; in this framework, the effective relative permittivity ε of a material can be written as

$$\varepsilon = 1 + (P/\varepsilon_0 E) \tag{1}$$

where P is the material's polarization, ε_0 is the permittivity of free space, and E is the applied electric field. In analogy, the material's effective relative permeability is defined by

$$\mu = 1 + (M/H) \tag{2}$$

where M denotes the material's magnetization and H indicates the applied magnetic field. The square root of ε and μ defines the refractive index ($n = \sqrt{\varepsilon\mu}$), which provides a measure of the relative speed of light in a material with respect to that in vacuum. The attenuation coefficient k (also referred to as the extinction coefficient) is another basic property of a material relevant to describing its interaction with light. In general, the spatial modulation of ε, μ, and k within a material, achieved, for instance, by locally adjusting material morphology and composition (i.e., lattice geometry, lattice dimensions, hierarchical structural complexity, and material constituents), enables precise control of light–matter interaction.

For the creation of novel optical materials through modification of their morphology, the type of suitable spatial modulations strongly depends on the ratio of the dimensions of the material morphology relative to the wavelength of light. At the subwavelength scale (e.g., ≪wavelength/5), individual

unit elements in a nanophotonic morphology with controlled ε, μ, and k act as "meta-atoms"; collective electron movements of meta-atoms—i.e., the electrons' resonant or quasistatic electromagnetic behavior—determine the material's overall photonic properties. This is the case for metamaterials and metasurfaces.[11,13,16,17,21,22,34,57,77,78,109,147–166] At the wavelength scale, the wave nature of light, resulting in prominent diffraction and interference effects, is important for explaining light–matter interaction phenomena that define the optical properties of diffraction gratings,[75,84,87,102] photonic crystals,[37,40,43,64–69,71,76,92–94,98,100,102,104,121,122,129,130,167–170] and photonic glasses.[39,40,43,95,96,101,171–173] The term nanophotonics encompasses systems that derive their optical properties from light–matter interactions resulting from morphological and compositional variations at the subwavelength and wavelength scales.

Geometric optics approaches are used for describing materials with structural features at scales that exceed the coherence length of the illuminating light, which is typically the case above length scales of a couple of tens of micrometers when sunlight or other broadband incoherent sources are used.[3,24,25,38,45–47,174–179] Typical examples of optical systems at this scale are lenses,[24,25,47] macroscale waveguides,[45,178,179] and whispering gallery mode (WGM) cavities.[46,174,175] Thus, strategies for the control of light–matter interaction can, in principle, be classified in two regimes as a function of the ratio of material feature size to wavelength: 1) the nanophotonics regime and 2) the geometric optics regime (**Figure 1**). Soft materials can be used to create and modify ultrasmall and complex morphologies of a photonic architecture, providing opportunities for the design of advanced optical modes and dynamic photonic systems. In this regard, different design principles apply for the use of soft materials to conceive systems that exploit the two different optical regimes, defined above.

2.1.1. Nanophotonics: Colloidal Nanoparticle Plasmonics and Metamaterials

The field of metamaterials and plasmonics is representative for strategies and the design of systems that enable subwavelength-scale control of light–matter interaction. Plasmonic materials, which rely on interactions between electromagnetic fields and free electrons in conducting materials (for instance, metals and graphene), allow for the confinement of light at the deep subwavelength scale.[180–183] Since such plasmonic waves have a momentum (represented by their wave vector), which is much higher than that of light, the mode volume of plasmonic optical components, such as nanocavities and nanowaveguides, is significantly reduced. Plasmonic excitations can exist in two distinct forms. Surface plasmon polaritons (SPPs) are propagating waves of electron density oscillations at the interface between metals and dielectrics. Localized surface plasmon resonances (LSPRs) are electron oscillations confined to discretized subwavelength areas and volumes, such as metallic nanoparticles (NPs) and isolated metal or graphene islands.[180–183]

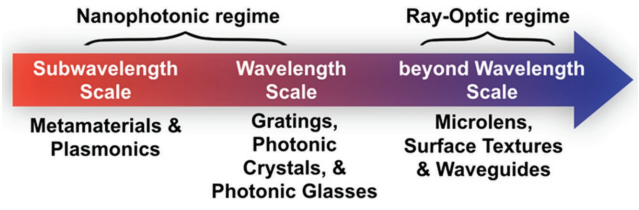

Figure 1. Strategies for the control of light–matter interaction as a function of material feature size in comparison to the light wavelength.

Both plasmonic phenomena are excited at the subwavelength scale. However, propagation of SPPs can be controlled at the wavelength scale or even at larger scales by adjusting length and dimensions of SPP pathways, as demonstrated for WGM systems and the gradual focusing of plasmons in 2D and 3D (**Figure 2**a,b).[18,174] For SPPs the correct design of material morphologies from the nano- to the microscale is crucial. Unlike SPPs, LSPRs are confined oscillations of electrons; thus, the control of the shape, size, and gap of the discretized subwavelength-scale object, which affects the electrons' permitted oscillation states, are the key design criteria (Figure 2c,d).[184]

Recent advances in the chemical synthesis of colloidal metallic nanowires (NWs) and NPs with exquisite shape and size control, combined with soft-matter self-assembly processes have enabled the controlled engineering of SPP and LSPR properties (**Figure 3**).[185–188] Atomic surface smoothness of metallic NWs (Figure 3a) permits highly efficient SPP waveguiding (Figure 3b–d).[189] In addition, soft lithographic transfer peeling (Figure 3e,f)[190] and soft photofluidic reconfiguration (Figure 3g–i)[86] have been explored as versatile strategies to shape deep-subwavelength-scale, 3D metallic holes in order to efficiently squeeze SPPs far beyond the diffraction limit.

The strength and resonant wavelength of LSPRs can be precisely tuned through fine-control of the size and shape of colloidal metal NPs.[185–187] LSPR behavior can further be tuned by carefully designing superstructures composed of different metallic NP species or by self-assembling NPs on flat metal films.[28,32,35,36,191] For example, when two spherical metal NPs are self-assembled into dimers with a gap of a few nanometers using DNA nanotechnology (Figure 3j–k), resonant electric fields can be strongly localized within this ultrasmall gap (Figure 3l).[28,33] Such feature sizes are difficult to achieve with conventional hard approaches.[28,191] The assembly of organic ligand-coated metallic NPs on flat metallic films allows for the creation of ultrasmall cavities between films and NPs, which dramatically focus the electromagnetic field within an ultrasmall mode volume (picocavity, Figure 3m).[32] This small mode volume between NPs (gold NPs (AuNPs)) and a flat Au film can be deterministically filled with a single fluorophore by using soft, organic cucurbituril molecules (Figure 3n).[32,35,36] In particular, cucurbituril molecules can force the fluorophore's electric dipole to be aligned vertically with respect to the surfaces of a flat Au film and AuNPs; thus, the dipolar oscillations of a single molecule and AuNPs can be strongly coupled to each other.[35] As such, advanced photonic modes such as Rabi splitting[35] and single-molecule optomechanical oscillations[36] resulting from sub-1-nm metallic gap-enabled strong interactions between the single molecule and the plasmonic resonance have been observed at room temperature for the first time using far-field scattering spectroscopy (Figure 3o).

Metamaterials are artificial media with structural units (meta-atoms) much smaller than the wavelength of light

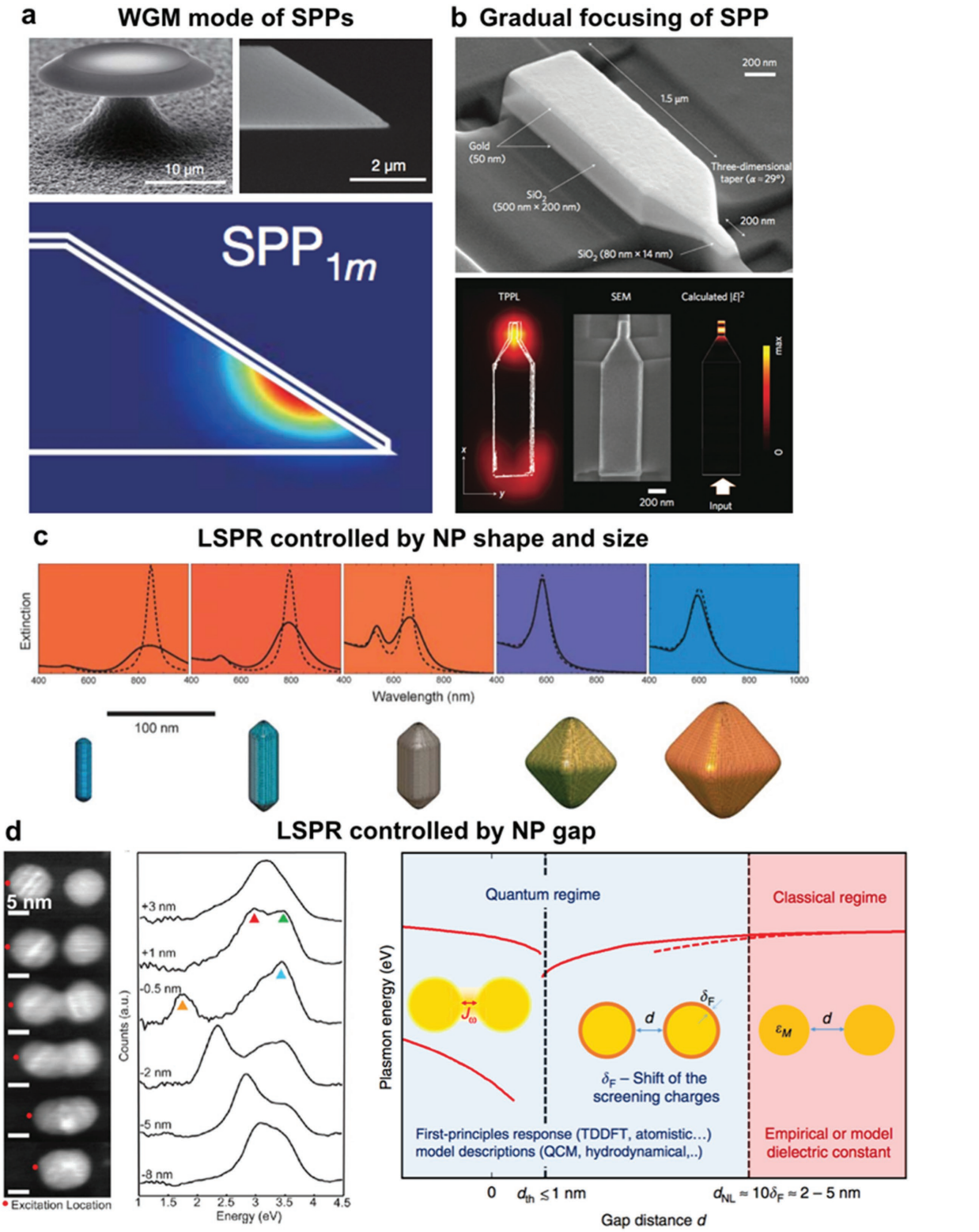

Figure 2. Surface plasmon polaritons (SPPs) and localized surface plasmon resonances (LSPR). a) Control of SPPs via a whispering gallery mode (WGM) cavity. Reproduced with permission.[174] Copyright 2009, Nature Publishing Group. b) Focusing of SPPs via 3D-tapered metallic waveguides. Reproduced with permission.[18] Copyright 2012, Nature Publishing Group. c) Control of LSPR by adjusting the shape of metallic nanoparticles (NPs). Reproduced with permission.[184a] Copyright 2008, Royal Society of Chemistry. d) Control of LSPR by adjusting the gap between metallic NPs. Reproduced with permission.[184b] Copyright 2016, Nature Publishing Group. Reproduced with permission.[184c] Copyright 2013, American Chemical Society.

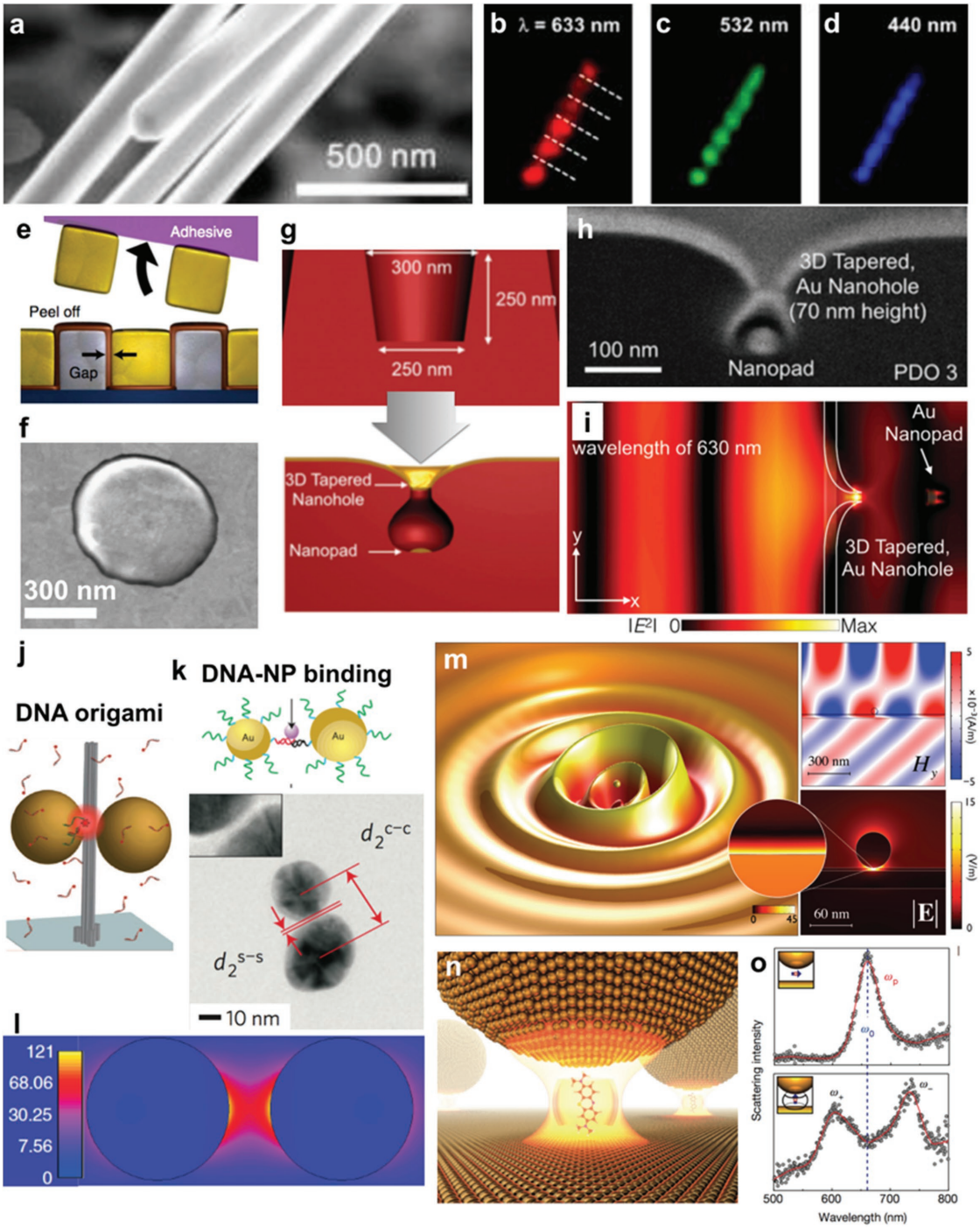

Figure 3. Deterministic control of SPPs and LSPRs by using colloidal systems. a) Atomically smooth Ag nanowires (NWs). b–d) SPPs on the atomically smooth AgNWs at different wavelengths. a–d) Reproduced with permission.[189] Copyright 2012, American Chemical Society. e) Soft lithographic peel-off process for the fabrication of ultrasmall gaps between metallic nanostructures. f) Circular ring gap between Au nanostructures, realized using the soft peel-off process. e,f) Reproduced with permission.[190] Copyright 2013, Nature Publishing Group. g) Controlled photofluidization of a polymer layer for the fabrication of 3D-tapered metallic nanohole arrays. h) A 3D-tapered Au nanohole with a 30 nm gap, fabricated by directional photofluidization lithography. i) Squeezing light beyond the diffraction limit using a 3D-tapered Au nanohole. g–i) Reproduced with permission.[86] Copyright 2014, Wiley-VCH. j,k) Assembly of AuNP dimers by using j) DNA origami–NP binding and k) DNA-coated NP binding. l) Light concentration in AuNP dimer, assembled by using DNA origami as template. j,l) Reproduced with permission.[33] Copyright 2012, American Association for the Advancement of Science. k) Reproduced with permission.[28] Copyright 2010, Nature Publishing Group. m) Light focusing in the cavity of AuNP on flat mirror. The light can be confined in an ultrasmall volume. Reproduced with permission.[32] Copyright 2012, American Association for the Advancement of Science. n) The deterministic coupling of a single molecular emitter with an AuNP on a mirror cavity. The cucurbituril molecules can force the fluorophore's electric dipole to be aligned vertically between the AuNP and a flat mirror. o) Rabi splitting can be observed by far-field scattering when the electric dipole of a single molecule is aligned vertically between an AuNP and a flat mirror. n,o) Reproduced with permission.[35] Copyright 2016, Nature Publishing Group.

($\leq\lambda/5$), in which collective electron movements and their ensemble effects can be induced in resonance or in the quasistatic limit.[11–13,16,17,21,22,34,57,77,78,109,147–166] These electron oscillations, together with the modifications of the light's phase, are responsible for a wealth of unnatural light–matter interactions, including artificial magnetism,[147,154,192] negative refraction,[12,13,113,149,153,154,159] epsilon-near-zero (ENZ),[21,56,158] and extremely high refractive indices.[16,151,157,166] Deep-subwavelength-scale ($\ll\lambda/5$) meta-atoms with controlled ε and μ can be spatially arranged in a single composite, so as to induce electric and magnetic responses that are nearly impossible to achieve with naturally occurring materials.[11–13,16,17,21,22,34,57,77,78,109,147–166] The most crucial parameters that determine light–matter interaction in metamaterials are the structural variables size, shape, and material composition of each individual meta-atom, the gap between adjacent meta-atoms, and the superlattice geometry of the meta-atom array. Fine adjustment of these parameters permits the control of electron movements on the subwavelength scale leading to unnatural electromagnetic effects. For homogenization theory,[193,194] meta-atoms need to be smaller than about 100 nm to operate in resonance and in the quasistatic regimes especially at optical frequencies. Furthermore, for realizing exotic electric responses, meta-atoms need to be located in close proximity from each other, with a few nanometer gaps in between. These two criteria represent demanding fabrication challenges that are difficult to address with conventional monolithic "hard" approaches. Controlled colloidal assembly of metallic NPs can address these challenges (referred to as nanoparticle metamaterials in this review).[30,34,56,58,62,78,116–118,192] NP metamaterials that cause unnatural light–matter interactions in the optical frequency spectrum can be categorized into two main classes: (1) magnetic and (2) electric metamaterials (**Figures 4** and **5**). These two classes are discussed in more detail below.

Magnetic Metamaterials: According to Maxwell's equations, the magnetic field of incident light can be coupled with materials through the unnatural circulating displacement current and electric field (i.e., magnetism); generally, except for ferrites, this magnetism cannot be induced (the magnetic permeability μ of naturally materials is, in general, limited to around unity). For this unnatural magnetism, the circular electron motion should be oriented perpendicularly to the incident magnetic field vector (Ampère's law in Maxwell's equations).[30,58,62,116,117,192,195] The circular electron movements, in turn, give rise to the generation of magnetic dipole moment and the resultant control of the permeability μ of the material, which can be reduced to negative values or enhanced far beyond unity. Thereby, the generation of magnetism in metals represents a promising avenue toward unnatural negative refractive index materials, since metals already have a negative permittivity ε.[12,13,113,149,153,154,159] Arrays of helically oriented metallic antennas (coils or helically coupled antennas)[153] or split ring resonators (SRRs)[13,30,58,62,116,117,192,195] are a representative design for artificial magnetism; such metamaterial structures have been successfully demonstrated at larger wavelength ranges (THz and microwave) using conventional hard approaches.[13] However, to date sub 100 nm scale helically structured meta-atoms or SRRs for optical systems in the IR, visible, and UV optical spectral ranges (optical frequencies) have not been realized with a high structural fidelity using top-down hard approaches. Alternatively, this miniaturization challenge can be addressed by self-assembly or atomic force microscopy (AFM) nanomanipulation of colloidal metallic NPs.[30,58,62,116,117,154] With this technique, subwavelength-scale clusters of at least three metallic nanospheres (NSs) or dimerized metallic nanorods (NRs) (collectively referred to as plasmonic metamolecules) have been realized with same functionality of SRRs. These structures display optical magnetism, since they support circulating displacement current and electric fields (see Figure 4a–c).[30,58,62,116,117,154] Because the circulation of both electron movements and electric field can be driven by the capacitive coupling between the electric dipolar oscillations of each NP in the cluster, the gaps between metallic NPs (generally less than 5 nm) should be as small as possible (≈1 nm) to maximize optical magnetism. From this perspective, self-assembly or AFM nanomanipulation of metallic NPs into clusters (plasmonic metamolecules) with controlled nanogaps can be viewed as a unique way toward optical magnetism at optical frequencies.[30,58,62,116,117] In particular, <1-nm-thick organic ligands, coated onto the metallic NPs of self-assembled clusters, can allow us to attain 1–2 nm gap between meta-atoms, which cannot be achieved with conventional hard approaches.

Additional structural complexities in plasmonic metamolecules enabled by taking benefit of the reconfigurable nature of soft matter can allow for further enhancement of optical magnetism. Generally, controlled geometrical asymmetry in colloidal NP clusters can improve the strength of optical magnetism by breaking orthogonality between electric and magnetic fields.[58,116,117,192] Recently, laser-induced plasmonic feedback control of colloidal assembly has been used to enable high-throughput assembly of NR pairs with controlled asymmetry (see Figure 4d–f). Normally, the assembly of colloidal NR dimers, driven by a controlled hydrophobic effect, give rise to an arbitrary symmetry or asymmetry, distributed statistically according to the Boltzmann equation; however, laser irradiation-enabled plasmonic heating can drive a process of repeated binding and unbinding of NRs until an NR-dimer structure with an LSPR wavelength not in resonance with the laser wavelength has formed (Figure 4d–f).[117] In this way, asymmetric NR dimers with a uniformly distributed offset can be assembled in a fluid massively (Figure 4f); in these structures, strong optical magnetism was observed by far-field scattering measurements performed on the colloidal solution (i.e., metafluids) (Figure 4g). Furthermore, refractive index could be reached to an unnatural negative value with increasing filling fraction of asymmetric NR dimers (Figure 4h).

Electric Metamaterials: Self-assembly of colloidal metallic NPs into periodically arranged 2D or 3D crystals within a dielectric medium (2D or 3D NP crystals) permits the tuning of the permittivity ε from near zero to extremely high values (Figure 5a–f).[34,56,78,196] Consequently, provided optical magnetism is suppressed (μ is limited to near unity), these NP metamaterials are able to achieve a near-zero refractive index (index near zero (INZ)) or an unnaturally high refractive index.[34,196] INZ metamaterials allow tunneling of electromagnetic waves through a physical barrier,[158,197] while metamaterials with extraordinarily high refractive index can enhance light trapping in solar cells according to Yablonovitch limit.[3,6]

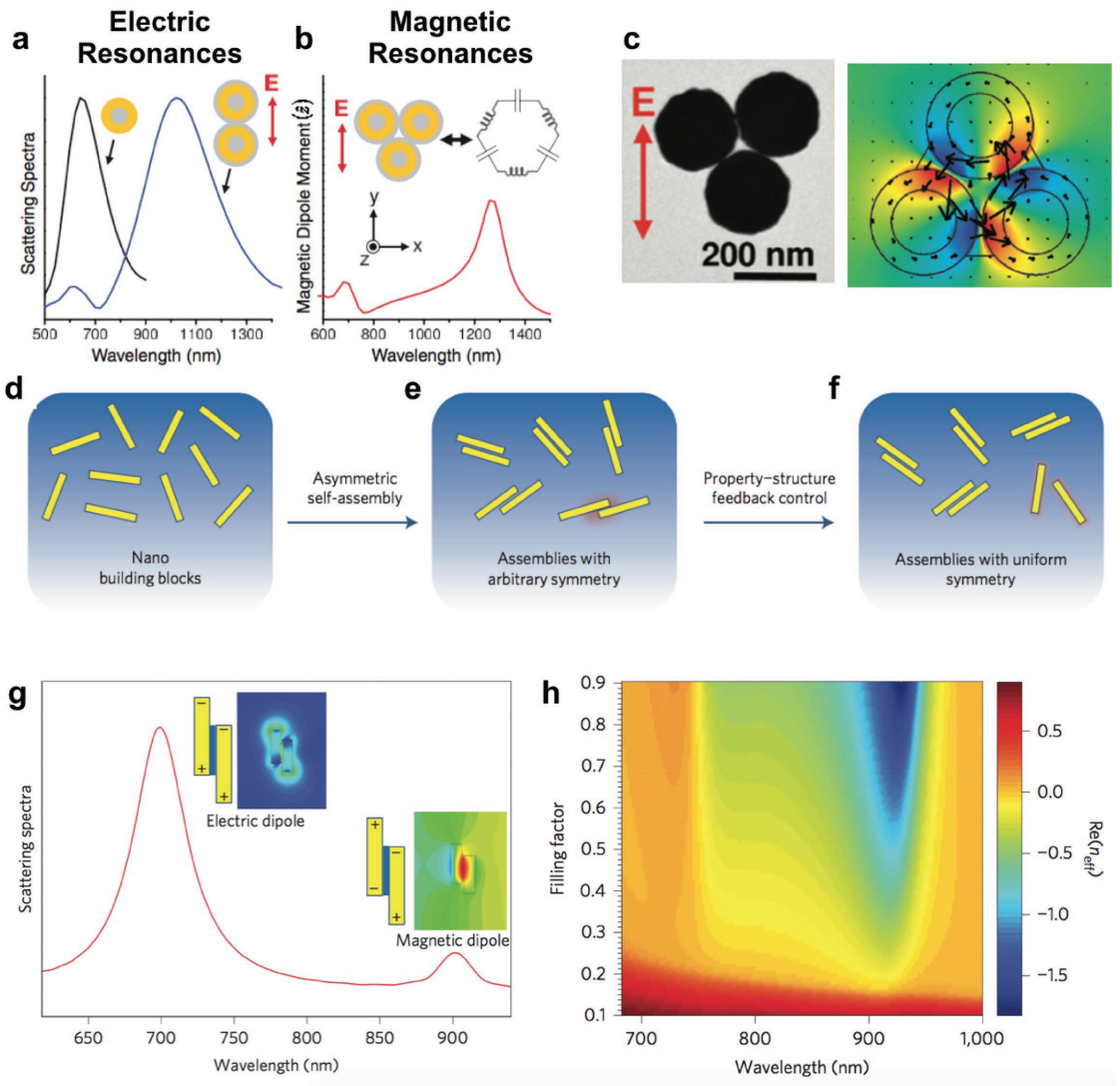

Figure 4. Realization of artificial magnetism at optical frequencies by using metallic colloids. a) Single AuNPs and AuNP dimers can exhibit only electric dipolar resonance. b) A ring motif formed by at least three AuNPs can induce a circular displacement current; as a result, a magnetic dipole can be induced (i.e., optical magnetism). c) An AuNP trimer, self-assembled by evaporation-induced capillary force (left) and the circular displacement current within the AuNP trimer (right). a–c) Reproduced with permission.[30] Copyright 2010, American Association for the Advancement of Science. d–f) Feedback control of colloidal assembly for Au nanorod (NR) dimers with uniform asymetry. g) Asymmetric AuNR dimers can induce a magnetic dipole together with an electric dipole. h) Highly concentrated asymmetric AuNR dimers dispersed in a liquid (i.e., referred to as an optical metafluid) can show unnatural negative refractive index. d–h) Reproduced with permission.[117] Copyright 2014, Nature Publishing Group.

INZ or high-refractive-index metamaterials using metallic NP crystals are based on the following principle: by controlling the gap between metallic particles in the of NP crystals, the strength of the linearized (not circular) electric dipole moment (P) confined within the gap of each NP pair can be tuned.[34,56,78,196] This controlled electric dipole moment in turn affects the effective permittivity ε according to the relation $\varepsilon = 1 + (P/\varepsilon_0 E)$. As P is confined via capacitive coupling between metallic NPs, control of the gap width, which is tunable by the length of the organic ligand of colloidal NPs, can enable the tuning of ε. Indeed, moderate spaces between NPs (comparable to NP size) in NP crystals formed via DNA complementary binding suffice to achieve 3D NP crystals with near zero ε (Figure 5a,b).[56] In particular, the length of the employed DNA ligand can be precisely tuned by benefitting from recent advances in polymerase chain reaction.

In contrast, the gap between metallic NPs, and the relative ratio of gap to NP size can be decreased dramatically (1–2 nm) by close packing of thin organic ligand-coated (<1 nm), colloidal metallic NPs, which leads to extreme enhancements of the electric resonance via strong capacitive coupling of the linear dipole moment (Figure 5c,d).[34] For example, an effective dielectric constant of about 200 was demonstrated in self-assembled, close-packed nanocube NP superlattices with 2 nm gap size (Figure 5e).[34] It is important to note that such a small gap can only reliably be achieved by self-assembly of colloidal metallic NPs coated with suitable ligands rather than with conventional hard approaches.

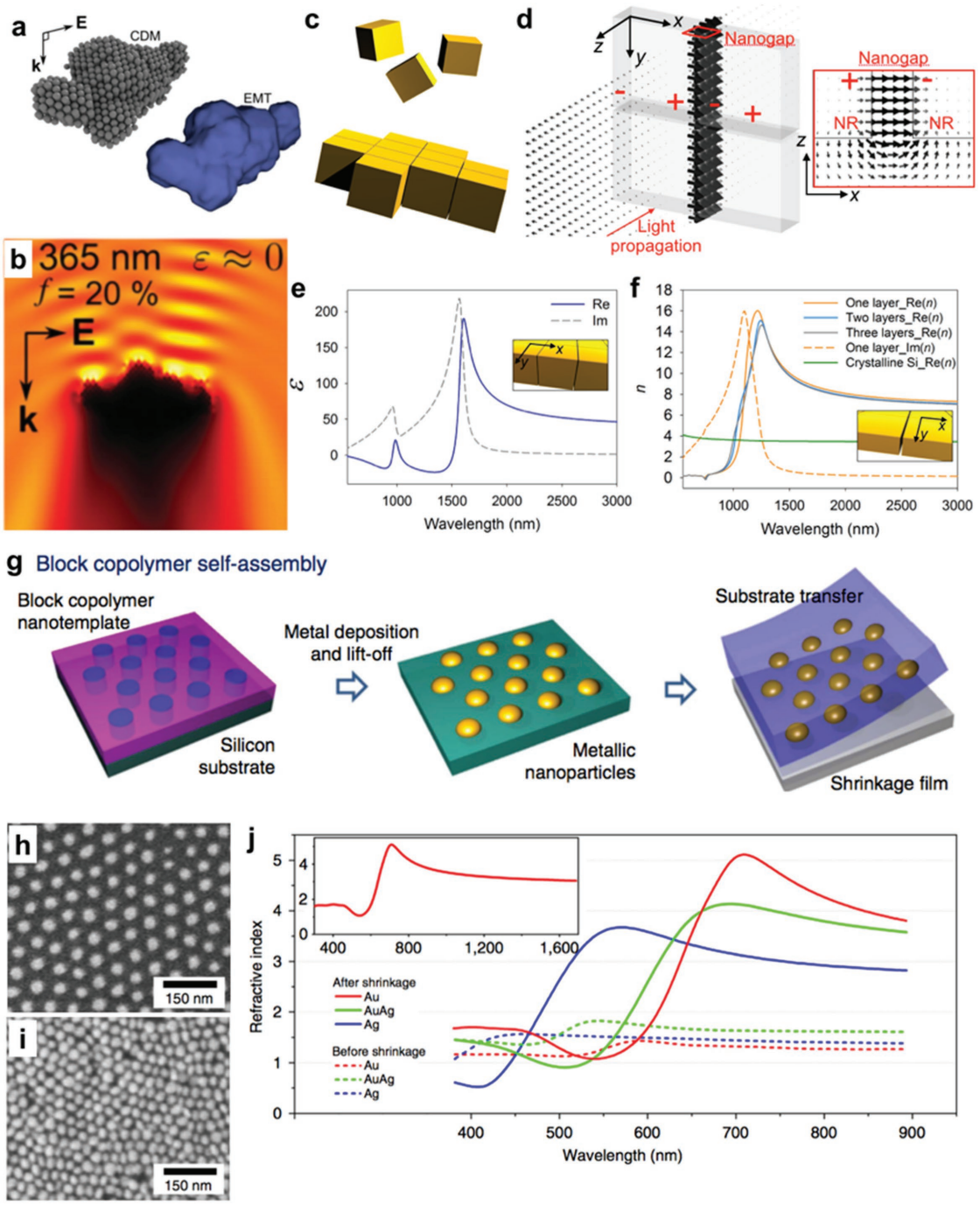

Figure 5. Achieving unnatural near zero epsilon and high refractive index. a,b) Crystallized AgNPs with a controlled volume fraction (top) can show near zero epsilon at a specific wavelength (bottom). Reproduced with permission.[56] Copyright 2014, Wiley-VCH. c,d) Cube-shaped AuNPs can be closely packed by c) colloidal self-assembly and d) the incoming electric field can be strongly squeezed into the gap between Au nanocubes (NCs) by capacitive coupling. e) The permittivity of closely packed AuNC monolayer can be increased unnaturally via resonant capacitive coupling. f) An AuNP monolayer with a relatively low aspect ratio can minimize diamagnetism, while still maximizing capacitive coupling. Thus, the refractive index of this effective optical medium can be unnaturally high at both electric resonance and quasistatic regimes. c–f) Reproduced with permission.[34] Copyright 2015, The Optical Society. g) AuNPs can be patterned over a large area by block copolymer lithography and then transferred to stretchable substrates. h–j) The gap between AuNPs depends on the amount of substrate stretching (h,i); this way, the capacitive coupling between AuNPs and the resulting refractive index can be controlled. g–j) Reproduced with permission.[78] Copyright 2016, Nature Publishing Group.

To achieve ultrahigh-refractive-index materials, optical magnetism should be suppressed as much as possible. By reducing the height of metallic NPs, electron circulation, vertical to the direction of the incident magnetic field, can be suppressed, and unnaturally high refractive index (e.g., Re(n) of 16 at a gap of 2 nm) can be achieved (Figure 5f).[34] In this regard,

self-assembly of low-aspect-ratio, plate-type metallic NPs, such as Au nanoprisms,[198] can be a versatile strategy to obtain unnaturally high n. Alternatively, self-assembled block copolymers can be used to template low-aspect-ratio AuNP arrays in order to achieve high n (Figure 5g).[78] More importantly, the resulting AuNP metamaterial can be transferred onto stretchable substrates and the gap size and the resultant capacitive coupling between AuNPs in the arrays can be precisely tuned through controlled substrate stretching (Figure 5h,i). In this way, the refractive index n can be reconfigured over a broad range of optical frequencies by stretching and relaxing the substrate (Figure 5j).[78]

Although the above-discussed control of effective permittivity ε and permeability μ is for the manipulation of "bulk" optical properties (i.e., effective medium theory), phase discontinuities Φ, imposed on incident light due to controlled spatial arrangement of plasmonic meta-atoms in a metamaterial surface (metasurface), have enabled the design of flat optical components for natural and unnatural light refraction.[17,22,77] LSPRs usually induce phase delays, which depend on several structural features of the meta-atoms including shape, size, and gap; consequently, the phase of incident light ($\Phi(x)$) can be modified spatially through controlled geometrical arrangement of different meta-atoms in a metasurface.[17,22,77] Control of $\Phi(x)$ with 2D metasurfaces can result in arbitrary bending of light propagation direction (extremely strong refraction or negative refraction) or focusing of scattered light.[17] The refraction of light by metasurfaces is described by a generalization of Snell's law of refraction given by[77]

$$n_t \sin\theta_t - n_i \sin\theta_i = \frac{\lambda}{2\pi}\frac{d\Phi(\vec{x})}{d\vec{x}} \tag{3}$$

where n_i and n_t are the refractive indices of the medium in which the light originates and the medium into which it is transmitted, θ_i and θ_t represent the angles of incident and transmitted light with respect to the normal of the optical interface, λ is the light wavelength, and $\vec{x}$ is the 2D spatial coordinate vector. Once the size and shape of meta-atoms in a metasurface are fixed, the phase $\Phi(\vec{x})$ can be controlled through variation of the gap between meta-atoms (**Figure 6**a).[77] As with high-refractive-index NP metamaterials, stretchable elastomer substrates provide a convenient strategy to reconfigure the space between meta-atoms by stretching and relaxing; this can, for instance, be used to tune the focal length of a flat metalens through a mechanical stimulus (Figure 6b).[77]

In addition to the permittivity ε, the permeability μ, the wave-vector k, and the spatial variation in phase $\Phi(\vec{x})$, the optical chirality ξ is an important parameter in the full description of light–matter interaction. Optical chirality ξ, a measure of the electromagnetic field's local helicity density, is quantitatively analyzed by determining circular dichroism (CD) in a material, defined by the difference of light absorption (ΔA) for left- and right-handed circular light polarizations. For monochromatic fields, ΔA is proportional to the optical helicity (h), the projection of the spin angular momentum (i.e., circular polarization state) onto the momentum, which is given by[199,200]

$$h = -\frac{\varepsilon_0 \mu_0}{2\omega}\mathrm{Im}\left(\tilde{E}^* \cdot \tilde{H}\right) \tag{4}$$

here, ε_0 and μ_0 are the vacuum permittivity and vacuum permeability, ω is the angular frequency of the incident light, and $\tilde{E}$ and $\tilde{H}$ are the electric and magnetic fields, respectively.

Furthermore, the difference of light absorption ΔA is proportional to the decay rate; thus, the optical chirality ξ can be coupled to the concept of the Purcell factor, which describes the magnitude of the enhancement of an emitter's spontaneous emission rate by its environment, giving the chiral Purcell factor F_c as[201]

$$F_c = \frac{1}{4\pi^2}\left(\frac{\lambda_0}{n}\right)^3\left(\frac{Q}{V_c}\right) \tag{5}$$

where $\frac{\lambda_0}{n}$ is the wavelength in the material with refractive index n, V_c is chiral mode volume, defining spatial confinement of optical helicity, and Q is the quality factor of the resonant structures. In order to maximize ξ, the chiral mode volume V_c, in which optical helicity h is confined, should be as small as possible. To squeeze optical helicity h within a small volume, colloidal plasmonic components including metallic NRs and NSs can be assembled into helical and tetragonal structures.[51,52,55] To maximize helical coupling between NPs (confining optical helicity h in small volume), colloidal NRs and NSs need to be controllably assembled with a small gap (e.g., 1 or 2 nm). This sophisticated assembly of colloidal NRs or NSs with nanoscale precision so far has only been achieved with DNA programmable binding, as summarized in Figure 6c,d.[51,52,55]

2.1.2. Nanophotonics: Coherent and Diffusive Light Scattering and Diffraction by Colloids and Advanced Polymers

While the preceding discussion was focused on subwavelength-scale photonic materials, in this section, we will focus on wavelength-scale photonic structures. Now, we have to take into account the wave properties of light in its interaction with the material, instead of relying on treating light–matter interaction in the quasistatic limit as done for subwavelength-scale photonic structures. Diffraction is a representative example for the importance of the wave nature of light. A general, qualitative description of diffraction of light by a regular surface grating is given by the equation

$$m\lambda = d(\sin\theta_i + \sin\theta_d) \tag{6}$$

where m denotes the diffraction order, λ the wavelength of diffracted light, d the grating period, and θ_i, and θ_d, the incident and the diffraction angle, respectively. In general, light diffracts from a grating into several distinct diffraction orders with the specific behavior inherently governed by the ratio of light wavelength λ to grating periodicity d. The efficiency of light diffraction into each order is influenced by a variety of variables including the refractive index contrast of grating and surrounding media, the fill factor of the grating, and the shape and height of grating unit elements. A full description of the diffraction of light by an arbitrary periodic surface relief phase or

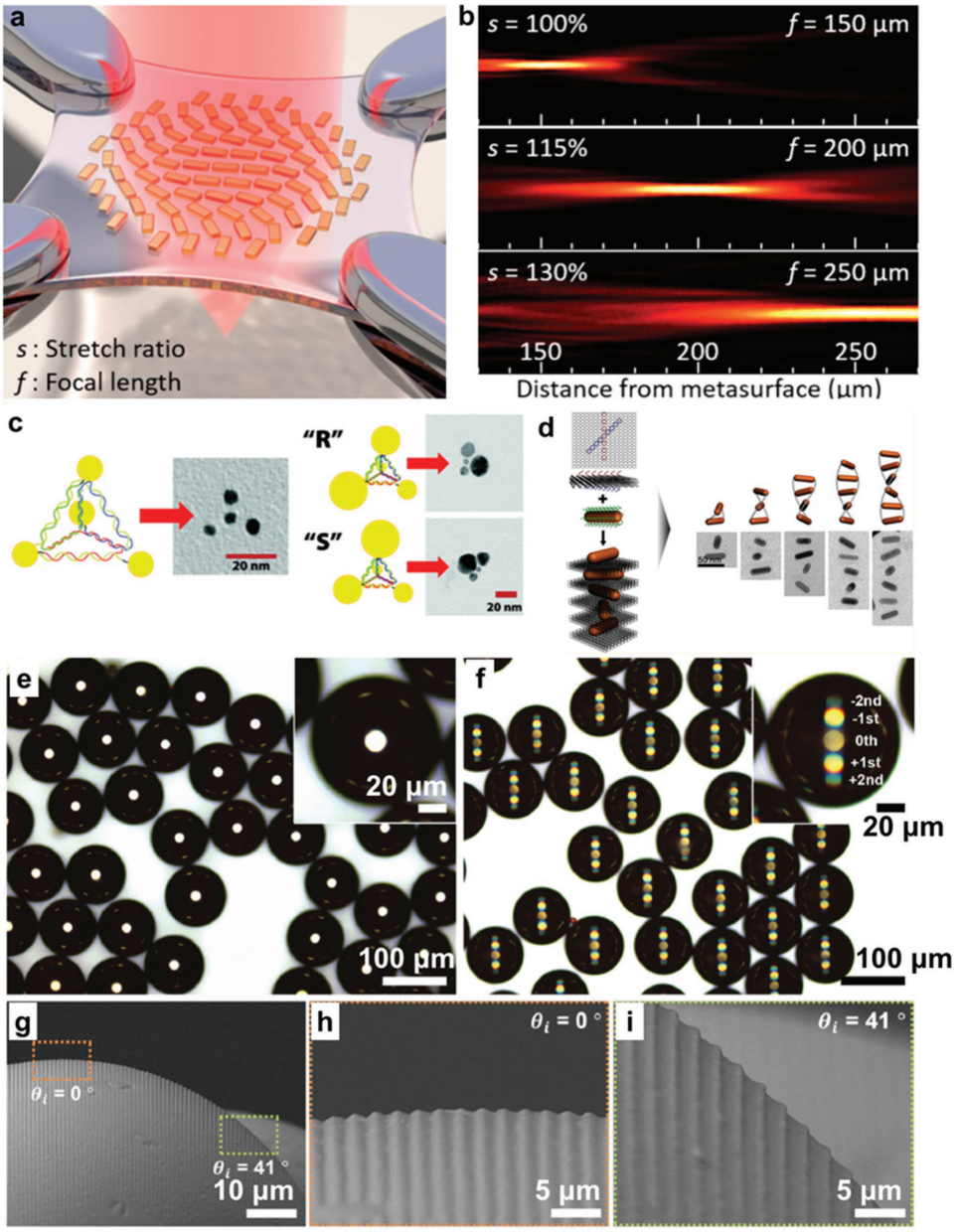

Figure 6. a) Stretchable metasurfaces for tunable flat optical components. b) By controlling the stretching ratio of metasurfaces, their focal length can be tuned. a,b) Reproduced with permission.[77] Copyright 2016, American Chemical Society. c) Controlled chirality can be achieved by DNA-enabled self-assembly of AuNPs into a pyramidal geometry. Reproduced with permission.[51] Copyright 2009, American Chemical Society. d) Helical arrangement of AuNRs realized by using stacked DNA origami nanoplates as a self-assembly template. Reproduced with permission.[55] Copyright 2014, American Chemical Society. e,f) Surface relief gratings (SRGs), inscribed onto microspheres by directional photofluidization, can exhibit structural colors: reflection-mode optical microscopy images of e) bare and f) SRG-inscribed polymeric microspheres. g–i) Scanning electron microscopy (SEM) images of the SRGs on microspheres. e–i) Reproduced with permission.[87a] Copyright 2016, Wiley-VCH.

amplitude grating usually requires numerical simulation and solving of Maxwell's equations on using frequency-domain or time-domain solvers.

Wavelength-scale surface relief gratings (SRGs) can be realized in a rich variety of 1D and 2D periodicity, height, and unit cell profile using conventional monolithic hard fabrication approaches for semiconductors and metals.[202] However, application of soft materials and soft-matter processing strategies can allow us to further expand the achievable structural complexity of SRGs.[87,102] Tailoring of the grating signature that allows for scalable grating production and dynamic tuning of grating performance is highly relevant for a variety of spectroscopic sensing and light manipulation applications. For instance, holographic photo-migration of azobenzene polymeric microspheres (Figure 6e–i)[87] have been used to realize SRGs on curved substrates (i.e., SRG-textured microspheres), which allows us to induce polychromatic structural colorization on the microspheres.

Analog to surface relief gratings, wavelength scale periodicity in 1D, 2D, and 3D in bulk materials can strongly affect the propagation of light wave. In 1887, Load Rayleigh analyzed the suppression of wave propagation occurring for a well-defined frequency/wavelength range (stop-band) in media of 1D periodicity.[203] While Rayleigh focused on acoustic phenomena, he noted that a similar argument should hold for the propagation of light waves in media with periodic refractive index variation.[203] For light propagating in stratified optical media with wavelength-scale refractive index periodicity, Rayleigh's equation[203] that determines the position of the edges of the spectral stop-band is given by

$$\frac{\lambda^2}{4d^2} - 1 = \pm\frac{\rho_1}{2\rho_2} \tag{7}$$

where ρ is the density. In 1987, 100 years after Rayleigh's derivation for a 1D periodic medium, Yablonovitch and John established the theoretical framework for describing photonic bandgaps in 2D and 3D periodic materials, now known as photonic crystals.[167,168]

PhC structures with controlled and dynamically tunable optical properties can be realized through the self-assembly of colloidal silica- or polymer-based NPs in elastomeric 3D crystals.[69,71] These materials are similar in their structure to the regular architecture found in precious opal. Colloidal photonic crystals are therefore also called opals. Opal PhCs display structural color analogous to precious opal and many examples of periodic biological photonic crystal structures. The periodicity of opal PhCs can easily be controlled by adjusting the size of colloidal NPs allowing for the tuning of the crystals' photonic bandgap in a wide frequency range. More importantly, opals embedded within an elastomeric matrix (**Figure 7**a,b) can be deformed by mechanical force, which results in a controlled increase of the PhC periodicity along the axis of deformation and a simultaneous reduction in periodicity perpendicular to the deformation axis.[69,71] This reduction in periodicity leads to a corresponding shift of the PhC's band edges, to lower wavelengths (see Equation (7)), which results in a blue-shift of the material's coloration.[69,71]

The engineering of the lattice motif of colloidal PhC represents an important challenge as the make-up of the PhC unit cell strongly influences the PhC's optical properties. For example, the 3D diamond lattice is unique among other PhC morphologies (face-centered cubic (FCC), hexagonal close packed (HCP), and so on), as it displays the largest photonic bandgap.[205] However, self-assembled colloidal NPs tend to have the lattice geometry of the densely packed FCC and HCP configurations according to a packing consideration. However, recent efforts utilizing DNA origami techniques proved successful in creating a tetragonal cage geometry containing AuNPs in order to implement the assembly of 3D diamond lattice structures from colloidal nanoparticles (see Figure 7c–e).[204] In this approach, the lattice periodicity can be precisely tuned by controlling the length of the molecules in the DNA patch at the four vertices of the tetragonal DNA origami cages.[204]

It is noteworthy that the design of more complex PhC-based motifs such as elastomeric concentric multilayered PhC fibers (Figure 7f–h)[76] requires the use of soft materials; the inclusion of soft materials in PhC design is therefore essential for significantly extending the functionality of current state-of-the-art PhCs. For example, the stop-band position of elastomeric 1D PhC fibers can be tuned mechanically (Figure 7h).[76] In general, the use of soft matter and soft-material processing approaches enable advanced performance and multifunctionality of novel PhC materials.

In contrast to PhC structures with regular long-range order, aggregates of wavelength-scale objects that possess only short-range order and are randomly disordered on length scales exceeding the length of a few unit elements exhibit coherent diffuse light scattering or coherent random lasing if actively light-emitting materials are present.[37,39,40,43,95,96] Recent work shows that the controlled aggregation of colloidal nanoparticles accompanied by phase separation of light-emitting polymer matrix within emulsion droplets can result in angle-independent structural colorization.[206] Very recent theoretical studies suggest that randomly distributed graphene nanoislands within a dye-doped polymeric matrix can be used to achieve cavity-free lasing by benefitting from the extraordinarily low threshold of graphene's saturable absorption.[207] The advancement of optical systems based on 3D random media with noniridescent colorization capable of coherent lasing will strongly rely on recent advances in soft material nanoscale engineering and processing.

2.1.3. Ray-Optics Regime: Dynamic Geometry Changes in Fluids

At scales much larger than the wavelength of light, ray optics (geometrical optics) and associated ray-tracing approaches are sufficient to quantify light–matter interactions. Reflection, transmission, and refraction from macroscopically structured material interfaces, such as that found in microlenses, lenses, macroscopic waveguides, and concentration optics, (used, for instance, in solar concentrators) can be modeled using ray optics. The focusing of light through convex lenses, total internal reflection underlying light guiding in optical fiber with macroscale cores, and statistical light trapping in macroscopically thick solar cells (Yablonovitch limit) are representative phenomena that can be investigated and explained by using ray-optical analysis.[3,45–47,178,179] Once the materials that compose the optical system are fixed, geometrical variables such as the curvature of optical interfaces determine the systems optical behavior and the path that light rays take through it. Many macro- and microscale fluid-based optical systems (optofluidics) with adjustable optical properties can be modeled using geometrical optics.[3,38,41,44–47,178,179] In such systems, the geometrical shape and size of a specific fluid morphology, such as a waveguide, a fluidic lens, and fluid-based optical fibers, can be precisely tuned, which leads to a controlled variation in optical properties. The variation of fluid species with different refractive index n and attenuation coefficient k in an optofluidic system can provide additional functionality for real-time modification of light absorption and refraction properties.

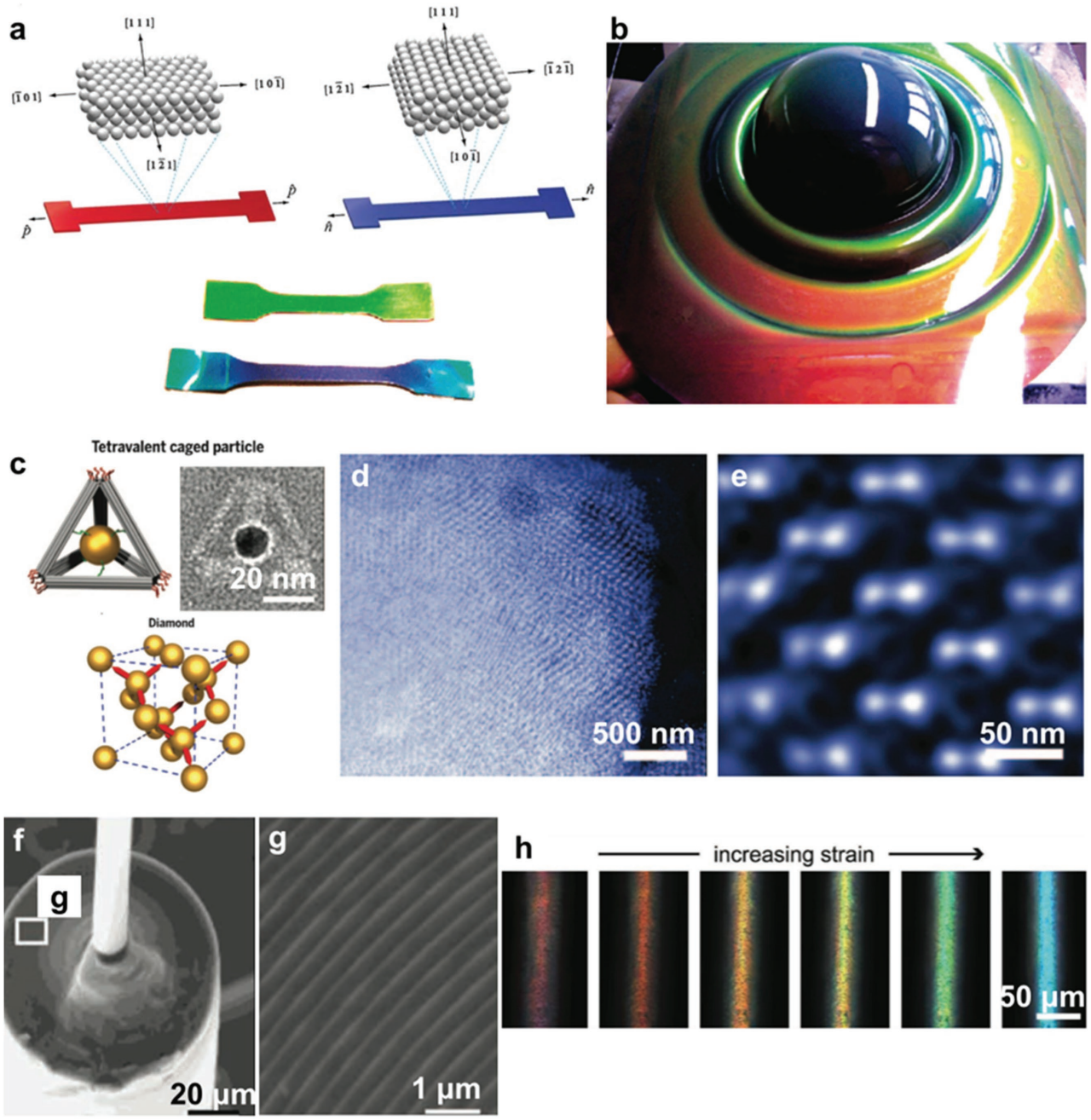

Figure 7. Periodic photonic structures in soft materials. a,b) Opal photonic crystals (PhCs) embedded within an elastomeric matrix can be deformed by mechanical force, in order to tune their photonic bandgap and the resultant structural color. a) Reproduced with permission.[71] Copyright 2010, American Physical Society. b) Reproduced with permission.[69] Copyright 2007, American Chemical Society. c) Tetravalency of AuNP binding sites can be achieved by NP encapsulation in tetrahedral cages made by DNA origami. These DNA-origami-patched AuNPs can be self-assembled into diamond lattices. d,e) A diamond lattice assembled from DNA-origami-based AuNPs imaged at different magnifications. c–e) Reproduced with permission.[204] Copyright 2016, American Association for the Advancement of Science. f,g) Cylindrical Bragg reflectors form photonic fibers. These multilayered clad fibers can be stretched and h) their structural color changes with applied strain. f–h) Reproduced with permission.[76] Copyright 2013, Wiley-VCH.

2.2. Soft Matter Manufacturing for Complex and Dynamic Photonic Systems

2.2.1. Structural DNA Nanotechnology for Metamaterial Engineering

In 1983, Seeman founded the field of "structural DNA nanotechnology," using DNA polymers (or oligomers) as building block to construct molecular architectures in a highly programmable fashion.[208] The most appealing feature of DNA is that it can carry complex information (i.e., the sequence of A, T, G, and C bases is designed to be complementarily paired). Particularly, as all bases of DNA are thermodynamically favorable to bind fully with their complementary sequences, each DNA sequence can find its specific position to be paired to a complementary

strand (i.e., programmable binding of single-stranded DNA and forming of DNA double helix).[209] More importantly, according to the monomer (nucleotide) number of DNA (N), a space of 4^N differently programed DNA molecules can be generated. Based on that, DNA oligomers with 8–50 bases have been used to build nanostructures; in principle, ≈65 000 up to ≈1.2×10^{30} different DNA oligomers are possible. However, due to sequence homology and possible secondary structure (i.e., partial intramolecular binding of DNA), the practically available number of DNA oligomers that can be used in structural DNA nanotechnology is much lower, for example, ≈240 000 for $N = 25$.[209] This imposes a minor constraint and still enables a wealth of distinct structurally complex DNA architectures.

Over the last three decades, the field of structural DNA nanotechnology has rapidly advanced in increasing the structural complexity and size of DNA nanostructures, from the algorithmic assembly and crystallization of DNA tiles (also called by brick) and DNA-coated metallic NPs to the seminal breakthrough of DNA origami.[210–214] Very recently, this success in structural DNA nanotechnology has been translated to the fabrication of optical metamaterials. DNA-based metamaterials can mainly be classified into two groups: 1) materials formed by programmable 3D crystallization of DNA oligomer-coated metallic NPs[56,57,59,63] and 2) structures generated by assembly of metallic NP onto DNA origami pegboards.[52,54,58,60,62] These two approaches will be discussed below.

1) DNA-Assisted 3D Crystallization of Metallic NPs: in 1996, Mirkin and Alivisatos simultaneously reported that DNA-coated AuNPs can be arranged, organized, and aggregated in a programmable way.[210,211] In particular, DNA-coated AuNPs can be clustered with tightly controlled particle distance. Their aggregation can be reversibly varied according to the temperature. Much of the advances that build on this initial breakthrough are focused on the extension of ordering distance (long-range-ordered crystallization of metallic NPs) by optimizing DNA base sequences and the relevant thermodynamics. For instance, the initial demonstrations of the assembly of DNA-coated NPs used full binding of DNA and were limited to short-range ordering, primarily due to kinetic trapping, which occurs before the thermodynamic equilibrium state can be established.[210,211] In 2008, this problem was addressed through rational DNA base sequence design by the groups of Mirkin and Gang.[215,216] Through dressing NPs with a relatively short DNA sequence to be partially bounded with a complementary DNA oligomer, kinetic trapping can be prevented, enabling the metallic NPs to find equilibrium state and to form well-crystallized 3D metallic NP superlattices.[215,216] In this way, diverse superlattices have been obtained by engineering the size, shape, and organic ligands of metallic NPs in order to tailor the crystallization kinetics.[56,57,59,63,217–219]

3D crystals of metallic NPs can have unique optical properties. They can form ENZ materials (see Chapter 2.1.1) and PhCs with plasmonic cavities at visible frequencies.[59,63] As shown in Figure 5a,b, DNA-coated 20-nm-sized silver NPs (AgNPs) can be crystallized into 3D superlattices with body-centered-cubic (BCC) lattice; once the size of AgNPs is fixed, the filling fraction can be controlled via changing the DNA oligomer length. When the filling fraction is ≈20%, this AgNP superlattice is found to show unnatural ENZ at a specific frequency (365 nm wavelength, presented in Figure 5b).[56] Basically, the dipolar oscillations of individual metallic NPs can be coupled to each other via LSPRs (i.e., capacitive coupling); the strength of this dipolar coupling in turn controls the polarization P and the dielectric strength ε (see Equation (1)). Hence, adjustment of the spacing between AgNPs in the BCC lattice offers a strategy for controlling ε from negative to positive values. In this work, the AgNP superlattice is assumed to be embedded within a dielectric material with refractive index $n = 1.4$; some amount of reflection and attenuation at the surface of ENZ AgNP superlattices is owed to the impedance mismatch between the metamaterial and air (Figure 5b).

In addition, DNA complementary binding enables the crystallization of the metallic NPs into the shape of rhombic dodecahedrons (see **Figure 8**a);[59,63] in these structures, the incoming light can resonate in Fabry–Perot mode (i.e., photonic modes). Since the PhC is made of crystalline AuNPs with a BCC lattice, the resonant photonic mode inherently couples to the LSPRs of individual AuNPs (Figure 8b,c).[59] The photonic modes are unable to propagate within a rhombic dodecahedron PhC due to the presence of a bandgap (i.e., polariton bandgap). Indeed, as shown in Figure 8d, a rhombic dodecahedron consisting of 9.0-nm-sized AuNP BCC lattice (center-to-center distance is 32.2 nm (gap is 23.2 nm)) shows oscillatory backscattering spectra as evidence of Fabry–Perot resonance (marked by a triangle). It is noteworthy that at the LSPR wavelength of AuNPs (520 nm), the hallmark of Fabry–Perot resonance is obscured due to coupling to the LSPR mode.[59] The polariton bandgap can be precisely engineered by adjusting the size of and the gap between AuNPs by controlling the DNA interconnect length. For instance, when the size of AuNPs within a BCC lattice is increased to 20.0 nm with a center-to-center distance of 44.0 nm (a gap of 24 nm), Fabry–Perot modes cannot be induced below a wavelength of 500 nm (see Figure 8e). This effect occurs, because an increase in AuNP size results in a larger lattice filling fraction, which leads to a strengthening of interband transitions. In addition to these effective ε and photonic–plasmonic interactions, other mesoscopic optical properties including refractive indices and extinction coefficients can be deterministically controlled by tuning various structural parameters such as filling fraction and shape of metallic NPs.[56,59,63]

2) DNA-Origami-Enabled organization of Metallic Nanoparticles: In 2006, Rothemund pioneered the concept of DNA origami, showing that a long, single-stranded M13 DNA sequence can be folded into almost any desired shape by using assistive, short, single-stranded DNA sequences that act as a clamp specifying folding position.[213] Since then, DNA nanotechnology has flourished into a rich, active field by increasing structural size and complexity of DNA origami constructs, ranging from fundamental achievements in realizing 2D and 3D complex,[213,214] bending and twisting[220] DNA origami motifs to their practical applications in biomedicine and photonics.[52,54,58,60,62,221,222] In particular, due to the ability to arbitrarily locate DNA sticky handles onto any desired DNA origami surface, various nanomaterials including NPs, QDs, lipid, proteins, and other building blocks can heterogeneously be integrated into a single molecular composite.[52,54,58,60,62,221–223] This remarkable ability of DNA origami to act as a molecular pegboard has enabled the realization of various molecular photonic devices.[52,54,58,60,62]

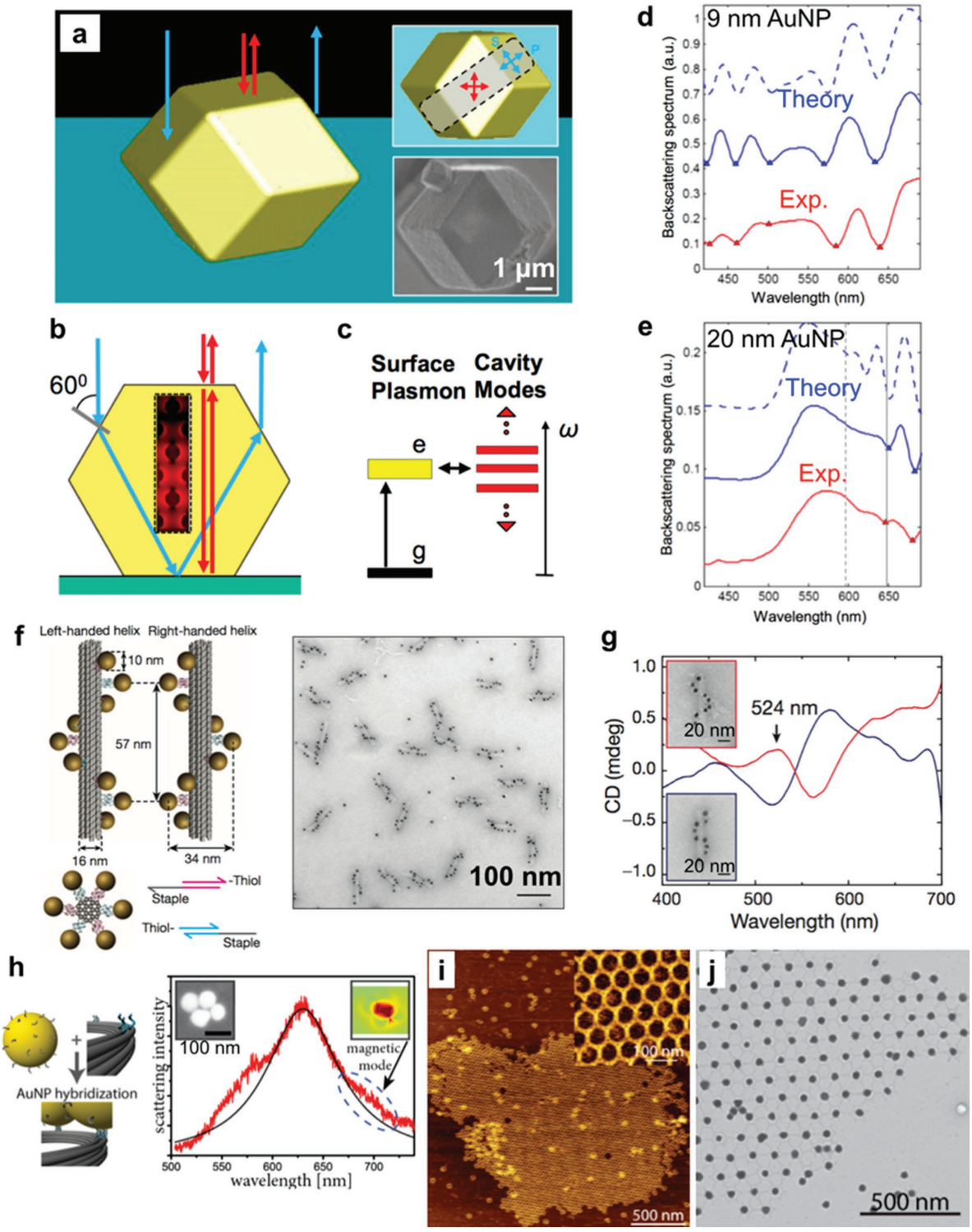

Figure 8. DNA nanotechnology for nanophotonics. a–c) A microscale crystal made from a) AuNPs can induce b,c) dielectric cavity modes and LSPR modes for each constituent AuNP. d,e) Normal scattering spectra of 9 and 20 nm AuNP crystal. a–e) Reproduced with permission.[59] Copyright 2015, National Academy of Sciences. f) Self-assembly of AuNP into a helical geometry by using tube-shaped DNA origami. g) Circular dichroism (CD) spectrum obtained from the structures shown in panel (f). f,g) Reproduced with permission.[52] Copyright 2012, Nature Publishing Group. h) Four AuNPs can be assembled into a ring motif onto donut-shaped DNA origami; these structures exhibit optical magnetism. Reproduced with permission.[58] Copyright 2015, American Chemical Society. i) Hexagonal tiling of DNA hierarchically assembled into a 2D lattice. j) This 2D lattice can act as a template for large-area arrangements of AuNPs, which could be used for electric metamaterials. i,j) Reproduced with permission.[62] Copyright 2016, American Chemical Society.

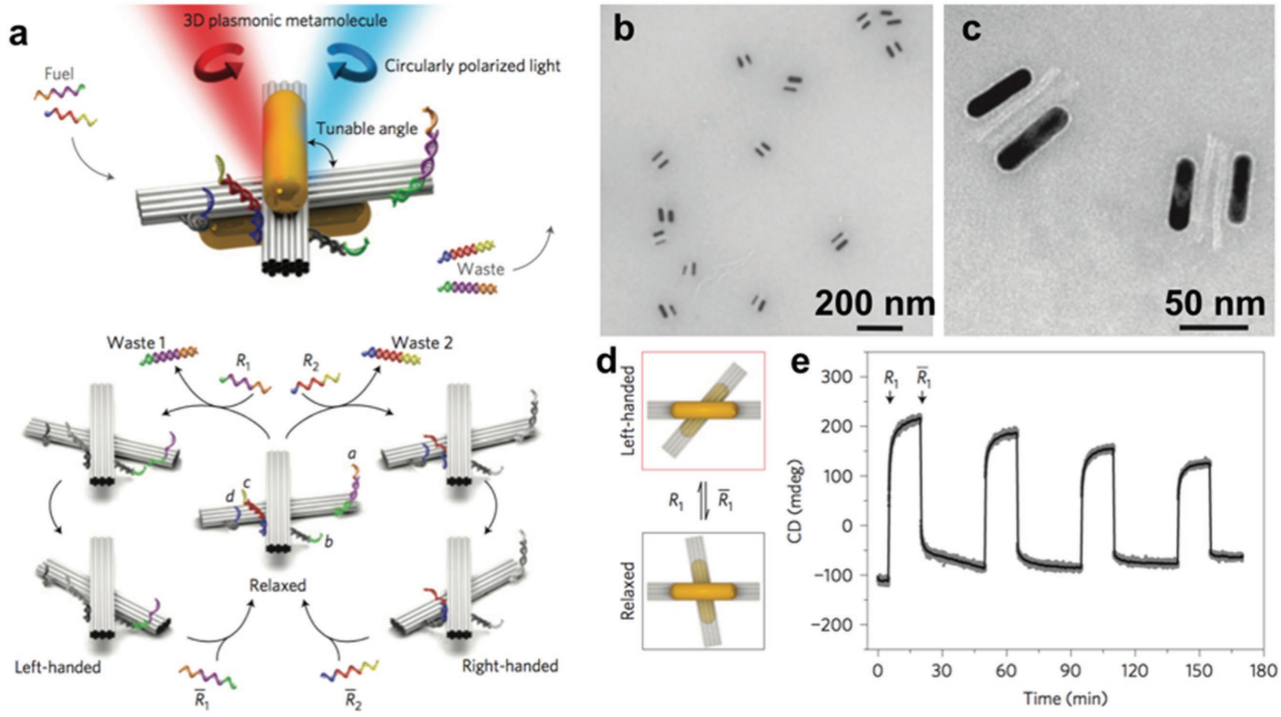

Figure 9. Reconfigurable plasmonic metamolecules assembled onto DNA origami. a) DNA strand displacement allows for the reconfiguration of DNA origami motifs, leading to a rearrangement of the associated AuNRs. b,c) The self-assembled plasmonic metamolecules made from AuNR dimers. d) The chirality of AuNR dimers changes according to the configuration of DNA origami, which can be controlled via DNA strand displacement. e) Circular dichroism (CD) spectrum of plasmonic metamolecule-dispersed fluid. a–e) Reproduced with permission.[54] Copyright 2014, Nature Publishing Group.

In 2012, T. Liedl and co-workers reported that 3D DNA origami constructs with longitudinal tubular structures can be decorated in a helical geometry with small AuNPs (≈10 nm in size, see Figure 8f);[52] in this material, the optical chirality ξ can be tuned precisely. By using an optimized experimental protocol, small AuNPs can be attached with almost 100% yield (see transmission electron microscope image of Figure 8f); the obtainable concentration of 3D DNA origami is generally on the orders of a few nanomolars. In line with this, the plasmonic chiral features (ξ), which are engineered at a molecular level, can be measured in a bulk solution (metafluids) and evidenced by bulk circular dichroism (see Figure 8g).

Furthermore, SRR motifs consisting of at least three metallic NPs can be realized with 3D DNA origami.[58] As presented in Figure 8h, donut-shaped 3D DNA origami tubes can serve as a template for arranging AuNP ring motifs with a controlled structural symmetry. In general, during colloidal self-assembly solvent evaporation-induced convective forces push NPs into a close-packed configuration that imparts highest structural stability. Thus, without any modification of the particle interaction (for instance, achieved through localized chemical binding spots on the particles—patchy particles), dense and packed clusters will be the result of any colloidal self-assembly approach.[92–104] However, the use of DNA origami as a template enables the formation of nondense assemblies. An example is the construction of NP 3D diamond lattices.[204] Through DNA-origami-enabled colloid assembly sophisticated structural motifs of AuNP ring clusters with controlled symmetry can be achieved (Figure 8h). By tailoring the structural symmetry of the ring cluster, the structure's electric and magnetic responses can be controlled precisely. Consequently, DNA-origami-based engineering of metamolecules enables artificial magnetism (control of the permeability μ) and the establishment of metamaterials with controlled dielectric constant ε (ENZ or very high ε materials).

Besides ring cluster motifs and their use as optical metamolecules, DNA origami can also be used to produce crystalline lattices with long-range order, using suitable DNA origami motifs and connection strand designs. In 2016, Ke and co-workers demonstrated the formation of hexagonal lattices using rationally designed hexagonal DNA origami tiles (Figure 8i).[62] Their hexagonal lattice of DNA origami crystals can be decorated with AuNPs (Figure 8j). DNA origami offers materials programmability with a precision of a few nanometers. This allows for the precise positioning of individual particles in AuNP arrangements enabling fine-tuning of the material's effective dielectric permittivity ε (i.e., electric metamaterials).[62]

The versatility of DNA nanotechnology for soft photonics is not limited to the exquisite control of clusters and lattices made from metallic NPs. Using dynamic molecular DNA strand displacement motifs,[224] reconfigurable and tunable photonic materials can be formed. **Figure 9**a schematically depicts the DNA displacement-enabled reconfiguration of 3D plasmonic metamolecules.[54] Two DNA origami beams are cross-stacked (see Figure 9b,c). The angle between them can be controlled by toehold-mediated DNA strand displacement.[224] Consequently, the configuration of AuNRs attached onto the facet of the two DNA origami beams can be reconfigured, changing the angle

between two stacked AuNRs; this dynamic change in turn affects the plasmonic interparticle coupling. This way, the plasmonic chirality ξ resulting from the interparticle coupling can be tuned, as shown in Figure 9d,e. This result indicates that the unique characteristics of DNA can provide a platform for realizing adaptable, tunable photonic systems that allow for in situ control of the material's dielectric permittivity ε, magnetic permeability μ, and optical chirality ξ.

2.2.2. Mechanoresponsive Elastomeric Photonic Systems

Taking advantage of rapid advances in soft lithography,[225] stretchable and soft elastomers have successfully been implemented in a variety of mechanically reconfigurable photonic materials for mechanosensitive optical systems.[69–78]

For instance, wrinkling instabilities driven through relaxation of a prestrained laminate that consists of a hard film on top of a soft layer can be exploited to form optical materials. As shown in **Figure 10**a, the oxygen plasma treatment of a prestrained polydimethylsiloxane (PDMS) elastomer sheet induces a conversion of the sample's top surface into a thin glassy hard film with a modulus that changes gradually from higher to lower values with the sample depth. Uniaxial stretching of the pristine PDMS prior to oxygen plasma treatment and the subsequent relaxation after plasma exposure results in the formation of characteristic quasiordered 1D wrinkling patterns.[75] Importantly, the period of winkles can be precisely controlled by adjusting the plasma exposure conditions and the prestrain. Periodicities of the order of a few micrometers can be achieved in the regular patterns, and consequently the samples show light diffraction that obeys the simple relation in Equation (4). Generally, the grating vector of the quasiordered wrinkles is oriented along the direction of prestretching. However, when the wrinkled PDMS surface is stretched beyond the initial prestrain, the wrinkle pattern switches to an orientation perpendicular to the initial grating direction. Furthermore, when stretching up to the prestrain value, the wavelength of wrinkles increases while the amplitude decreases; when the applied strain becomes comparable to the prestrain, the winkle line patterns undergoes a transient state forming 2D surface morphologies. For strains beyond the prestrain, the wrinkles, which are now aligned parallel to the axis of strain decrease in wavelength and increase in amplitude. Overall, the wrinkles can be reversibly stretched and relaxed by controlled mechanical strain; consequently, the corresponding diffraction behavior can be reconfigured reversibly as a function of strain (i.e., mechanosensitive diffractive components).[75] This can be seen beautifully in the strain-dependent far-field diffraction pattern (Figure 10b,c). For strains below the prestrain value, a line diffraction pattern aligned with the strain direction is apparent. For strains close to the prestrain value, a 2D diffraction pattern occurs due to wrinkles being present on the surface in both orientations parallel and perpendicular to the strain direction. For strains higher than the prestrain, the diffraction patterns turn into a line of diffraction spots now oriented perpendicular to the strain direction. The change in wrinkle wavelength is captured in the distance between diffraction orders (Figure 10c) according to the general diffraction equation (Equation (4)).

Surface wrinkling can also be employed to form tunable metamaterials.[74] Irreversible chemical bonding of hard metamaterial layers onto stretched PDMS substrates and subsequent strain release can result in the formation of a periodically wrinkled superstructure superimposed onto the periodically arranged meta-atoms, as shown in Figure 10d–f.[74] In this work, an electric terahertz (THz) metamaterial, which exhibits unnaturally high refractive index[16,226] is first encapsulated within a hard polymeric thin film (2-μm-thick polyimide layer), which is then deposited on a prestretched PDMS substrate. In this metamaterial, an array of hexagon frames with a small gap between individual unit cells can strongly concentrate the electric field via capacitive coupling between the hexagons, which leads to a dramatic enhancement of the dielectric permittivity ε (see Figure 10g). Simultaneously, thin hexagon frames suppress magnetism ($\mu \approx 1$). This resonant electric behavior can be seen in the single spectral transmission dip shown in Figure 10h. The frequency at which this electric resonance is located depends on the light incidence angle.

The rearrangement of individual meta-atoms (hexagons) in the wrinkled superstructures imposed by the substrate upon strain relaxation leads to a mode splitting, as evidenced by several dips in the transmission spectra. Also, structuring into 1D wrinkling drives the degeneracy lift in "polarization insensitive" electric THz metamaterials (see Figure 10h). Such tuning of electric resonance can be reversibly carried out by stretching and relaxation; the modulation depth (a relative change in transmission) can reach to about 90%.[74]

Lattices of subwavelength- (metasurfaces) and wavelength-sized (photonic crystals) optical units can easily be embedded within stretchable elastomers (for instance, PDMS) to be dynamically reconfigured by mechanical strain. This way, a wide range of mechanically tunable, soft optical systems can be realized, including stretchable metasurfaces, polymeric opals, PhC fibers, and nanolasers, exemplified by the specific systems discussed in Section 2.1. In particular, the lattice variables including Φ in metasurfaces (see Equation (3)) and d (periodicity) in PhCs (see Equations (5) and (6)) can be readily tuned according to the stretching ratio; in that, the relevant optical mode (i.e., light bending and photonic bandgap (coupling mode)) is reconfigured.

2.2.3. Fluidic Reconfiguration

The shape of fluids is very susceptible to externally applied forces and can easily be reconfigured by a variety of mechanical, electrical, or thermal stimuli. Fluids will retain an imposed shape as long as the stimulus is active. This can be used to control various geometrical parameters in fluidic optical elements, such as the curvature of liquid lenses and the dimensions of liquid waveguides.[45,47] A large variety of fluids are available for optical design. For example, numerous combinations of various liquids (water, organic oils, solvents, and so on) and dissolvable molecules with useful optical properties (e.g., fluorescence and absorption) can be used to gain precise control of basic optical properties, including refractive index and attenuation coefficient. In the field of "optofluidics"—the implementation of fluids as functional elements in optical devices—the recent development

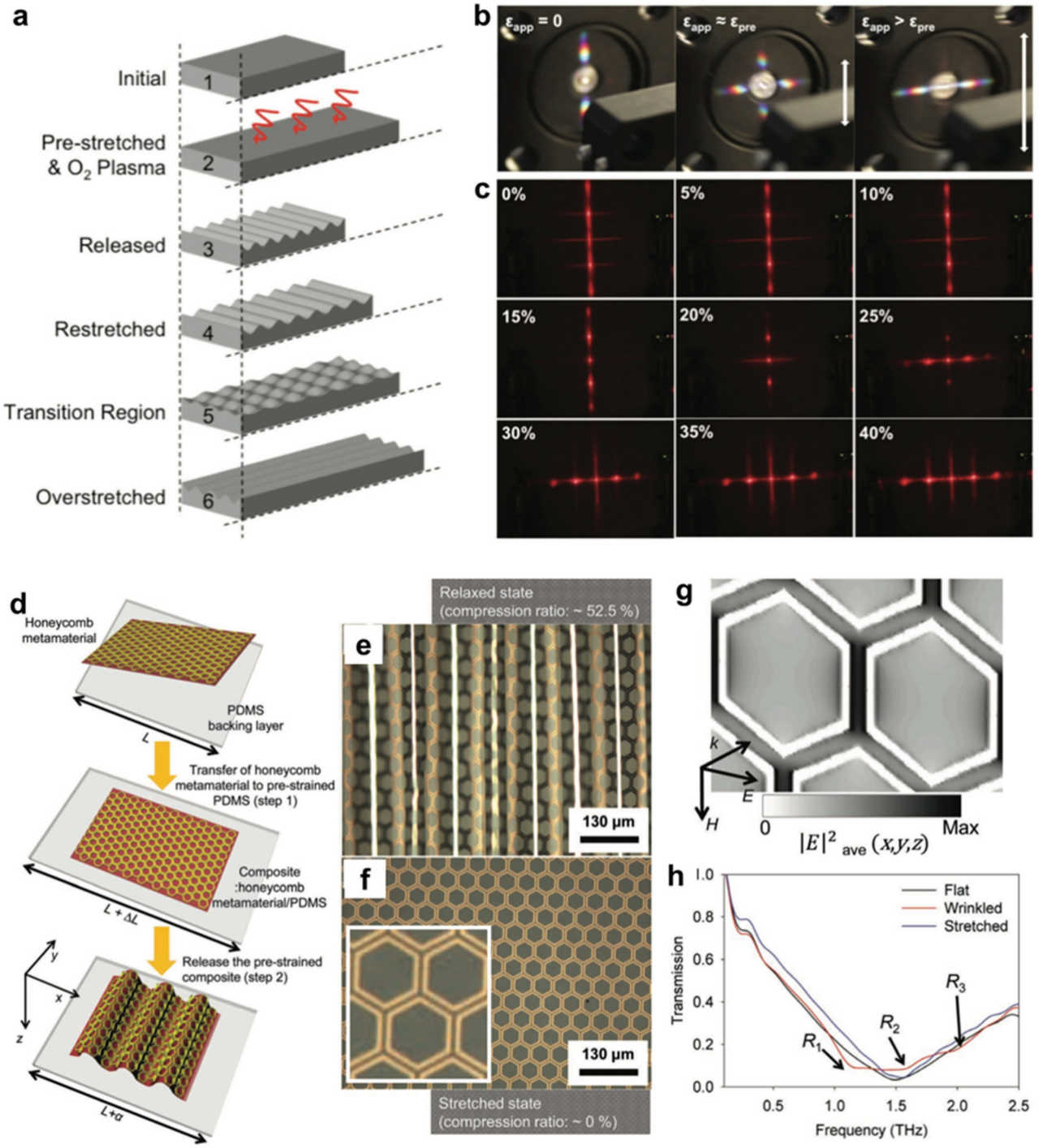

Figure 10. Elastomeric micro- and nano-optical systems that respond to mechanical reconfigurations. a) Wrinkling instabilities caused by the relaxation of oxygen-treated elastomer surfaces lead to the formation of periodic SRGs. b,c) The diffraction effects caused by the SRGs inscribed onto the elastomer depend on the applied strain. a–c) Reproduced with permission.[75] Copyright 2013, Wiley-VCH. d) Electric terahertz (THz) metamaterials (i.e., array of hexagonal frame with small gap) also can be patterned via wrinkling instabilities. e,f) Wrinkled THz metamaterials can be reversibly e) relaxed and f) stretched. g) These THz metamaterials exhibit electrical resonances as evidenced by the strongly confined electric field within the gap between hexagonal meta-atom frames. h) The resonant behavior can be altered by applying a strain, because the geometrical relationship between the incoming electric field and the gap is different for each stretching ratio. d–h) Reproduced with permission.[74] Copyright 2012, Wiley-VCH.

of microfluidic technologies that benefits from the advanced soft lithography has enabled opportunities for unprecedented control of fluidic optical components.[38,41,44–47,178,179] Representative examples of optofluidic light manipulation, including tunable liquid/liquid lenses[46] and emulsion droplet-enabled WGM lasers,[47] are shown in **Figure 11**. Using microfluidic channels,

a tunable liquid lens system was designed from three immiscible fluids, where two distinct fluids acted as cladding phases for a third liquid (Figure 11a).[46] In this system, appropriate flow adjustment permits the tuning of the fluid interface curvatures; the two cladding fluids force the core fluid to form elliptically shaped interfaces within an expansion chamber. The fluids are formulated to maximize the refractive index contrast. Mixtures of benzyl alcohol and benzothiazol are used for the core fluid, and compositions of trifluoroethanol, methanol, ethylene glycol, and ethanol make up the cladding fluid.[46] Clear interfaces between the fluids are established due to laminar flow in the channel. Microscale channels with characteristic dimensions on the order of a few 100 μm typically have Reynolds numbers smaller than 10, which allows for laminar flow of the three fluids, resulting in a stable operation of the fluid lens (Figure 11b).[46] More importantly, the curvature of this optofluidic lens can be readily tuned by varying the flow rate of core fluid (see Figure 11c), so as to adjust the lens' focal distance in real time.

Emulsion droplet-based tunable WGM microlasers can be generated with uniform sizes using microfluidics (Figure 11d,e).[47] The microscale droplets have ultrasmooth surfaces that allow for very high WGM quality factors when used in optofluidic devices. In addition, various gain materials can easily be incorporated into the WGM droplet lasers, enabling a wide range of operating wavelengths. By alternatingly generating laser droplets with two different gain materials (rhodamine 560 and rhodamine 640 in benzyl alcohol), which exhibit a mutually distinct spectral emission, a fast-switching microfluidic laser system was realized (Figure 11d). This laser system, which demonstrates switching times of less than 100 ms, relies on temporarily exciting individual droplets by flowing them through an excitation beam. Adjusting the droplet generation parameters and the flow rate of formed droplets allows for the tuning of switching duration, the duty cycle, and the switching sequence (Figure 11e).

An alternative strategy for the creation of microscale components with variable texture and reversibly tunable optical properties for photonic devices consists in exploiting the photofluidic reconfiguration of solid-state azobenzene-based materials (**Figure 12**).[82–87] The azobenzene-based materials, formed by incorporating photochromic azobenzene molecules

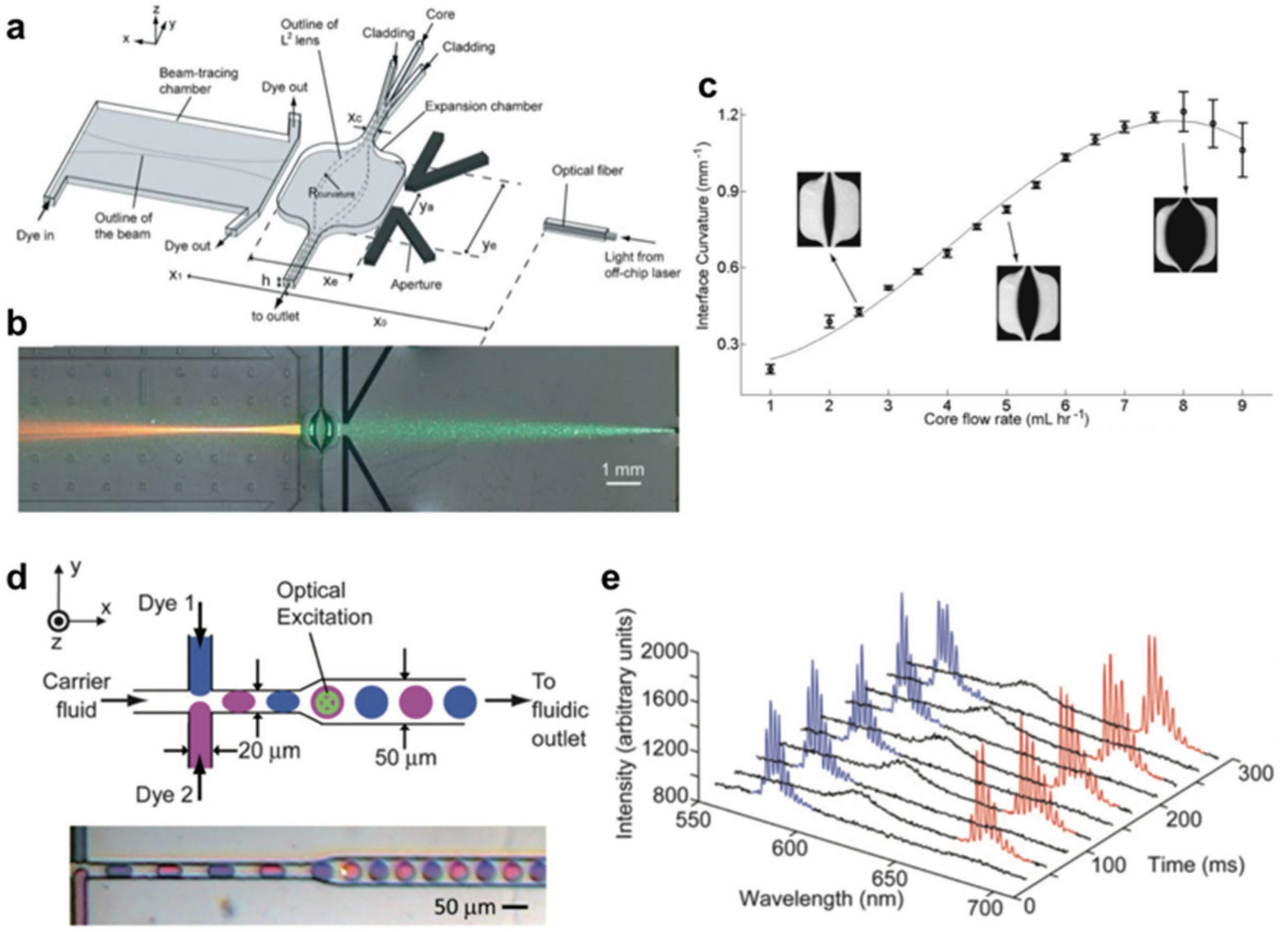

Figure 11. Optofluidics for reconfigurable and adaptable photonic systems. a) Device schematic for an optofluidic microlens system. Two fluid cladding layers can force a core fluid to assume shapes with variable curvature, which could act as a microlens. b) Light focusing via an optofluidic microlens system. c) By changing the flow rate between core and cladding fluids, the lens curvature can be tuned. a–c) Reproduced with permission.[46] Copyright 2008, Royal Society of Chemistry. d) T-junction of a microfluidic channel that can form uniformly sized microemulsion droplets containing fluorescent dye. e) The microemulsion droplet can act as a WGM cavity; thus, fluorescence from dye molecules can be boosted via stimulated emission. d,e) Reproduced with permission.[47] Copyright 2009, Royal Society of Chemistry.

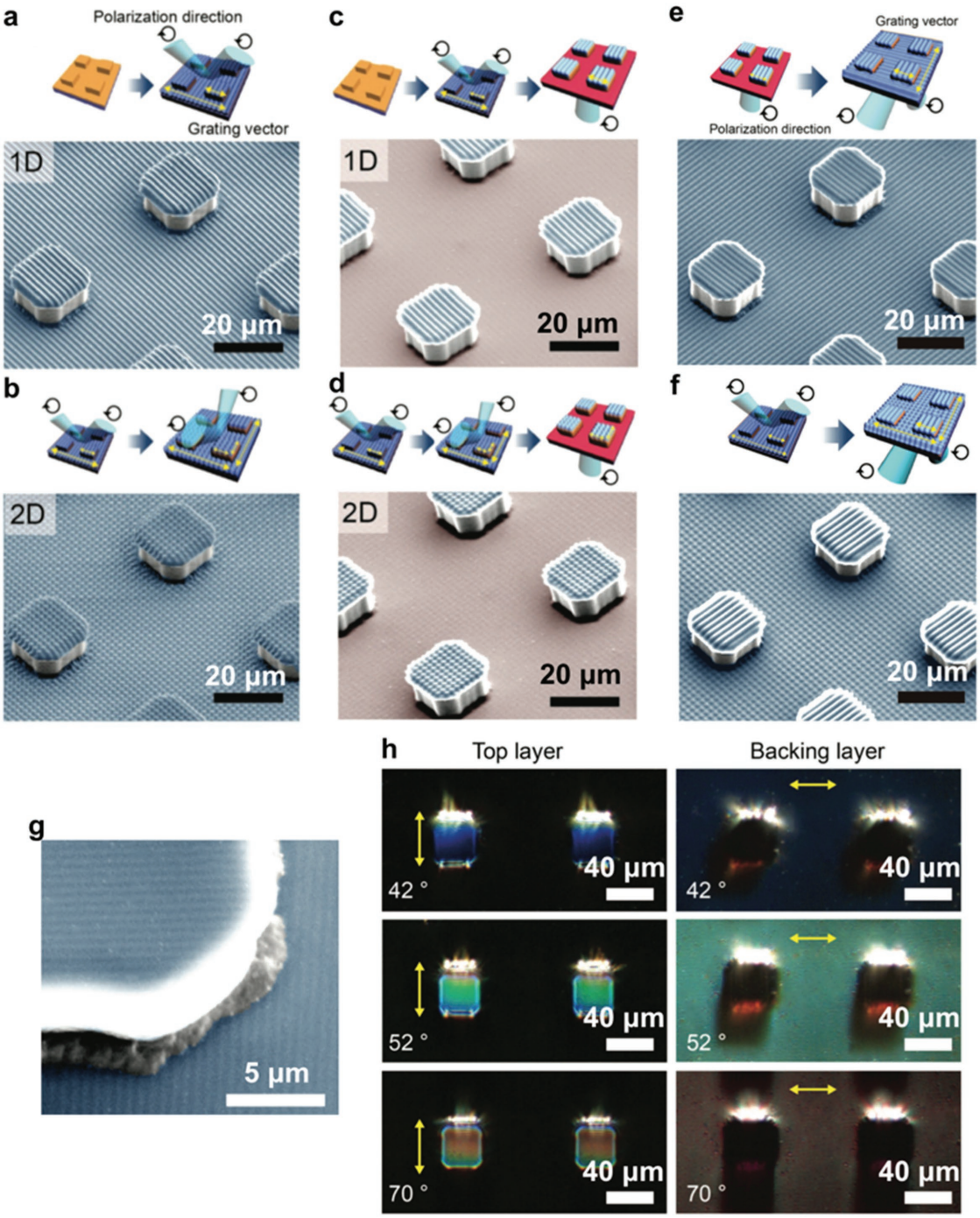

Figure 12. The use of photofluidization for reconfigurable nanophotonic systems. Photofluidization is a specific softening effect occurring in photochromic materials (i.e., azobenzene-molecule-incorporated soft materials) in response to illumination with light. Photofluidization is driven by photoisomerization of azobenzene molecules, which can switch between a *trans*- and a *cis*-conformations. a,b) Flat surfaces on microsized posts made of azobenzene polymer can be inscribed with SRGs, when exposed to interference patterns of polarized light. This photofluidic inscription is capable of the reversible generation of SRGs without the need for chemical wet-etching or other processing. c,d) When the SRG-inscribed microposts are illuminated with backside single beam rather than interference beam, the backing layer can be selectively fluidized. As such, the inscribed SRGs are selectively erased, while the SRGs on the top of microposts remain intact. This can be achieved because photofluidization can be induced selectively at the illuminated surface (superficial photofluidization). e,f) By taking advantage of superficial photofluidization, the erased surface can be inscribed with a different SRG. g) Representative example of heterogeneously integrated SRGs at the top of micropost and at the backing layer. At the top and the backing layer, the grating vectors of 1D SRGs differ from each other, whereas the periods are the same. h) Thus, SPP holograms either in the backing layer or on the top surface of microposts can selectively be excited by adjusting the wavevectors of incident light. a–h) Reproduced with permission.[84] Copyright 2013, Wiley-VCH.

into various polymers or supramolecules, can be fluidized at room temperature using light illumination; this photofluidization effect is driven by photoisomerization of azobenzene molecules, which can switch between a *trans*- and a *cis*-conformation.[82] Notably, in stark contrast to isotropic thermal melting, the photofluidization of azobenzene materials is highly directional and dependent on the polarization of incident light.[82] Consequently, flat thin films made of azobenzene materials can be inscribed with SRGs, when exposed to interference patterns of polarized light.[82–87] SRGs result from the localized directional photofluidic migration of azobenzene molecules in the direction of polarization within high intensity regions of the light interference pattern. Azobenzene derivatives are generally highly light-absorbing materials; consequently, the inscription of SRGs can be selectively confined at the surface. This process is reversible as the generated SRGs can be erased by thermal treatment, i.e., heating above the material's glass transition temperature or by exposure to a circularly polarized light beam of homogeneous intensity.[82–87] This approach enables the reversible generation of SRGs without the need for chemical wet-etching or other processing. Structured surfaces consisting of azobenzene-containing microposts on an azobenzene-rich backing layer have been used to demonstrate the generation of hierarchical surface patterns by reversible inscription of 1D and 2D SRGs onto micropatterned surfaces with structured front-side illumination (Figure 12a,b).[84] By subsequently irradiating the sample from the backside with a uniform circularly polarized beam, the SRG on the backing layer that supports the patterned microposts can be selectively erased (Figure 12c,d) and then can be inscribed by another SRG with a different orientation than the SRG previously generated on the top of the microposts (Figure 12e,f). After the deposition of a metallic thin film (e.g., Au), the dielectric and diffractive hierarchically patterned SRG surfaces can be used for SPP holography (Figure 12g,h). By appropriately choosing the light incidence direction, i.e., by controlling the wavevector component of incident light that is parallel to the surface plane, SPP holograms inscribed in either the backing layer or the top surface of micrometer post (Figure 12g) can be selectively excited.[84] Furthermore, reversible photofluidic texturing of micropatterned optical surfaces can be employed for the integration of pixelated plasmonic color filters (Figure 12h).

2.2.4. Thermally Responsive Soft Photonic Materials

Materials conducive to thermal tuning can provide additional flexibility in adaptive photonic systems.[227,228] The metallic NP superlattices with controlled volume fraction form materials with unnatural ENZ in the visible spectral range.[56] Furthermore, liquid crystalline organic ligand-coated AgNPs (**Figure 13**a,b), recently reported by Lewandowski et al., can form superlattice structures that reversibly switch between lamella (Lm) and isotropic (Iso) phases as a function of applied temperature (Figure 13c,d).[227] Particularly, at 90 °C, the liquid-crystalline organic ligand undergoes melting, resulting in a rearrangement of AgNPs (Figure 13c,d). This structural reorganization from isotropic to lamellar phases in the AgNP superlattice leads to a change in the particles' dipolar interactions resulting in a variation of the material's mesoscopic optical properties such as the extinction coefficient and the effective dielectric permittivity (Figure 13e).

Hydrogel-based PhCs can form thermally tunable gels (Figure 13f,g).[228] Such gels can be formed by using colloidal crystals (i.e., opals) as a template to form a structures with regular porosity in a hydrogel. For example, a liquid hydrogel precursor can be infiltrated into a colloidal crystal template and subsequently solidified through a cross-linking reaction. Then, the colloidal crystal can be selectively etched out, leaving behind a hydrogel inverse opal. Hydrogels immersed in water can undergo dramatic volume changes as a function of temperature near the lower critical solution temperature. This effect can be exploited to induce significant variations in the periodicity of hydrogel-based inverse opals to tune their photonic bandgaps (Figure 13f).[228] The structural parameters of hydrogel inverse opals can also be varied using light. This can be achieved by incorporating azobenzene molecules within the hydrogel. Upon irradiation with UV light, azobenzene molecules undergo photo-isomerization between *trans*- and *cis*-states, which leads to a significant change in their dipole moment: in the *trans*-state, azobenzene molecules do not have a strong dipole moment, whereas in the *cis*-state a distinct dipolar electron distribution is present.[228] This dipolar momentum in the *cis*-state alters the free energy of the hydrogel network and affects its expansion behavior in water: In the presence of polarized *cis*-state azobenzene molecules, the hydrogel attracts more water molecules and displays stronger swelling compared with a pure hydrogel or a hydrogel with azobenzene molecules in the nonpolar *trans*-state.[228] Reversible optical patterning can be achieved using this effect (Figure 13g). Patterned exposure of an azobenzene-containing hydrogel inverse opal to UV light leads to localized swelling of a hydrogel accompanied by a pronounced redshift in perceived coloration allowing to display image features with submillimeter resolution. In summary, inverse opals made of azobenzene-containing hydrogels can be thermally and optically tuned.[228]

3. Biologically Inspired Photonic Materials

3.1. Cephalopod Skin: A Versatile Soft Photonic Material

The field of soft photonics has seen tremendous advances over the last decade, in large parts due to the interdisciplinary efforts of researchers in chemistry, materials science, engineering, and physics. Now, let us imagine the following challenge for a tunable, soft, optical material. Given around 800 g of water, 160 g of proteins, 9 g of fat, and a select, but finite list of other minor ingredients,[229,230] can you create a material that contains spatially distributed, expandable absorbing components, iridescent elements, and bright white scatterers, which together allow for in situ control of the material's emergent optical behavior? Can you also render this material deformable and compliant, capable of sensing light levels in its environment, and changing texture and color, while being able to control its configuration with your brain? If your answer to these questions is "Yes," congratulations for a remarkable achievement—your material should be poised to change optical technology and product

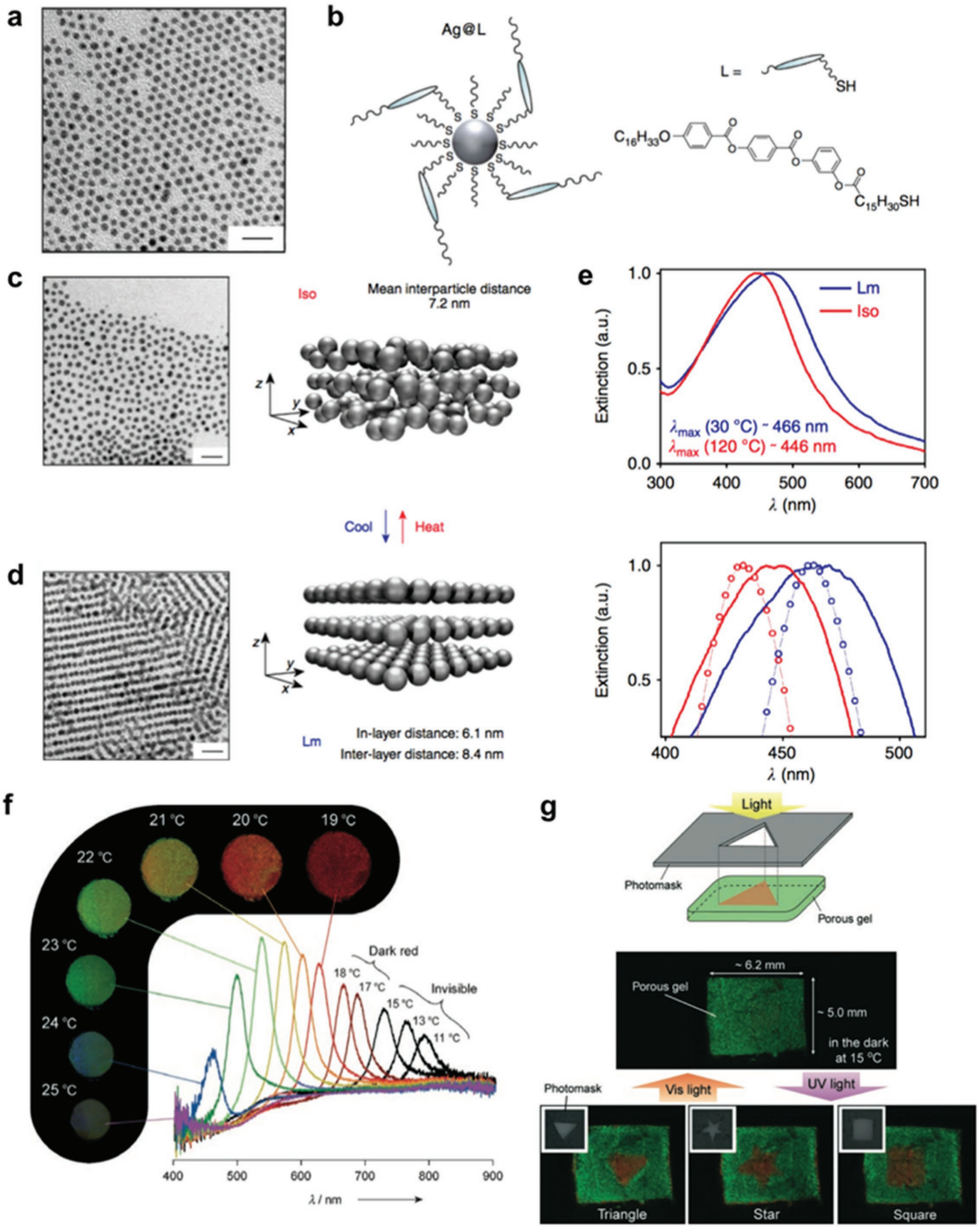

Figure 13. Thermally controllable nanophotonic systems. a,b) A superlattice of AgNPs with controlled volume fraction can act as an optical metamaterial with unnatural near-zero permittivity. These AgNPs can be coated with thermally responsible, liquid crystalline organic ligands. c,d) The superlattice structures consisting of liquid crystalline organic-ligand-coated AgNPs can reversibly switch between lamella (Lm) and isotropic (Iso) phases as a function of applied temperature. As a result, the arrangement of AgNPs can be thermally switched between c) a randomly dispersed state and d) a regularly arrayed state. e,f) By controlling the arrangement of AgNPs, the electric dipolar interaction is tuned; this way, the extinction caused by the AgNP superlattice structure is thermally reconfigurable. a–e) Reproduced with permission.[227] Copyright 2014, Nature Publishing Group. f) Hydrogel-based, inverse opals can exhibit thermally tunable photonic bandgaps and variable structural colorization. In general, hydrogels immersed in water undergo dramatic volume changes as a function of temperature near the lower critical solution temperature. This effect can be used to effectively modulate the periodicity of hydrogel-based inverse opals to tune their photonic bandgaps. g) The period of hydrogel inverse opals, in which azobenzene molecules are incorporated, can be modulated by light illumination. The illumination with UV light makes azobenzene molecules undergo photoisomerization; in that, their dipole moment is significantly changed. In particular, in the *trans*-state azobenzene molecules cannot show a strong dipole moment, whereas in the *cis*-state, a distinct dipolar distribution can be induced. This photo-tuned dipolar state affects the expansion behavior of hydrogel in water; reversible optical patterning of structural colors of hydrogel opal can be attained using this effect. f,g) Reproduced with permission.[228] Copyright 2007, Wiley-VCH.

design dramatically. Why is this not yet published anywhere in its full glory?

While parts of this challenge have indeed recently been addressed,[231–234] most likely your answer—regarding a complete synthetic realization of a material with all the properties described above—will be "No." That, however, does not mean that such a material does not exist; the organisms that are capable of realizing it just have not made academic publishing and device engineering for mankind's sake their highest priority. Take, for instance, the longfin inshore squid (*Doryteuthis pealeii* formerly *Loligo pealeii*), a well-studied example[235,236] of the diversity of optical elements in the multifunctional skins of cephalopods (**Figure 14**).[131–134] This squid species, like many other cephalopods, employs chromatophores and iridophores to create specific camouflage or signaling patterns through local control of chromatophore and iridophore configurations. It achieves high spatial and temporal control of the configuration of its microscale optical components using a complex nervous system distributed within its skin. The squid also sports a system of leucophores—cells that contain randomized, incoherently scattering micro- and nanoarchitectures, which create a white canvas for chromatophores and iridophores.

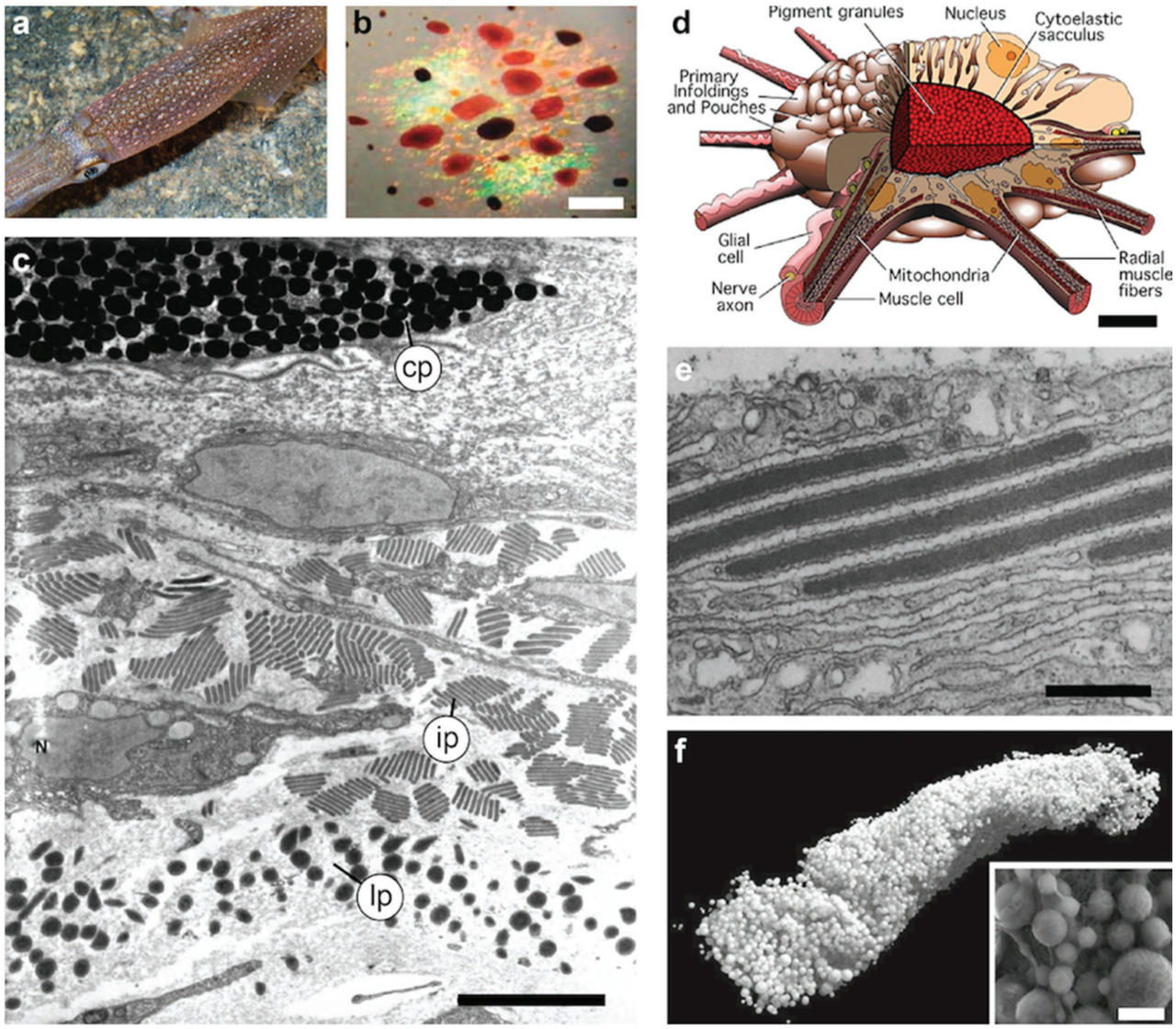

Figure 14. Photonic elements in cephalopod skin. a) The longfin inshore squid (*Doryteuthis pealeii*). b) The squid's variable skin color results from the interplay between light-absorbing chromatophores (brown, red, and yellow), iridophores containing regularly layered nanostructures that cause Bragg reflection (blue, green, and yellow), and leucophores that exhibit strong multiple scattering and provide a white backdrop. Scale bar is 1 mm. a,b) Reproduced with permission.[236] Copyright 2009, The Royal Society. c) Scanning electron microscopy image of squid skin tissue displaying part of a chromatophore (cp), iridophores (ip), and leucophores (lp). Scale bar is 5 µm. Reproduced with permission.[131] Copyright 2001, John Wiley & Sons. d) Anatomy of a chromatophore. Adapted with permission.[240] Copyright 1968, Springer-Verlag. e) High-refractive-index protein platelets within an iridophore forming a Bragg reflector. Scale bar is 500 nm. Reproduced with permission.[241] Copyright 1990, Springer International Publishing AG. f) Tomographic reconstruction of a leucophore from 3D electron microscopy, visualizing the strongly scattering leucosomes. Leucophore dimensions: $55 \times 20 \times 15$ µm. The inset shows a SEM of the spherical leucosomes. Scale bar is 1 µm. Reproduced with permission.[237] Copyright 2013, Wiley-VCH.

Leucophores have been studied in great detail in cuttlefish and other squid species.[237,238] Furthermore, the longfin inshore squid's chromatophores might even function as a system of distributed light detectors providing the organism with information about its environment needed for adapting in its skin coloration and patterns.[239]

The unique ability of cephalopods to control their coloration has inspired the creation of various synthetic photonic systems that emulate features of the biological system to a varying degree, partly even exploiting the reflectin proteins involved in forming cephalopods' photonic architectures.[231–234] Examples are discussed in more detail below. A recent review compared cephalopods' photonic elements to electronic adaptive coloration systems.[242] Importantly, this review emphasizes mutual benefits for biologists, material scientists, and engineers interested in optical materials. An understanding of biological light manipulation strategies can help to advance technology, while the implementation of the thorough standards and metrics from optical engineering in investigations of biological optical materials can impart a deeper insight into biological photonic systems. This synergy is a fundamental underpinning of the efforts in the field of biological and bioinspired photonics.

In the following paragraphs, let us first provide our definition of the term "bioinspired photonics" as used in this review, before advancing to a discussion of the benefits of this approach, enriched with examples of bioinspired optical materials that capture versatile aspects of biological light manipulation. Throughout the discussion of bioinspired photonics, we aim to stress the relevance of soft materials and the link and synergy with the field of soft nanophotonics.

3.2. Bioinspired Photonics: Definition and Benefits

The term "bioinspired photonics" encompasses a set of strategies for the design, material configuration, and manufacturing of photonic components based on the understanding of unparalleled and desirable biological light manipulation concepts. Many approaches for the realization of photonic elements with unique designs, material compositions, and function can be identified by taking a careful look at nature's light manipulation strategies.[135–142]

In essence, light manipulation strategies in nature are concerned with reflecting, redistributing, or absorbing parts or all of the UV, visible, and IR light spectra. For these purposes, a great variety of material architectures combining functional features on the molecular scale with nano-, micro-, and even macroscale structures have evolved independently in a wide variety of nonrelated animal and plant species (**Figure 15**).[243–254] These structures not only are frequently formed from soft organic materials (**Figure 16**),[241,255–259] but also have been observed to involve the use of minerals or hybrid organic–inorganic

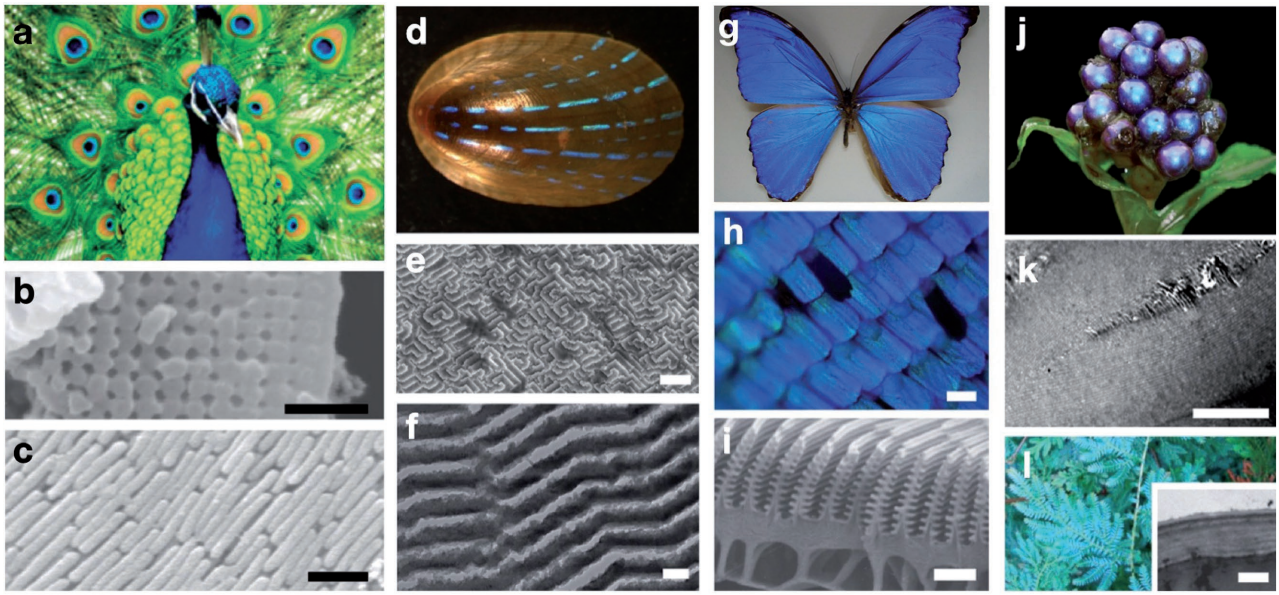

Figure 15. Photonic structures in fauna and flora. a) The peacock's brilliant feathers. Reproduced with permission.[275] Copyright 2011, American Chemical Society. b) Scanning electron microscopy image cross section of a peacock's green feather barbule revealing a 2D photonic crystal of melanine granules. c) Top view of the granules after removal of the surface keratin layer of a green barbule. Scale bars are 500 nm. b,c) Reproduced with permission.[276] Copyright 2003, National Academy of Sciences. d) Shell of the blue-rayed limpet. e) Top view of lamellar calcite structures in the area of the blue stripes. Scale bar is 2 µm. f) Cross section of the lamellar architecture revealing a multilayered reflector with gap spacing and calcite lamella thickness tuned to reflect blue light. Scale bar is 200 nm. d–f) Reproduced with permission.[261] Copyright 2015, Nature Publishing Group. g) *Morpho* butterfly. h) Optical image of the blue scales of a *Morpho menelaus*. Scale bar is 100 µm. i) Cross section through a single scale revealing the regular architecture on each scale ridge that is responsible for the blue color. Scale bar is 1 µm. Reproduced with permission.[277] Copyright 2006, Royal Society Publishing. j) Fruits of the tropical plant *Pollia condensata*. k) Cross section of cells in the fruits' exterior layers showing a regular cellulose architecture. Scale bar is 5 µm. j,k) Reproduced with permission.[278] Copyright 2012, National Academy of Sciences. l) Blue leaves of *Selaginella willdenowii*. The inset shows the layered structure in the leaves' cuticle that causes the blue color. Scale bar is 500 nm. Reproduced with permission.[254] Copyright 2010, The Royal Society.

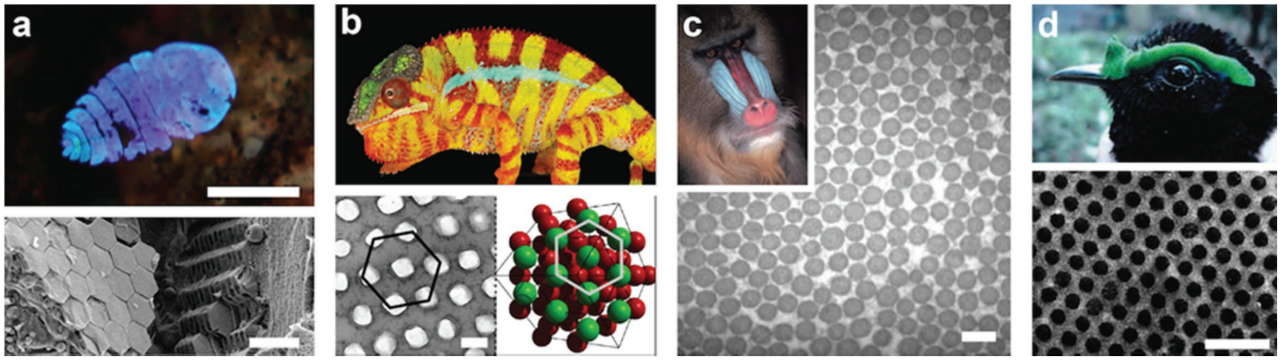

Figure 16. Photonic structures in soft tissues. a) A copepod showing iridescent colors that originate from regularly packed hexagonal guanine platelets. Scale bars are ≈500 µm (top panel) and 2 µm (bottom panel). Reproduced with permission.[259] Copyright 2015, American Chemical Society. b) The panther chameleon's coloration results from a regular arrangement of guanine crystals, of which a scanning electron microscopy cross section (scale bar is 200 nm) and a 3D reconstruction are shown. Color change is achieved by changing the spacing between guanine crystallites in the 3D photonic crystal. Reproduced with permission.[257] Copyright 2015, Nature Publishing Group. c) The blue facial coloration of male mandrills results from a disordered 2D photonic structure of collagen fibrils within the skin. Scale bar is 250 nm. Reproduced with permission.[256] Copyright 2004, The Company of Biologists. d) The green coloration of the bird *Philepitta castanea* originates from a regular arrangement of collagen fibrils shown in cross section in the bottom image. Scale bar is 500 nm. Reproduced with permission.[255] Copyright 2003, The Company of Biologists.

material composites.[260–262] Biological photonic structures enable organisms to display vivid structural coloration for intraspecific communication, including agonistic interactions, advertising sexual attractiveness, or for interspecies interactions, such as aposematic warning signals.[263,264] Photonic structures are also involved in camouflage,[132,265–268] enhanced light collection for photosynthetic processes,[269,270] radiation protection and thermal management.[271–273] In addition, they have been reported to enhance light emission in bioluminescent species.[274]

Recent research efforts suggest that the most inspiring materials science accomplishments of organisms that employ photonic systems are

1) The implementation of optical components from functional, responsive, durable, soft materials;[235,257]
2) The handling of a limited material variety for creating a large diversity of hierarchical, length-scale-bridging micro- and nanoarchitectures;[246,251,253,279]
3) The integration of soft and hard constituents in functional composites;[260,280]
4) The integration of multiple functions into one system;[262,281,282] and
5) The dynamic control of the system's optical properties (**Figure 17**).[143,235,257,283–285]

It is precisely for these reasons—in addition to the pure curiosity of scientists with regard to the wonderfully dazzling color displays of nature—that over the last two decades many scientists across disciplines have been compelled to study the underpinnings of biological photonics, benefiting in their efforts from the availability of rapidly advancing analysis tools.[252,286] Beyond the mere prospecting for blue-prints of useful artificial photonic structures, the study of nature's light manipulation approaches can provide us with a more refined understanding of the interplay of material composition and morphology, the basics of length scale bridging structure formation control, and the synergistic integration of function and co-optimization constraints when aiming to satisfy different functional requirements simultaneously.

A wealth of reviews assess the progress in bioinspired materials[282,287–292] and bioinspired photonics in partic ular.[135–138,140–143,293–295] As the field continues to evolve vibrantly, this section of the present review is aimed at providing an overview of recent insights and achievements, while also putting emphasis on presenting a perspective and an evaluation of recent developments and their benefits for future progress.

The potential of utilizing inspiration from biological photonic systems for the realization of novel optical technologies is assessed with respect to four important criteria, where insights from natural light manipulation strategies can be pivotal:

1) The dynamic nature and functionality of bioinspired photonic materials and devices;
2) The morphologies and structural designs that impart desirable functionality;
3) The material composition; and
4) The process by which the material or device is formed.

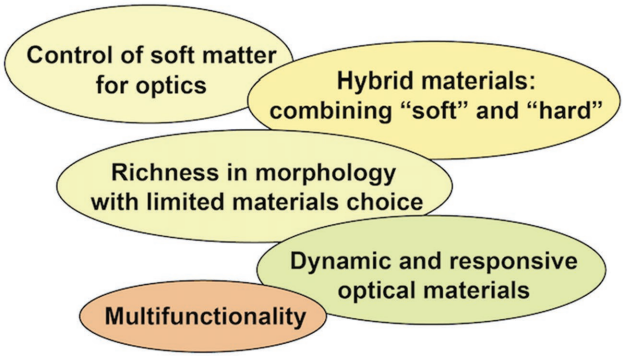

Figure 17. Materials science accomplishments of organisms relevant to optical design.

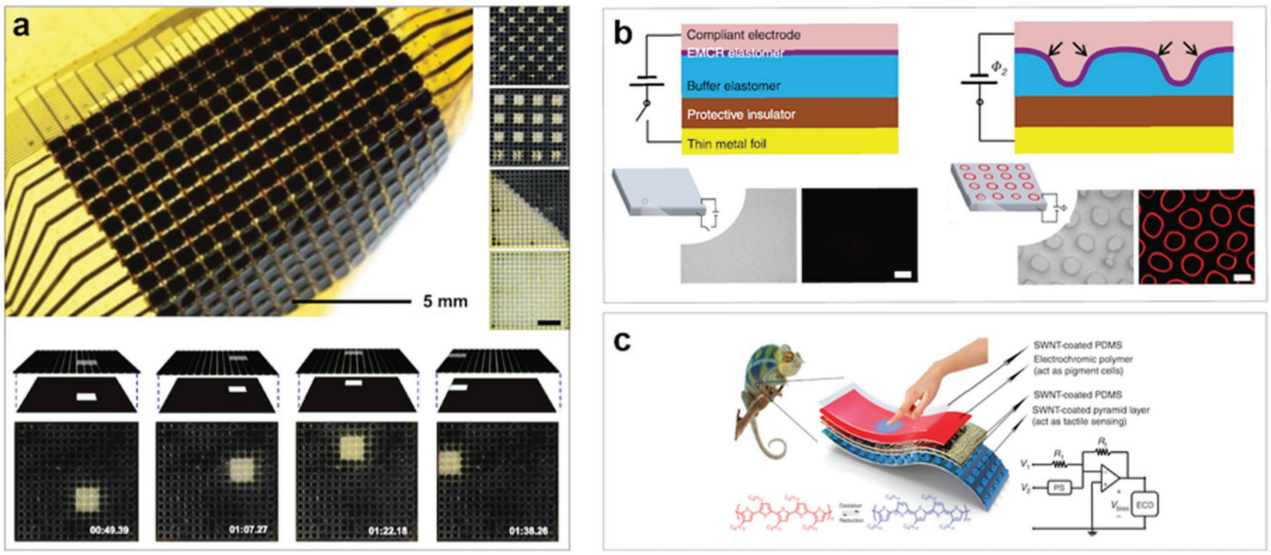

Figure 18. Synthetic materials and devices that emulate the dynamic color of cephalopods and chameleons. a) Image of a flexible device that mimics the interplay of chromatophores and leucophores in cephalopod skin. Top right side: the device displaying different static contrast patterns. Bottom row of images: the device is capable of autonomic, dynamic, adaptive pattern matching to a continuously changing background. Scale bars are 5 mm. Reproduced with permission.[233] Copyright 2014, National Academy of Sciences. b) Actuation of electro-mechanochemically responsive elastomer films that contain spiropyran mechanophores, which change color and emit strong fluorescent signals under mechanical stress. Electric fields can be used to switch the films on-demand between a nondeformed, nonfluorescent state and a deformed, fluorescent configuration. Scale bars are 250 µm. Reproduced with permission.[234] Copyright 2014, Nature Publishing Group. c) All-solution-processed, chameleon-inspired, stretchable electronic skin, consisting of elastic pyramidal-microstructured polydimethylsiloxane surfaces with a layer of spray-coated single-wall carbon nanotubes and electrochromic polymer, poly(3-hexylthiophene-2,5-diyl). Reproduced with permission.[299] Copyright 2015, Nature Publishing Group.

3.3. Dynamic Bioinspired Photonic Systems: Design Concepts and Applications

Let us start with taking a closer look at the dynamic coloration of cephalopods. The unparalleled control of absorption, reflection, and scattering of light on the cellular level, which earned this class of mollusks world fame as "kings of camouflage,"[296] has inspired scientists across disciplines to create photonic systems with unprecedented functionality. Cephalopods are masters of the creation, control, and application of functional, stimuli-responsive, soft materials for environmental sensing, adaptive color, and skin texture variation. A comprehensive investigation of cephalopod skin morphology, the working principles of individual optical components, and their functional purpose conducted by several research groups around the world has laid the foundation for collaborative efforts of engineers, biologists, material scientists, chemists, and biologists aimed at creating artificial materials that match or even exceed the performance characteristics of cephalopod skin.[297] The three overarching functional optical elements in cephalopod skin responsible for the creation of color are chromatophores—stretchable cells with dense internal pigmentation that can be extended to achieve a 500% change in chromatophore surface area during actuation (Figure 14d),[240,298] iridophores—cells that contain layered protein stacks acting as iridescent Bragg reflectors (Figure 14e),[241] and leucophores—cells that are densely packed with randomly organized scattering spherical leucosomes that provide a white backdrop (Figure 14f).[237]

The interplay of chromatophores and leucophores has been captured convincingly in an artificial material recently developed in a collaborative effort between biologists and material scientists.[233] The reported system—current prototypes are up to 2 cm^2 in size—combines the artificial equivalent of switchable chromatophores and leucophores on a flexible, layered, optoelectronic sheet design (**Figure 18**a). Like the skin of cephalopods, this artificial system also contains photosensing elements, which provide information about the illumination environment. Endowed with this sensing ability, the artificial system can autonomously create black-and-white patterns that match its surroundings. In its flexibility, ability to adaptively alter the displayed patterns and switching speed, it matches the functionality of cephalopod skin and captures a large part of its morphological architecture. While it is obviously formed from different materials using processes that nature does generally not have access to, its anticipated application in adaptive camouflage systems is identical to the purpose for which the natural system has evolved to its current state of optimization in cephalopods.

Another notable attempt to capture some of the key features of adaptive coloration in cephalopods consists of utilizing electro-mechanochemically responsive elastomers for on-demand fluorescent patterning (Figure 18b).[234] While unlike most cephalopods, this artificial system utilizes fluorescence as the main optical signature, it relies on the exploitation of large deformations in soft, responsive materials to actuate spiropyran mechanophores, and—to some extend like cephalopods[300]—is stimulated electrically. This study provides an example of implementing the essentials of an interesting natural light manipulation concept into an artificial bioinspired material, using libraries of well-developed constituents, combined with standard synthesis and fabrication approaches.

In a different study, inspired by the working principles and function of cephalopod iridophores, electrochemically tunable multilayered reflectors were fabricated from lamella-forming diblock copolymers.[301] The block copolymer consists of a hydrogel domain and a glass-forming block, which assemble into a periodic multilayered morphology. This material was used to form electrically controlled full color pixels that could be tuned throughout the whole visible spectrum. In general, the formation of specific material structures through the control of self-assembly processes by chemically programing a material's molecular components represents an enticing approach that likely will play a role in generating bioinspired optical materials with industrial throughput.

On terrestrial grounds, some chameleon species are rivaling cephalopods' ability to change color, with possibly even stronger contrasts in hue and reflection intensity.[257] Chameleons' adaptive coloration relies on the integration of guanine-based photonic crystals in the organism's skin localized in different types of iridophores, affording the animal with the ability to efficiently camouflage, to put on spectacular displays, and to potentially even ensure passive thermal shielding. This mechanism takes place in addition to the dispersion and aggregation of pigments in chromatophores. The latter effect combined with the chameleon skin's intrinsic deformability has been mimicked in chameleon-inspired stretchable electronic skin that can be induced to change color triggered by tactile cues (Figure 18c).[299] This approach involves the controlled spatial arrangement of single-walled carbon nanotubes on microstructured polydimethylsiloxane surfaces to form patterned electrodes. Compression of the structure results in a change in resistance and a current flow between the electrodes, inducing the variation of color of an integrated organic, electrochromic material. While using a very different set of materials and formation processes, the stretchable electronic skin mimics the mechanical properties and the color change of chameleons and lends itself to a wide variety of applications beyond camouflage and display technology.

Inspired by the iridescent nanostructures and graded surface chemistry found on the wing scales of *Morpho* butterflies,[302] a team of researchers has developed vapor sensor arrays based on a hierarchical photonic design (**Figure 19**).[303] These bio-derived and bioinspired sensing devices are responsive to a range of solvent vapors in pristine environments and can also quantify these vapors in mixtures under variable moisture conditions. The sensors rely on the colorimetric detection of spectral variations in detected light due to diffraction, interference, and absorption within the nanostructures. The detected signal is affected by changes in the gas phase surrounding the sensing structures, which optically amplify minute changes in the chemical environment. In an array of sensors, the spectral response of each element can be locally modulated, by adjusting refractive index and optical extinction in the structure, allowing for multivariable sensing in order to enhance vapor sensitivity and selectivity. Current developments suggest, that these bioinspired sensing structures are on the way to outperform conventional sensor arrays.[303]

The examples discussed above largely signify how underlying optical concepts, and—with some level of abstraction—control strategies and material properties are translated from biological role models to artificial counterparts in order to create similar or extended dynamic behavior and functionality. While our current abilities to form dynamic programmable photonic materials do not yet parallel all the sophistication, functionality, and control of the photonic architectures in the skins of

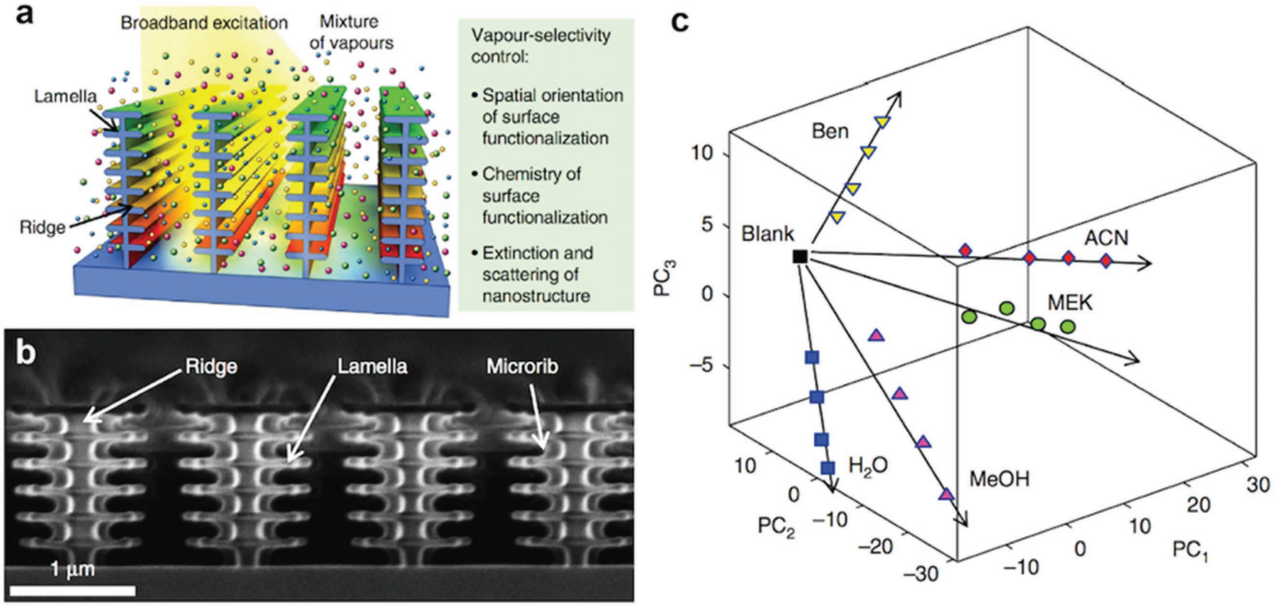

Figure 19. Vapor sensing using bioinspired photonic nanostructures. a) Schematics of the bioinspired nanostructure (emulating features found in the wing scales of *Morpho* butterflies) interacting with a vapor mixture under broadband excitation including factors that influence vapor selectivity. b) Scanning electron microscopy image of the vapor-sensing nanostructure. Scale bar is 1 µm. c) Principal component diagram visualizing the device's capability to distinguish vapors of benzene (Ben), acetonitrile (ACN), methyl ethyl ketone (MEK), methanol (MeOH), and water (H_2O). a–c) Reproduced with permission.[303] Copyright 2015, Nature Publishing Group.

cephalopods and chameleons, or the wing scales of butterflies, we are making big strides in that direction. Undoubtedly, photonic elements exploiting the favorable properties of soft materials will play a decisive role in achieving this goal.

Efforts aimed at conceiving soft, bioinspired photonic materials benefit from a wealth of investigations that focus specifically on the realization of biological structural architectures in man-made materials, the implementation of formation approaches that emulate natural processes, and the exploitation of biological materials for the formation of functional photonic elements. A representative choice of recent achievements that focus on these aspects in particular and therefore define promising avenues for the utilization of soft matter in bioinspired photonics is discussed below.

3.4. Morphologies in Bioinspired Photonic Systems

The palette of materials that humans use generally far outcompetes the selection of materials that other organisms have to content.[241] However, the structural complexity across length scales from the molecular to the macroscopic scales that organisms impose on their materials is, with few exceptions, unparalleled by humans (**Figure 20**). Here, we can learn a great deal. Once the choice of constituent components is made, the control of morphology from the molecular to the macroscopic scale can dramatically affect a material's performance characteristics and functional significance. Structural design can push the envelope of a specific material property; while a solid slap of cuticle provides a rather dull sight, the same material imbibed with tailored nano- and microscale structures acting in concert can have an incredibly colorful appearance as evident in the scales of the sunset moth or *Eupholus* beetles.[304,305] Prevalent in the field of bioinspired photonics is the desire to replicate such optically functional material morphologies. Beyond novel photonic devices, the ability to control material morphology across length scales would afford us with tremendous opportunities in other fields of materials science and engineering.

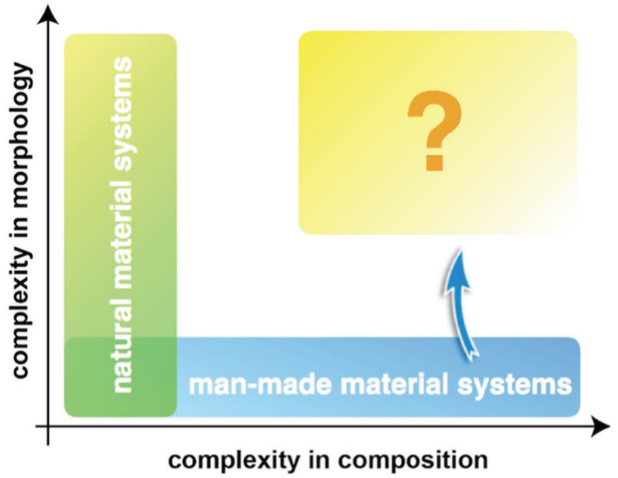

Figure 20. Complexity in composition and morphology in biological and in human-made functional materials and devices. Humans exploit a vast palette of elements to control material properties primarily by composition, while biology utilizes a reduced set of components but has great control over material morphology across all length scales.

Many microfabrication, templating, and replication approaches for the realization of bioinspired materials that either closely mimic morphologies found in butterflies and beetles or that realize the underlying essential light manipulation concepts using hard inorganic materials have been reported.[306–312] This review is focused on the intersection of soft and bioinspired photonics, so these achievements will not be extensively discussed here.

Many different approaches have been reported for the formation of bioinspired multilayered assemblies. These materials emulate the architectures found in many biological photonic systems, such as the cuticles of tortoise and jewel beetles, and the scales of butterflies and moths.[283,304,313,314] They are often called 1D photonic crystals, and can dynamically respond to a broad variety of stimuli, provided they are formed from stimuli-responsive constituents. Most responsive multilayered systems incorporate soft, deformable materials that are sensitive to the presence of water vapors, solvents, changes in pH, or material chemistry, pressure and strain, or electric/magnetic fields.[301,315,316]

Surface bound 2D photonic morphologies, such as the nanoscopic protrusions on insect eyes and wings that function as antireflection coatings,[268,317] the diffraction patterns on curved surfaces, found, for example, on the setae of the sea mouse,[318] and the wing scales of butterflies[319] have been mimicked in many different variants.[320–322] Structures on the back of the fog-collecting Namib desert beetle provided inspiration for the design of a photonic-crystal microchip for ultratrace chemical detection in highly dilute solutions.[323] The chip that is produced by inkjet printing of colloidal particles onto flexible substrates combines fluorescent signal enhancement with analyte enrichment based on tailoring the device's surface energy. The device showed very low detection limits (10^{-16} mol L^{-1}) for trace amounts of cocaine.

A rich variety of 3D material morphologies for the manipulation of light has evolved in natural organisms ranging from opal structures to gyroid morphologies.[324,325] These structures have been at the center of interest of many efforts aimed at creating dynamic bioinspired photonic materials.[93,101,102,326,327] Advantages of 3D photonic architectures include their dynamic response to a variety of different stimuli[100] and the existence of a rich variety of fabrication protocols that rely on combinations of controlled self-assembly[94] with other patterning techniques[104,328] to create specific hierarchical architectures (**Figure 21**).

While a rich variety of structural color materials in nature—found in the wing cases of beetles, the skin of fruits, and the scales of butterflies—are highly ordered, many birds owe their bright feather colors to disordered optically heterogeneous nanostructures with refractive index variations on a characteristic length scale.[95] These materials, which only possess short-range order across a length scale comparable to optical wavelengths, provide isotropic color and suppress iridescence. Recent investigations have specifically focused on the role of structural regularity and irregularity in biological architectures[279,305] and its translation into artificial systems (Figure 21d,f,g).[96,332,329] In nature, the concept of isotropic

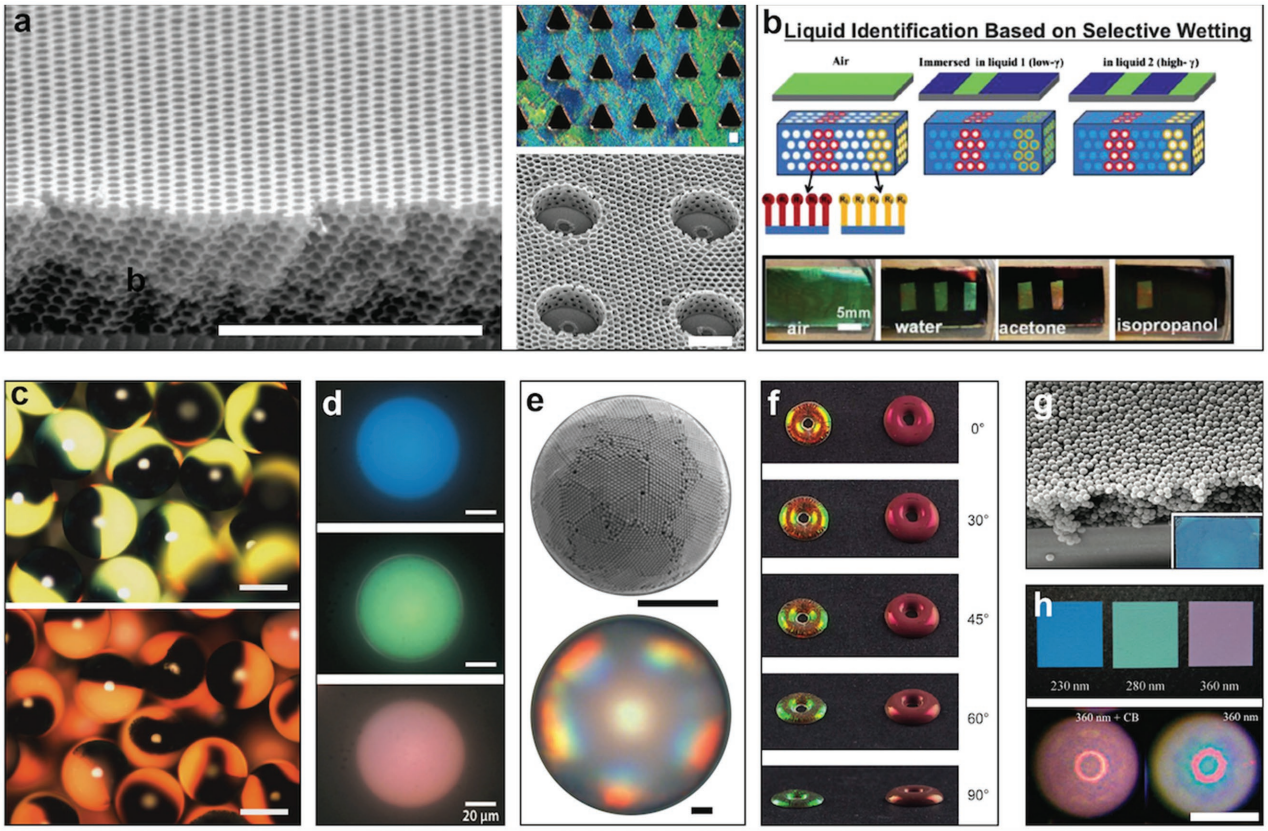

Figure 21. 3D photonic structures resulting from directed and confined self-assembly. a) Scanning electron microscopy images and optical image of inverse opal and direct opal structures co-assembled on flat and patterned substrates. Scale bars are 5 μm. Reproduced with permission.[94] Copyright 2010, National Academy of Sciences. Reproduced with permission.[98] Copyright 2017, The Optical Society. b) Chemically patterned inverse opals can be used to identify different liquids (including water, acetone, and isopropanol) based on their selective wetting behavior. Reproduced with permission.[100] Copyright 2013, Royal Society of Chemistry. c) Electroresponsive photonic Janus particles fabricated from 182 nm (top) and 198 nm (bottom) silica particles by optofluidic synthesis. Scale bars are 200 μm. Reproduced with permission.[93] Copyright 2008, Wiley-VCH. d) Blue, green, and red photonic microcapsules consisting of dense amorphous packings of core–shell particles of different shell thicknesses. Scale bars are 20 μm. Reproduced with permission.[101] Copyright 2014, Wiley-VCH. e) Scanning electron microscopy and optical images of photonic balls produced from 400 nm colloids using microfluidics. Scale bars are 10 μm. Reproduced with permission.[102] Copyright 2015, National Academy of Sciences. f) Biomimetic structural color pellets with iridescent and noniridescent hues seen at different angles. Reproduced with permission.[329] Copyright 2016, Nature Publishing Group. g) Scanning electron microscopy image of a film of disordered 226 and 271 nm polystyrene (PS) spheres spin-cast onto a glass coverslip. Reproduced with permission.[96] Copyright 2010, Wiley-VCH. The inset shows a photograph of the disordered colloidal film. h) Top: Variously colored membranes composed of silica particles and carbon black. Reproduced with permission.[330] Copyright 2013, Wiley-VCH. Bottom: Structurally colored photonic microparticles composed of black and white (left) and only white (right) colloids. Scale bar is 100 μm. Reproduced with permission.[331] Copyright 2013, Nature Publishing Group.

photonic materials culminates in the formation of brilliant white surfaces if the last constraint—the presence of a short-range order comparable to optical wavelengths between optical heterogeneities—is relaxed. A well-studied example is the *Cyphochilus* beetle. Its bright white color is generated by small scales that cover its body and contain a disordered filamentary network of cuticle, which causes strong, random, multiple scattering of light.[333–335] This approach is highly efficient—even if the scattering structure is only a couple of micrometers thick—beating any whiteness-enhancing coating currently used by the paper industry. Other concepts for the creation of white rely on disordered colloidal or multilayered architectures found, for instance, in the leucophores of cuttlefish and squid,[237,238] or the creation of white through mixing different structural colors as observed in white giant clams.[336]

In nature, strong blacks, which are used to provide spatial contrast or absorb undesirable spectral components in conjunction with a spectrally filtering photonic structure, are achieved by the interplay of scattering and light confining structures with pigmentation.[337] Scattering confines light within an absorbing medium by increasing its path length leading to a more pronounced light absorption by appropriately distributed absorbing elements. The importance of the interplay of structural color and absorption is evident in the example of the Steller's jay, where the missing pigmentation in an albino has drastic consequences on the appearance of the usually strongly saturated blue hues of the birds.[338] Interestingly, the interplay of white and black can lead to coloration, as has been recently shown in a series of articles (Figure 21g,h).[330,331]

Another rich source for inspiration is nature's ability to produce light. Fireflies are known for their ability to put on

nighttime displays of dazzling color with different spectra and time-pattern of light flashing. The production of light in internal compartments in the organisms' abdomen also necessitates good strategies to couple the light out. Recently it has been shown that fireflies use specialized, hierarchical surface patterns that improve light extraction efficiency from the high refractive index of the firefly lantern into air.[339] These structures have been mimicked in artificial systems in order to improve the light extraction efficiency of light-emitting diodes.[339]

Biological photosynthesis, the conversion of photons into chemical potentials for the formation of sugars and biomass, has long captured the interest of scientists. The molecular structure of the light-harvesting elements is often a crucial factor in the efficiency of light capture.[340] For instance, the light-harvesting antenna complexes in purple photosynthetic bacteria rely on highly symmetric wheel-like supramolecular architectures involving bacteriochlorophyll pigments.[341]

These structures incorporate a great number of chromophore units thereby achieving large absorption cross sections. They play an essential role in light capture and conversion. An understanding of these structural features allows chemists to design artificial light-harvesting antenna that form the basis for more efficient molecular electronics and photonics that can improve performance of photovoltaic cells, field-effect transistors, and light-emitting devices. Very recent research that focused on the epidermal, blue iridescent chloroplasts of shade-dwelling *Begonia* species showed that the plants within their chloroplasts exploit a photonic crystal structure formed from a periodic arrangement of the light-absorbing thylakoid tissue.[270] This increases photosynthetic efficiency by increasing light capture at the predominantly green wavelengths available in shade conditions, and by directly enhancing quantum yield by 5–10% under low-light conditions. The photonic structures in the chloroplasts enable a complex interplay between control of light propagation, light capture, and photochemistry and could provide inspiration for the design of advanced artificial solar energy capture systems.

3.5. Material Systems in Bioinspired Photonics

The choice of the constituent material components, in principle, roughly defines many of the system's base properties, such as the mechanical characteristics or the interfacial interaction with liquids and gases. For instance, a mineralized shell with calcite as the major constituent that provides fracture toughness and impact strength will likely not support the extreme deformation ranges known from soft tissue, such as cephalopod skin, no matter how complex the micro- and nanostructuring is. In turn, such soft tissues, which show an intriguing complexity of integrated dynamic optical components, are not known for the highest mechanical strength.

Control of structural integration of soft with hard materials can also simultaneously ensure a range of different functions. For some mollusks templating with soft materials appears to provide the organism with the ability to impose organic forms and curvature with optical functionality on a hard calcite shell made from calcite,[261] a material that is notoriously hard to pattern in synthetic approaches. The presence of the soft material phase in biomineralized shells improves their mechanical properties.[281,342] The design concepts underlying biomineralized photonic materials have recently been implemented in free-standing strong, transparent, layered organic–inorganic hybrid films that are reinforced with layered double hydroxide micro- and nanoplatelets (**Figure 22**a).[343] The films are fabricated through layer-by-layer assembly with a variety of colors, and they show tensile strength surpassing the strength of natural nacre. An insightful review on the role of soft organic materials in templating hard materials to create optical systems and structures with other functional purposes was recently published by Dunlop and Fratzl.[280]

Frequently, materials' unique molecular properties are key to the structure formation process. The photonic structures found in tropical fruits, such as *Pollia condensata*[278] or *Margaritaria nobilis*,[76,346] are composed majorly of cellulose. Cellulose, earth's most abundant biopolymer, known to consist of nanocrystals, can assemble in helicoidal patterns.[347] In the fruits, these patterns form with a periodicity on the order of 200 nm, leading to the fruits' strong, structural color-based blue reflections. A change in pitch, achieved, for instance, by swelling a fruit in water leads to a shift of the observed color to higher wavelengths. Recent work, aimed at exploiting cellulose—a very abundant and industrially relevant material—for the formation of artificial photonic elements, shows that films with structures and optical properties that match the fruits' performance can be assembled in vitro. Using controlled, bioinspired self-assembly processes, Vignolini and co-workers assembled cellulose-based chiral reflectors (Figure 22b).[344,348,349] Understanding and controlling distinctly different phases of film formation, the researchers were capable of tuning the resulting morphology and optical appearance of the chiral cellulose reflectors. This work shows tremendous promise for the exploitation of natural materials in structure formation analogous to the processes leading to biological functional systems.

Another biomaterial with a uniquely broad range of interesting mechanical, chemical, and optical properties is silk. Silk is produced by silk worms to form bright white cocoons and by spiders to form webs. Silk exists in different variants with distinct mechanical, chemical, and optical properties,[350] which make this material very interesting for the design of optical devices. A broad range of silk-based optical systems have recently been demonstrated,[351,352] including silk optical fibers,[353] superlenses,[354] and immunosensors.[355] Silk as a material for soft, bioinspired photonic systems appears to have a promising future for the design of 21st century optical devices.

Recently, the principles underlying adaptive coloration of cephalopods have been utilized to produce biomimetic infrared camouflage coatings on transparent and flexible adhesive substrates, using protein structures found in cephalopod skin. Reflectin proteins, isolated from cephalopods for the use of bioinspired optical materials for the first time in 2007,[231] were used to form thin, strain responsive films that adapt their reflection spectrum in response to an applied strain (Figure 22c).[232,345] These films can be utilized to disguise common objects with varied roughness and geometries from infrared visualization (Figure 22d). The morphology employed

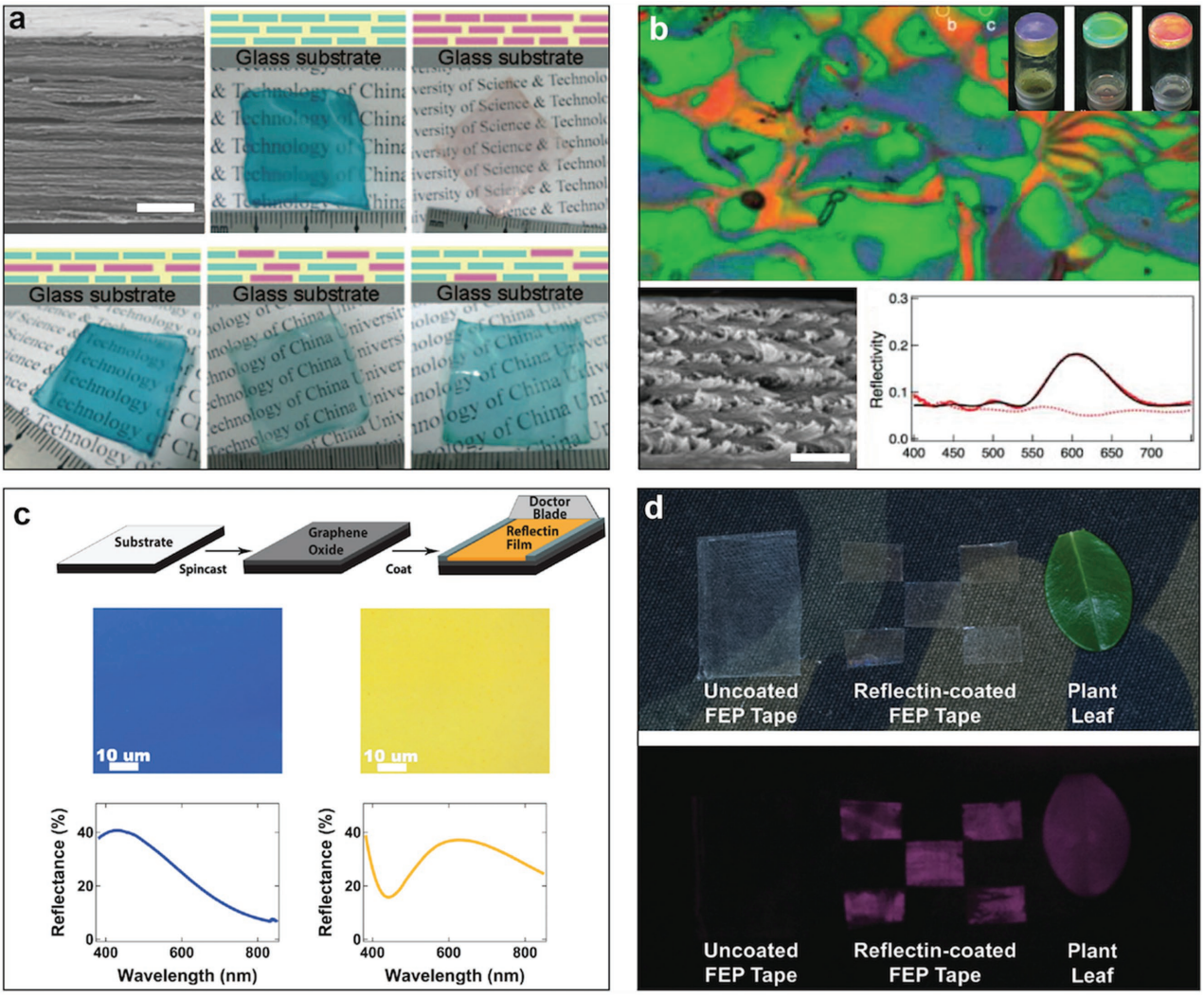

Figure 22. Biologically derived materials for optical devices. a) Structurally colored, partially transparent chitosan composite films. The top-left scanning electron microscopy image shows the layered architecture in the co-assembled 2D structure of a Cu–NO_3/Co–Al–CO_3–chitosan hybrid film. All other images show films of varying compositions. Scale bar is 5 µm. Reproduced with permission.[343] Copyright 2010, Wiley-VCH. b) A helicoidal cellulose nanocrystal film seen in a polarization microscope to reflect left-handed circularly polarized light. Differently colored domains correspond to variation in the pitch of the helical nanocrystal structure. Domain size varies between 2 and 20 µm. A cross section through a red domain is shown in the scanning electron microscopy image (scale bar is 500 nm) on the bottom left, and its reflection spectra are seen on the right. Reproduced with permission.[344] Copyright 2014, American Chemical Society. c) Thin film optical devices formed from graphene oxide and the cephalopod protein Reflectin (RfA1). Images and reflection spectra are shown for films with thicknesses of 125 and 207 nm. Reproduced with permission.[232] Copyright 2013, Wiley-VCH. d) Images acquired with a normal camera (top) and an infrared camera (bottom) from uncoated fluorinated ethylene propylene (FEP) tape (left), reflectin-coated FEP tape squares (middle), and a plant leaf (right). The reflectin coating allows us to modify the tapes' optical appearance in the infrared to produce easily deployable, disposable coatings that match the infrared signature of plant leafs, and therefore could provide benefits in camouflage applications. Reproduced with permission.[345] Copyright 2015, Royal Society of Chemistry.

in this approach is intriguingly simple and only remotely similar to the features found in cephalopods. However, the use of reflectin protein extracted from cephalopods to enable infrared camouflage represents an intriguing demonstration of the benefits of gaining inspiration from nature for material systems and for the realization of function in artificial materials that go beyond the intrinsic biological purpose.

Research on the structural color of avian species, in addition to insights gained from studying the structural coloration of many insects, has stressed the importance of pigmentation located beneath, adjacent or within photonic structures.[261,337,356,357] For the most part, bright and intense coloration in the animal kingdom results from a finely tuned interplay between material structures that induce light scattering, interference, or diffraction and well-positioned pigment containers that provide spectrally selective or broadband absorption. The role of pigmentation is especially evident from a recent investigation of the blue color of the Steller's jay, where the coloration of an albino individual of the species, lacking melanin pigmentation, was compared to a bird without pigment deficiency.[338] While the feather-internal morphology of the albino is identical to that of the other bird, the

complete lack of pigment resulted in a very different appearance of the albino. It completely lacked the saturated blue hues and only showed a slight metallic blue shimmer on a white backdrop in its feathers. In addition to changing the spectral composition, pigmentation can alter other characteristics of a photonic structure, such as the angle dependency of structural coloration. This has been shown for papilionid butterflies of the *Nireus* group.[358] In the scales of these organisms, the presence of pigment suppresses iridescence ensuring an angle- and polarization-independent blue–green wing coloration. The concept of inclusion of pigmentation in photonic architectures has been employed to enhance color contrast in ordered, dynamic opal materials produced by extrusion, where small amounts of carbon black significantly enhance color saturation.[359] It also found use in disordered colloidal photonic arrangements fabricated by spraying, where inclusion of a small amount of absorbing colloids allowed for the creation of isotropic coloration[330,331] and, in colloidal crystal particles, enriched with spectrally selective absorbers (Figure 21c,f,h).[101,102]

3.6. Processing and Manufacturing Approaches

Current difficulties in matching the structural complexity of natural materials in synthetic systems might partly be found in the stark differences between the processes applied by organisms and by humans. Processing approaches determine whether a desired morphology can be imposed on a constituent material. Processing conditions naturally also have a strong effect on the material characteristics imparted by the bulk material. Humans produce functional materials in a very different way from nature. Often, we rely on high-temperature approaches, while in nature most material formation processes occur at environmental temperatures. Reaction–diffusion processes,[360,361] self-assembly,[206] and complex biomechanical growth dynamics[362] appear to be the main routes underlying formation of complex material morphologies with optical function in nature. Proteins isolated from cephalopod iridophores form nanoparticles with β-sheet character,[363] which can be reversibly assembled by control of the proteins' net charge through phosphorylation and dephosphorylation achieved by controlling pH.[364,365] The protein nanoparticles form thin nanostructured, stimuli-responsive films with variable refractive index, reflectivity, and color,[231,364,366] and have been used to form coatings for infrared camouflage (Figure 22c,d).[232,345]

The blue and the green coloration in the feather and skins of many birds result from spongy keratin nanostructures with well-defined feature distance and varying degrees of order.[367] The feathers of the peacock owe their bright, iridescent coloration to an ordered 2D photonic crystal arrangement of melanin rods connected by keratin bridges,[276] while the blue noniridescent color of the Steller's jay and the kingfisher are the result of spongy amorphous keratin structures with a short-range order and narrow feature size distribution[338,368] with pigmentation also playing an important role, as discussed above. A prominent hypothesis for the formation of amorphous biophotonic nanostructures invokes the process of self-assembly due to the phase separation of immiscible biological material phases and kinetic arrest of the observed morphologies through vitrification or gelation of one or multiple phases.[206] The investigation of channel- or sphere-like spongy β-keratin nanostructures at the origin of bird feather color which appear to have formed during spinodal or binodal phase separation of β-keratin from other cytoplasmic components provides convincing evidence to support this hypothesis.

Processes that exploit self-assembly for the formation of photonic structures with varying degrees of disorder either by phase separation or by colloidal assembly have been receiving much attention in the scientific community.[40,369] For instance, reflectin proteins derived from the squid *D. (L.) pealeii* can be used to form films with stimuli-responsive optical properties by self-assembly. During film formation, the protein assembles into distinct, stimuli-responsive, nanoscale aggregate structures with an oblate geometry (**Figure 23**a). This structure can be slightly altered through exterior stimuli and is implied in the function of iridiphores in vivo and reflectin-based photonic structures in vitro.[365,366] Studied by many research groups, the assembly of colloidal particles in confined geometries, partially involving kinetic arrest of the forming morphologies, appears to bear many similarities with biological structure formation processes (Figure 23b).[104] Colloids assembling in the vicinity of regular microstructures will assume orientations and crystal configurations that are influenced by the presence of the confining surface yielding very specific patterns.[98] Assembly of colloids in microdroplets forms superstructures that vary depending on the droplet drying kinetics (Figure 21).[93,101,102] Crystalline colloidal structures can form throughout the particles, be only confined to the surface, or be completely absent in amorphous packing. Combined with exploiting surfaces with tailored wetting characteristics,[370] the droplet-based formation of colloidal architectures can lead to interesting applications in photonic and plasmonic sensing (Figure 23c,d).[371] A noteworthy example of the progress recently made in understanding the formation of intricate microscale morphologies is the work by Noorduin et al.[372] Using only inorganic components and intriguingly simple control mechanisms, the researchers were able to show that complex morphologies resembling the organic, sophisticated forms found so often in biology can result from very simple inorganic ingredients, provided the formation process is understood to the extent that all relevant parameters are controlled tightly (Figure 23e). This shows that, while the role of genes is, without doubt, crucial in providing this tight control, getting the physics, chemistry, and biomechanics right is likely of equal importance.

Biological formation processes and human approaches to material synthesis are subject to the same laws of physics. For the most part, human approaches to material synthesis are fundamentally different from the strategies of other biological organisms. While we rely on a much more developed library of material constituents and involve synthetic solvents and very high or low temperatures in our processes, organisms only master a much smaller choice of materials and have to comply with processes occurring mostly at ambient temperatures. Instead, organisms have managed to implement control instances on all relevant length scale and timescales, starting from genes that regulate time and space of material expression to cells that simultaneously form factory and compartment for the production and assembly of materials into functional

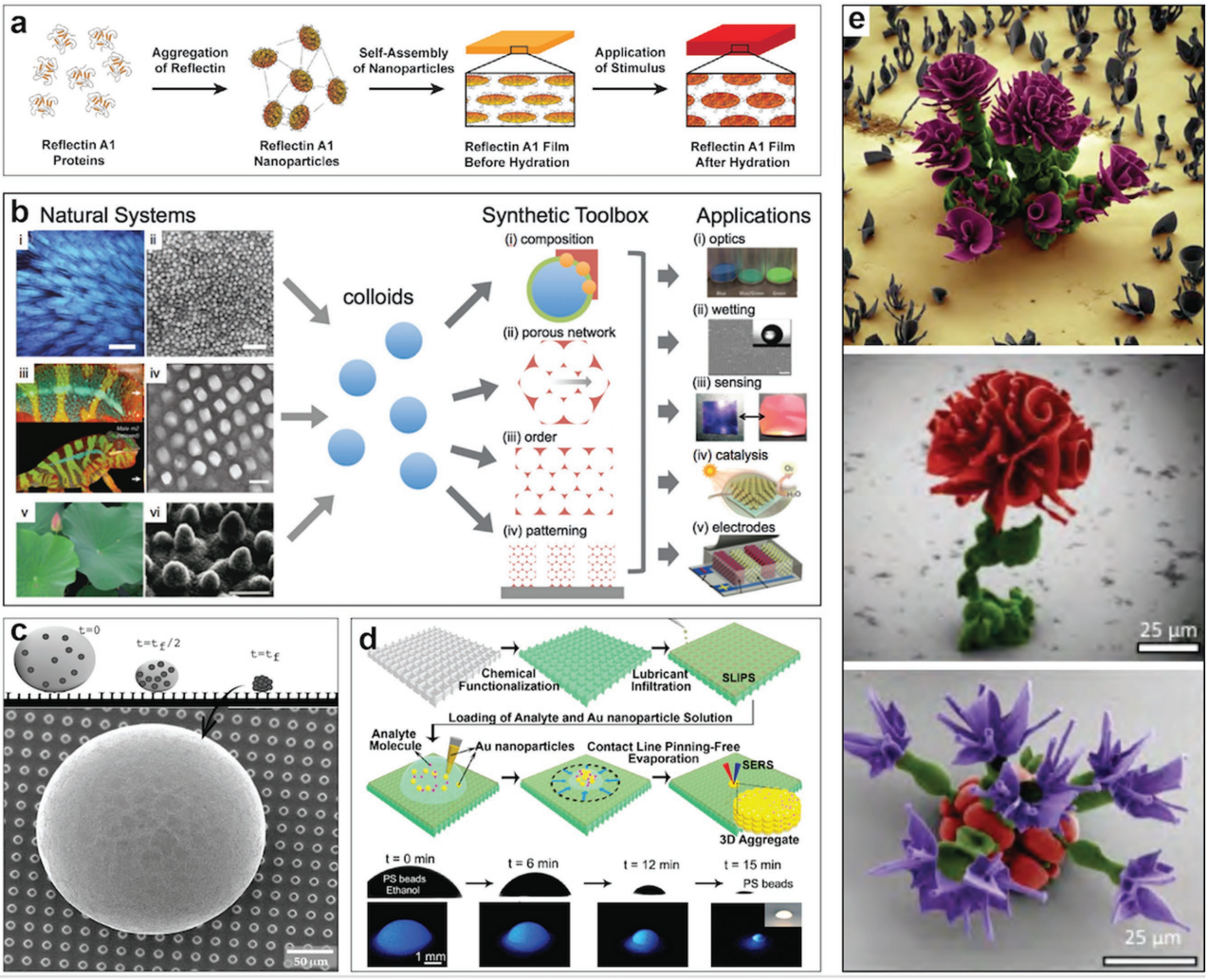

Figure 23. Self-assembly and controlled synthesis of functional and hierarchical complex structures. a) Schematic representing the self-assembly of reflectin proteins into nanoparticles and stimuli-responsive thin films. Reproduced with permission.[366] Copyright 2016, Wiley-VCH. b) Colloidal assembly in natural systems informs processes used in synthetic colloidal assembly strategies for functional materials and devices. Reproduced with permission.[104] Copyright 2016, Royal Society of Chemistry. c) Assembly of colloidal superstructures on superhydrophobic surfaces. Reproduced with permission.[370] Copyright 2012, National Academy of Sciences. d) One-step self-assembly of analyte molecules and gold nanoparticles on slippery liquid surfaces to enable high-resolution surface-enhanced Raman scattering analysis. Reproduced with permission.[371] Copyright 2017, National Academy of Sciences. e) Rational design of complex, hierarchical microarchitectures in processes that are comparable to biological growth phenomena. Artificial coloration in the scanning electron microscopy images indicates sequential growth steps. Top and middle: $BaCO_3/SiO_2$ coral (purple/red) grown on top of a $BaCO_3/SiO_2$ spiral (green); structures are altered by careful control of the growth conditions. Bottom: $SrCO_3/SiO_2$ (green) opened with CO_2 pulse (purple) ingrown in $BaCO_3/SiO_2$ (red). Reproduced with permission.[372] Copyright 2013, American Association for the Advancement of Science.

structures, while representing the building blocks for even more complex tissue superstructures. The key for this control of length scale bridging material structures and the control of the laws of chemistry and physics across all scales appear to be inscribed in the organisms' genetic material in ways that we are far from comprehending. The key to our ability to control structure formation with the same sophistication lies in understanding the interplay between genes and the boundary conditions imposed by chemistry and physics that enable the complex mechanisms, process pathways, and timescales observed in the development of biological functional materials. Due to their distinct morphologies, the narrow margin for variation permissible without compromising functionality and an extensive set of characterization knowledge, photonic structures can provide versatile model systems for studying biological structure formation processes. Recent work aimed at elucidating photonic structure formation in butterflies in situ shows great promise for revealing the processes underlying formation of functional biological micro- and nanoarchitectures.[362,373,374] Research aimed at modifying diatom growth and exploring diatoms' versatility in optical applications also is expected to provide significant insights and benefits for the development of optical technologies.[375–380] While learning about the processes governing biological material formation, we also can hope to glean useful insight into strategies for advancing synthetic manufacture of photonic materials. And while we are at

it, we might as well try to re-engineer some of the biological machinery to produce materials and structures of interest and gain more understanding of the underlying effects in the process of doing it.

4. Summary, Conclusions, and Outlook

Function and performance limits ultimately are a result of the interplay between the choice of material constituents, structural design, and processing history. Nature's optical materials have to realize a broad range of functions, such as enabling vision, creating conspicuous color displays, permitting efficient camouflage, ensuring thermal regulation abilities, enhancing light collection, and enabling light distribution management. In many applications, these functions are relevant to humans as well; however, we should not forget that biological solutions to one light manipulation problem might also be beneficial when applied to a completely different optics challenge.[146] Such lateral thinking has, for instance, resulted in beautiful demonstrations of the use of bioinspired photonic materials for vapor sensing, infrared photon imaging, and a host of other sensors based on *Morpho* wing scale structures,[277,302,381,382] and infrared invisibility stickers inspired by cephalopod optics.[345]

The biggest inspiration comes from organisms that are fighting the fiercest wars of survival and are rapidly evolving due to short life cycles and fast succession of generations, and that possess a large diversity of tool sets. Under these conditions, we expect strong selection pressures to act on any emerging variation in a material system leading to a rapid culling of the concepts that best ensure the organisms' survival. Insects—the most diverse group of animals—largely satisfy these criteria. They provide inspiration not only for photonic systems, but also for the multifunctional integration of optical properties with desirable mechanical characteristics, dynamics, and interfacial interactions. Another environment that forces great functional diversification of species is the ocean, where organisms are embedded in complex food chains, fierce arms races, and a tight competition for resources. More and more insights are emerging from the study of light manipulation in the marine environment, and great discoveries might just be around the corner.

Understanding a biological solution to an optical challenge can provide an advanced starting point for the creation of novel artificial photonic materials. We can learn from organisms how to realize the hierarchical integration of multiple structural elements to enhance functionality and create novel effects. We can also learn from nature how to form multifunctional materials that show desired performance according to multiple metrics, including optical appearance, mechanical strength, thermoregulation, and interfacial interactions. We can gain insights about the interplay of different structural components to create a specific optical function, and we can get inspired for the creations of structures in soft, stimuli-responsive, adaptive materials to obtain tunable optical characteristics, or the integration of soft components with hard material constituents, for the creation of composite systems with superior optical and mechanical functions. We anticipate that advances at the intersection between soft and biologically inspired photonics (**Figure 24**), two young but rapidly diversifying fields, will enable significant breakthroughs in the design of novel optical technology and address 21st century's challenges in manufacturing, energy conversion, medical instrumentation design, biosensing, data processing, and communication.

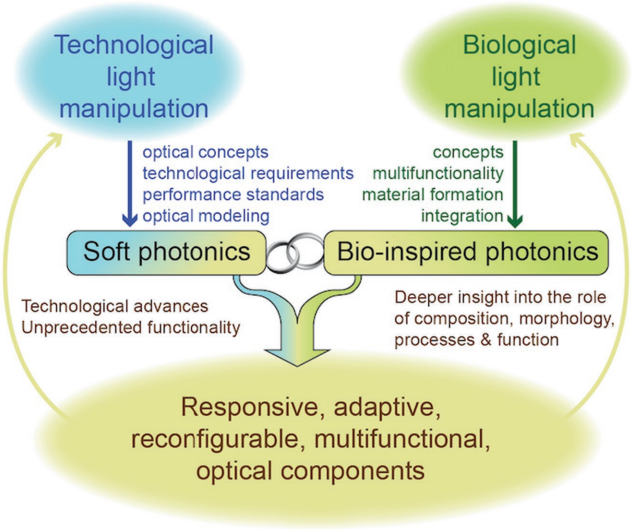

Figure 24. Advances at the intersection of soft and biologically inspired photonics promise to enable major breakthroughs in optical technology development in the coming decades.

Acknowledgements

The preparation of this review was supported by the National Research Foundation of Korea under grant of NRF-2014R1A1A2057763, NRF-2016R1D1A1B03930454, the Samsung Research Funding Center for Samsung Electronics under Project Number SRFC-MA1402-09 (for S.L.) and the US National Science Foundation through the "Designing Materials to Revolutionize and Engineer our Future" program, DMREF-1533985 (for M.K.).

Conflict of Interest

The authors declare no conflict of interest.

Keywords

bioinspired optics, natural materials, soft matter, soft photonics

Received: May 12, 2017
Revised: June 13, 2017
Published online:

[1] M. A. Green, J. Zhao, A. Wang, P. J. Reece, M. Gal, *Nature* **2001**, *412*, 6849.
[2] S. Pimputkar, J. S. Speck, S. P. EndBaars, S. Nakamura, *Nat. Photonics* **2009**, *3*, 180.
[3] E. Yablonovitch, *J. Opt. Soc. Am.* **1982**, *72*, 899.
[4] C. W. Tang, *Appl. Phys. Lett.* **1986**, *48*, 183.

[5] S. Pillai, K. R. Catchpole, T. Trupke, M. A. Green, *J. Appl. Phys.* **2007**, *101*, 093105.
[6] Z. Yu, A. Raman, S. Fan, *Proc. Natl. Acad. Sci. USA* **2010**, *107*, 17491.
[7] P. L. Stiles, J. A. Dieringer, N. C. Shah, R. P. Van Duyne, *Annu. Rev. Anal. Chem.* **2008**, *1*, 601.
[8] X. Huang, I. H. El-Sayed, W. Qian, M. A. El-Sayed, *J. Am. Chem. Soc.* **2006**, *128*, 2115.
[9] J. Clark, G. Lanzani, *Nat. Photonics* **2010**, *4*, 438.
[10] K.-H. Brenner, A. Huang, N. Streibl, *Appl. Opt.* **1986**, *25*, 3054.
[11] H.-T. Chen, W. J. Padilla, J. M. O. Zide, A. C. Gossard, A. J. Taylor, R. D. Averitt, *Nature* **2006**, *444*, 597.
[12] J. Valentine, S. Zhang, T. Zentgraf, E. Ulin-Avila, D. A. Genov, G. Bartal, X. Zhang, *Nature* **2009**, *455*, 376.
[13] S. Zhang, Y.-S. Park, J. Li, X. Lu, W. Zhang, X. Zhang, *Phys. Rev. Lett.* **2009**, *102*, 023901.
[14] M. D. Kelzenberg, S. W. Boettcher, J. A. Petykiewicz, D. B. Turner-Evans, M. C. Putnam, E. L. Warren, J. M. Spurgeon, R. M. Briggs, N. S. Lewis, H. A. Atwater, *Nat. Mater.* **2010**, *9*, 239.
[15] T. Xu, Y.-K. Wu, X. Luo, L. J. Guo, *Nat. Commun.* **2010**, *1*, 59.
[16] M. Choi, S. H. Lee, Y. Kim, S. B. Kang, J. Shin, M. H. Kwak, K.-Y. Kang, Y.-H. Lee, N. Park, B. Min, *Nature* **2011**, *470*, 369.
[17] N. Yu, P. Genevet, M. A. Kats, F. Aieta, J.-P. Tetienne, F. Capasso, Z. Gavurro, *Science* **2011**, *334*, 333.
[18] H. Choo, M.-K. Kim, M. Staffaroni, T. J. Seok, J. Bokor, S. Cabrini, P. J. Schuck, M. C. Wu, E. Yablonovitch, *Nat. Photonics* **2012**, *6*, 838.
[19] P. Spinelli, M. A. Verschuuren, A. Polman, *Nat. Commun.* **2012**, *3*, 692.
[20] K. Kumar, H. Duan, R. S. Hegde, S. C. W. Koh, J. N. Wei, J. K. W. Yang, *Nat. Nanotechnol.* **2012**, *7*, 557.
[21] P. Moita, Y. Yang, Z. Anderson, I. I. Kravchenko, D. P. Briggs, J. Valentine, *Nat. Photonics* **2013**, *7*, 791.
[22] D. Lin, P. Fan, E. Hasman, M. L. Brongersma, *Science* **2014**, *345*, 298.
[23] F. Duerr, Y. Meuret, H. Thienpont, *Opt. Express* **2011**, *19*, A207.
[24] J. S. Price, X. Sheng, B. M. Meulblok, J. A. Rogers, N. C. Giebink, *Nat. Commun.* **2015**, *6*, 1.
[25] A. Lamoureux, K. Lee, M. Shlian, S. R. Forrest, M. Shtein, *Nat. Commun.* **2015**, *6*, 8092.
[26] S. Lee, B. Kang, H. Keum, N. Ahmed, J. A. Rogers, P. M. Ferreira, S. Kim, B. Min, *Sci. Rep.* **2016**, *6*, 27621.
[27] S. Kim, *IEEE Potentials* **2016**, *35*, 14.
[28] D.-K. Lim, K.-S. Jeon, H. M. Kim, J.-M. Nam, Y. D. Suh, *Nat. Mater.* **2010**, *9*, 60.
[29] A. Kinkhabwala, Z. Yu, S. Fan, Y. Avlasevich, K. Müllen, W. E. Moerner, *Nat. Photonics* **2009**, *3*, 654.
[30] J. A. Fan, C. Wu, K. Bao, J. Bao, R. Bardhan, N. J. Halas, V. N. Manoharan, P. Nordlander, G. Shvets, F. Capasso, *Science* **2010**, *328*, 1135.
[31] D.-K. Lim, K.-S. Jeon, J.-H. Hwang, H. Kim, S. Kwon, Y. D. Suh, J.-M. Nam, *Nat. Nanotechnol.* **2011**, *6*, 452.
[32] C. Ciracì, R. T. Hill, J. J. Mock, Y. Urzhumov, A. I. Fernández-Domínguez, S. A. Maier, J. B. Pendry, A. Chikoti, D. R. Smith, *Science* **2012**, *337*, 1072.
[33] G. P. Acuna, F. M. Möller, P. Holzmeister, S. Beater, B. Lalkens, P. Tinnefeld, *Science* **2012**, *338*, 506.
[34] S. Lee, *Opt. Express* **2015**, *23*, 28170.
[35] R. Chikkaraddy, B. de Nijs, F. Benz, S. J. Barrow, O. A. Scherman, E. Rosta, A. Demetriadou, P. Fox, O. Hess, J. J. Baumberg, *Nature* **2016**, *535*, 127.
[36] F. Benz, M. K. Schmidt, A. Dreismann, R. Chikkaraddy, Y. Zhang, A. Demetriadou, C. Carnegie, H. Ohadi, B. de Nijs, R. Esteban, J. Aizpurua, J. J. Baumberg, *Science* **2016**, *354*, 726.
[37] C. López, *Adv. Mater.* **2003**, *15*, 1679.
[38] D. Psaltis, S. R. Quake, C. Yang, *Nature* **2006**, *442*, 381.
[39] P. D. García, R. Sapienza, Á. Blanco, C. López, *Adv. Mater.* **2007**, *19*, 2597.
[40] S.-H. Kim, S. Y. Lee, S.-M. Yang, G.-R. Yi, *NPG Asia Mater.* **2011**, *3*, 25.
[41] H. Schmidt, A. R. Hawkins, *Nat. Photonics* **2011**, *5*, 598.
[42] S. J. Tan, M. J. Campolongo, D. Luo, W. Cheng, *Nat. Nanotechnol.* **2011**, *6*, 268.
[43] J. F. Galisteo-López, M. Ibisate, R. Sapienza, L. S. Lroufe-Pérez, Á. Blanco, C. López, *Adv. Mater.* **2011**, *23*, 30.
[44] D. Erickson, D. Sinton, D. Psaltis, *Nat. Photonics* **2011**, *5*, 583.
[45] D. B. Wolfe, R. S. Conroy, P. Garstecki, B. T. Mayers, M. A. Fischbach, K. E. Paul, M. Prentiss, G. M. Whitesides, *Proc. Natl. Acad. Sci. USA* **2004**, *101*, 12434.
[46] S. K. Y. Tang, C. A. Stan, G. M. Whitesides, *Lab Chip* **2008**, *8*, 395.
[47] S. K. Y. Tang, Z. Li, A. R. Abate, J. J. Agresti, D. A. Weitz, D. Psaltis, G. M. Whitesides, *Lab Chip* **2009**, *9*, 2767.
[48] J. G. Cuennet, A. E. Vasdekis, L. De Sio, D. Psaltis, *Nat. Photonics* **2011**, *5*, 234.
[49] S. A. Morin, R. F. Shepherd, S. W. Kwok, A. A. Stokes, A. Nemiroski, G. M. Whitesides, *Science* **2012**, *337*, 828.
[50] C. Sönnichsen, B. M. Feinhard, J. Liphardt, A. P. Alivisatos, *Nat. Biotechnol.* **2005**, *23*, 741.
[51] A. J. Mastroianni, S. A. Claridge, A. P. Alivisatos, *J. Am. Chem. Soc.* **2009**, *131*, 8455.
[52] A. Kuzyk, R. Schreiber, Z. Fan, G. Pardatscher, E.-M. Roller, A. Högele, F. C. Simmel, A. O. Govorov, T. Liedl, *Nature* **2012**, *483*, 311.
[53] a) V. V. Thacker, L. O. Herrmann, D. O. Single, T. Zhang, T. Liedl, J. J. Baumber, U. F. Keyser, *Nat. Commun.* **2013**, *5*, 3448; b) R. Schreiber, N. Luong, Z. Fan, A. Kuzyk, P. C. Nickels, T. Zhang, D. M. Smith, B. Yurke, W. Kuang, A. O. Govorov, T. Liedl, *Nat. Commun.* **2013**, *4*, 2948; c) A. Kuzyk, M. J. Urban, A. Idili, F. Ricci, N. Liu, *Sci. Adv.* **2017**, *3*, e1602803; d) A. Gopinath, E. Miyazono, A. Faraon, P. W. K. Rothemund, *Nature* **2016**, *535*, 401.
[54] A. Kuzyk, R. Schreiber, H. Zhang, A. O. Govorov, T. Liedl, N. Liu, *Nat. Mater.* **2014**, *13*, 862.
[55] X. Lan, X. Lu, C. Shen, Y. Ke, W. Ni, Q. Wang, *J. Am. Chem. Soc.* **2014**, *137*, 457.
[56] K. L. Young, M. B. Ross, M. G. Blaber, M. Rycenga, M. R. Jones, C. Zhang, A. J. Senesi, B. Lee, G. C. Schatz, C. A. Mirkin, *Adv. Mater.* **2014**, *26*, 653.
[57] M. B. Ross, J. C. Ku, V. M. Vaccarezza, G. C. Schatz, C. A. Mirkin, *Nat. Nanotechnol.* **2015**, *10*, 453.
[58] E.-M. Roller, L. K. Khorashad, M. Fedoruk, R. Schreiber, A. O. Govorov, T. Liedl, *Nano Lett.* **2015**, *15*, 1368.
[59] D. J. Park, C. Zhang, J. C. Ku, Y. Zhou, G. C. Schatz, C. A. Mirkin, *Proc. Natl. Acad. Sci. USA* **2015**, *112*, 977.
[60] M. J. Urban, P. K. Dutta, P. Wang, X. Duan, X. Shen, B. Ding, Y. Ke, N. Liu, *J. Am. Chem. Soc.* **2016**, *138*, 5459.
[61] C. Zhou, X. Duan, N. Liu, *Nat. Commun.* **2016**, *6*, 8102.
[62] P. Wang, S. Gaitanaros, S. Lee, M. Bathe, W. M. Shih, Y. Ke, *J. Am. Chem. Soc.* **2016**, *138*, 7733.
[63] D. J. Park, J. C. Ku, L. Sun, C. M. Lethiec, N. P. Stern, G. C. Schatz, C. A. Mirkin, *Proc. Natl. Acad. Sci. USA* **2017**, *114*, 457.
[64] K. Lee, S. A. Asher, *J. Am. Chem. Soc.* **2000**, *122*, 9534.
[65] A. C. Sharma, T. Jana, R. Kesavamoorthy, L. Shi, M. A. Virji, D. N. Finegold, S. A. Asher, *J. Am. Chem. Soc.* **2004**, *126*, 2971.
[66] S. A. Asher, V. L. Alexeev, A. V. Goponenko, A. C. Sharma, I. K. Lednev, C. S. Wilcox, D. N. Finegold, *J. Am. Chem. Soc.* **2003**, *125*, 3322.
[67] E. Tian, J. Wang, Y. Zheng, Y. Song, L. Jiang, D. Zhu, *J. Mater. Chem.* **2008**, *18*, 1116.
[68] J.-H. Kang, J. H. Moon, S.-K. Lee, S.-G. Park, S. G. Jang, S. Yang, S.-M. Yang, *Adv. Mater.* **2008**, *20*, 3061.

[69] B. Viel, T. Ruhl, G. P. Hellmann, *Chem. Mater.* **2007**, *19*, 5673.
[70] I. M. Pryce, K. Aydin, Y. A. Kelaita, R. M. Briggs, H. A. Atwater, *Nano Lett.* **2010**, *10*, 4222.
[71] A. Kontogeorgos, D. R. E. Snoswell, C. E. Finlayson, J. J. Baumberg, *Phys. Rev. Lett.* **2010**, *105*, 233909.
[72] S. Aksu, M. Huang, A. Artar, A. A. Yanik, S. Selvarasah, M. R. Dokmeci, H. Altug, *Adv. Mater.* **2011**, *23*, 4422.
[73] M. G. Millyard, F. M. Huang, R. Shite, E. Spigone, J. Kivioja, J. J. Baumberg, *Appl. Phys. Lett.* **2012**, *100*, 073101.
[74] S. Lee, S. Kim, T.-T. Kim, Y. Kim, M. Choi, S. H. Lee, J.-Y. Kim, B. Min, *Adv. Mater.* **2012**, *24*, 3491.
[75] P. Kim, Y. Hu, J. Alvarenga, M. Kolle, Z. Suo, J. Aizenberg, *Adv. Opt. Mater.* **2013**, *1*, 381.
[76] M. Kolle, A. Lethbridge, M. Kreysing, J. J. Baumberg, J. Aizenberg, P. Vukusic, *Adv. Mater.* **2013**, *25*, 2239.
[77] H.-S. Ee, R. Agarwal, *Nano Lett.* **2016**, *16*, 2818.
[78] J. Y. Kim, H. Kim, B. H. Kim, T. Chang, J. Lim, H. M. Jin, J. H. Mun, Y. J. Choi, K. Chung, J. Shin, S. Fan, S. O. Kim, *Nat. Commun.* **2016**, *7*, 12911.
[79] X. Shen, T. J. Cui, D. Martin-Cano, F. J. Garcia-Vidal, *Proc. Natl. Acad. Sci. USA* **2013**, *110*, 40.
[80] Y. Morikawa, S. Nagano, K. Watanabe, K. Kamata, T. Iyoda, T. Seki, *Adv. Mater.* **2006**, *18*, 883.
[81] M. Yamada, M. Kondo, J.-i. Mamiya, Y. Yu, M. Kinoshita, C. J. Barrett, T. Ikeda, *Angew. Chem., Int. Ed.* **2008**, *47*, 4986.
[82] S. Lee, H. S. Kang, J.-K. Park, *Adv. Mater.* **2012**, *24*, 2069.
[83] N. S. Yadavalli, S. Santer, *J. Appl. Phys.* **2013**, *113*, 224304.
[84] H. S. Kang, S. Lee, S.-A. Lee, J.-K. Park, *Adv. Mater.* **2013**, *25*, 5490.
[85] A. Priimagi, A. Shevchenko, *J. Polym. Sci., Part B: Polym. Phys.* **2014**, *52*, 163.
[86] S.-A. Lee, H. S. Kang, J.-K. Park, S. Lee, *Adv. Mater.* **2014**, *26*, 7521.
[87] a) S. J. Yeo, K. J. Park, K. Guo, P. J. Yoo, S. Lee, *Adv. Mater.* **2016**, *28*, 5268; b) K. J. Park,J. H. Park, J.-H. Huh, C. H. Kim,D. H. Ho, G. H. Choi, P. J. Yoo, S. M. Cho, J. H. Cho,S. Lee, *ACS Appl. Mater. Interfaces* **2017**, *9*, 9935.
[88] S. N. Sheikholeslami, H. Alaeian, A. L. Koh, J. A. Dionne, *Nano Lett.* **2013**, *13*, 4137.
[89] J. Fontana, W. J. Dressick, J. Phelps, J. E. Johnson, R. W. Rendell, T. Sampson, B. R. Ratna, C. M. Soto, *Small* **2014**, *10*, 3058.
[90] R. P. M. Höller, M. Dulle, S. Thomä, M. Mayer, A. M. Steiner, S. Föster, A. Fery, C. Kuttner, M. Chanana, *ACS Nano* **2016**, *10*, 5740.
[91] A. Tao, P. Sinsermsuksakul, P. Yang, *Nat. Nanotechnol.* **2007**, *2*, 435.
[92] S.-H. Kim, S.-J. Jeon, S.-M. Yang, *J. Am. Chem. Soc.* **2008**, *130*, 6040.
[93] S.-H. Kim, S.-J. Jeon, W. C. Jeong, H. S. Park, S.-M. Yang, *Adv. Mater.* **2008**, *20*, 4129.
[94] B. Hatton, L. Mishchenko, S. Davis, K. H. Sandhage, J. Aizenberg, *Proc. Natl. Acad. Sci. USA* **2010**, *107*, 10354.
[95] H. Noh, S. F. Liew, V. Saranathan, S. G. J. Mochrie, R. O. Prum, E. R. Dufresne, H. Cao, *Adv. Mater.* **2010**, *22*, 2871.
[96] J. D. Forster, H. Noh, S. F. Liew, V. Saranathan, C. F. Schreck, L. Yang, J.-G. Park, R. O. Prum, S. G. J. Mochrie, C. S. O'Hern, H. Cao, E. R. Dufresne, *Adv. Mater.* **2010**, *22*, 2939.
[97] S. Mühlig, A. Cunningham, S. Scheeler, C. Pacholski, T. Bürgi, C. Rockstuhl, F. Lederer, *ACS Nano* **2011**, *5*, 6586.
[98] Y. Cho, J.-H. Huh, K. J. Park, K. Kim, J. Lee, S. Lee, *Opt. Express* **2017**, *25*, 13822.
[99] B. Gao, G. Arya, A. R. Tao, *Nat. Nanotechnol.* **2012**, *7*, 433.
[100] I. B. Burgess, M. Lončar, J. Aizenberg, *J. Mater. Chem. C* **2013**, *1*, 6075.
[101] J.-G. Park, S.-H. Kim, S. Magkiriadou, T. M. Choi, Y.-S. Kim, V. N. Manoharan, *Angew. Chem. Int. Ed.* **2014**, *53*, 2899.
[102] N. Vogel, S. Utech, G. T. England, T. Shirman, K. R. Phillips, N. Koay, I. B. Burgess, M. Kolle, D. A. Weitz, J. Aizenberg, *Proc. Natl. Acad. Sci. USA* **2015**, *112*, 10845.
[103] Z. Qian, S. P. Hastings, C. Li, B. Edward, C. K. McGinn, N. Engheta, Z. Fakhraai, S.-J. Park, *ACS Nano* **2015**, *9*, 1263.
[104] K. R. Phillips, G. T. England, S. Sunny, E. Shirman, T. Shirman, N. Vogel, J. Aizenberg, *Chem. Soc. Rev.* **2016**, *45*, 281.
[105] S. Vignolini, N. A. Yufa, P. S. Cunha, S. Guldin, I. Rushkin, M. Stefik, K. Hur, U. Wiesner, J. J. Baumberg, U. Steiner, *Adv. Mater.* **2011**, *24*, 2012.
[106] K. Hur, Y. Francescato, V. Giannini, S. A. Maier, R. G. Hennig, U. Wiesner, *Angew. Chem. Int. Ed.* **2011**, *50*, 11985.
[107] B. A. Grzybowski, K. J. M. Bishop, C. J. Campbell, M. Fialkowski, S. K. Smoukov, *Soft Matter* **2005**, *1*, 114.
[108] V. Colizza, R. Pastor-Satorras, A. Vespignani, *Nat. Phys.* **2007**, *3*, 276.
[109] D. Chanda, K. Shigeta, S. Gupta, T. Cain, A. Carlson, A. Mihi, A. J. Baca, G. R. Bogart, P. Braun, J. A. Rogers, *Nat. Nanotechnol.* **2011**, *6*, 402.
[110] T.-H. Kim, K.-S. Cho, E. K. Lee, S. J. Lee, J. Chae, J. W. Kim, D. H. Kim, J.-Y. Kwon, G. Amaratunga, S. Y. Lee, B. L. Choi, Y. Kuk, J. M. Kim, K. Kim, *Nat. Photonics* **2011**, *5*, 176.
[111] S. Kim, Y. Su, A. Mihi, S. Lee, Z. Liu, T. K. Bhandakkar, J. Wu, J. B. Geddes III, H. T. Johnson, Y. Zhang, J.-K. Park, P. V. Braun, Y. Huang, J. A. Rogers, *Small* **2012**, *8*, 901.
[112] J. Yoon, S.-M. Lee, D. Kang, M. A. Meitl, C. A. Bower, J. A. Rogers, *Adv. Opt. Mater.* **2015**, *3*, 1313.
[113] D. Franklin, Y. Chen, A. Vazquez-Guardado, S. Modak, J. Boroumand, D. Xu, S.-T. Wu, D. Chanda, *Nat. Commun.* **2015**, *6*, 7337.
[114] F. P. G. de Arquer, A. Mihi, G. Konstantatos, *ACS Photonics* **2015**, *2*, 950.
[115] M. Rein, E. Levy, A. Gumennik, A. F. Abouraddy, J. Joannopoulos, Y. Fink, *Nat. Commun.* **2016**, *7*, 12807.
[116] F. Shafiei, F. Monticone, K. Q. Le, X.-X. Liu, T. Hartsfield, A. Alù, X. Li, *Nat. Nanotechnol.* **2013**, *8*, 95.
[117] S. Yang, X. Ni, X. Yin, B. Kante, P. Zhang, J. Zhu, Y. Wang, X. Zhang, *Nat. Nanotechnol.* **2014**, *9*, 1002.
[118] a) M. Kim, S. Lee, J. Lee, D. K. Kim, Y. J. Hwang, G. Lee, G.-R. Yi, Y. J. Song, *Opt. Express* **2015**, *23*, 12766; b) K. J. Park, J.-H. Huh, D.-W. Jung, J.-S. Park, G. H. Choi, G. Lee, P. J. Yoo, H.-G. Park, G.-R. Yi, S. Lee, *Sci. Rep.* **2017**, *7*, 6045.
[119] X. Guo, H. Li, B. Y. Ahn, E. B. Duoss, K. J. Hsia, J. A. Lewis, R. G. Nuzzo, *Proc. Natl. Acad. Sci. USA* **2009**, *106*, 20149.
[120] D. B. Burckel, J. R. Wendt, G. A. T. Eyck, A. R. Ellis, I. Brener, M. B. Sinclair, *Adv. Mater.* **2010**, *22*, 3171.
[121] A. Mihi, M. Ocaña, H. Miguez, *Adv. Mater.* **2006**, *18*, 2244.
[122] Q. Zhao, C. E. Finlayson, D. R. E. Snoswell, A. Haines, C. Schäfer, P. Spahn, G. P. Hellmann, A. V. Petukhov, L. Herrmann, P. Burdet, P. A. Midgley, S. Butler, M. Mackley, Q. Guo, J. J. Baumberg, *Nat. Commun.* **2015**, *7*, 11661.
[123] J. J. Adams, E. B. Duoss, T. F. Malkowski, M. J. Motala, B. Y. Ahn, R. G. Nuzzo, J. T. Bernhard, J. A. Lewis, *Adv. Mater.* **2011**, *23*, 1335.
[124] D. A. Pawlak, S. Turczynski, M. Gajc, K. Kolodziejak, R. Diduszko, K. Rozniatowski, J. Smalc, I. Vendik, *Adv. Funct. Mater.* **2010**, *10*, 1116.
[125] W. X. Jiang, T. J. Cui, X. M. Yang, H. F. Ma, Q. Cheng, *Appl. Phys. Lett.* **2011**, *98*, 204101.
[126] Y. L. Kong, I. A. Tamargo, H. Kim, B. N. Johnson, M. K. Gupta, T.-W. Koh, H.-A. Chin, D. A. Steingart, B. P. Rand, M. C. McAlpine, *Nano Lett.* **2014**, *14*, 7017.
[127] A. Kuzyk, Y. Yang, X. Duan, S. Stoll, A. O. Govorov, H. Sugiyama, M. Endo, N. Liu, *Nat. Commun.* **2016**, *7*, 10591.

[128] T. Ding, V. K. Valev, A. R. Salmon, C. J. Forman, S. K. Smoukov, O. A. Scherman, D. Frenkel, J. J. Baumberg, *Proc. Natl. Acad. Sci. USA* **2016**, *113*, 5503.
[129] J. H. Kim, J. H. Moon, S.-Y. Lee, J. Park, *Appl. Phys. Lett.* **2010**, *97*, 103701.
[130] Y. Y. Diao, X. Y. Liu, G. W. Toh, L. Shi, J. Zi, *Adv. Funct. Mater.* **2013**, *23*, 5373.
[131] J. B. Messenger, *Biol. Rev.* **2001**, *76*, 473.
[132] R. Hanlon, *Curr. Biol.* **2007**, *17*, R400.
[133] D. G. DeMartini, D. V. Krogstad, D. E. Morse, *Proc. Natl. Acad. Sci. USA* **2013**, *110*, 2552.
[134] C.-C. Chiao, C. Chubb, R. T. Hanlon, *J. Comp. Physiol., A* **2015**, *201*, 933.
[135] L. P. Lee, R. Szema, *Science* **2005**, *310*, 1148.
[136] A. R. Parker, H. E. Townley, *Nat. Nanotechnol.* **2007**, *2*, 347.
[137] L. P. Biró, J. P. Vigneron, *Laser Photonics Rev.* **2011**, *5*, 27.
[138] A. Saito, *Sci. Technol. Adv. Mater.* **2011**, *12*, 64709.
[139] S. Johnsen, *The Optics of Life*, Princeton University Press, Princeton, NJ, USA **2012**.
[140] Y. Zhao, Z. Xie, H. Gu, C. Zhu, Z. Gu, *Chem. Soc. Rev.* **2012**, *41*, 3297.
[141] V. Greanya, *Bioinspired Photonics: Optical Structures and Systems Inspired by Nature*, CRC Press, Boca Raton, FL, USA **2015**.
[142] L. Wu, J. He, W. Shang, T. Deng, J. Gu, H. Su, Q. Liu, W. Zhang, D. Zhang, *Adv. Opt. Mater.* **2016**, *4*, 195.
[143] H. Fudouzi, *Sci. Technol. Adv. Mater.* **2011**, *12*, 64704.
[144] R. Brunner, O. Sandfuchs, C. Pacholski, C. Morhard, J. Spatz, *Laser Photonics Rev.* **2012**, *6*, 641.
[145] K. Yu, T. Fan, S. Lou, D. Zhang, *Prog. Mater. Sci.* **2013**, *58*, 825.
[146] L. Wu, W. Zhang, D. Zhang,*Small* **2015**, *11*, 5004.
[147] J. B. Pendry, A. J. Holden, D. J. Robbins, W. J. Stewart, *IEEE Trans. Microwave Theory Tech.* **1999**, *47*, 2075.
[148] D. R. Smith, W. J. Padilla, D. C. Vier, S. C. Nemat-Nasser, S. Schultz, *Phys. Rev. Lett.* **2000**, *84*, 4184.
[149] R. A. Shelby, D. R. Smith, S. Schults, *Science* **2001**, *292*, 77.
[150] J. B. Pendry, *Science* **2004**, *306*, 1353.
[151] J.-T. Shen, P. B. Catrysse, S. Fan, *Phys. Rev. Lett.* **2005**, *94*, 197401.
[152] D. Schurig, J. J. Mock, B. J. Justice, S. A. Cummer, J. B. Pendry, A. F. Starr, D. R. Smith, *Science* **2006**, *314*, 977.
[153] J. B. Pendry, D. Schurig, D. R. Smith, *Science* **2006**, *312*, 1780.
[154] A. Alù, A. Salandrino, N. Engheta, *Opt. Express* **2006**, *14*, 1557.
[155] V. M. Shalaev, *Nat. Photonics* **2007**, *1*, 41.
[156] N. Engheta, *Science* **2007**, *317*, 1698.
[157] J. A. Schuller, R. Zia, T. Taubner, M. L. Brongersma, *Phys. Rev. Lett.* **2007**, *99*, 107401.
[158] B. Edwards, A. Alù, M. E. Young, M. Silveirinha, N. Engheta, *Phys. Rev. Lett.* **2008**, *100*, 033903.
[159] S. Xiao, V. P. Drachev, A. V. Kildishev, X. Ni, U. K. Chettiar, H.-K. Yuan, V. M. Shalaev, *Nature* **2010**, *466*, 735.
[160] B. Luk'yanchuk, N. I. Zheludev, S. A. Maier, N. J. Halas, P. Nordlander, H. Giessen, C. T. Chong, *Nat. Mater.* **2010**, *9*, 707.
[161] N. I. Zheludev, *Science* **2010**, *328*, 582.
[162] Y. Zhao, M. A. Belkin, A. Alù, *Nat. Commun.* **2012**, *3*, 870.
[163] N. I. Zheludev, Y. S. Kivshar, *Nat. Mater.* **2012**, *11*, 917.
[164] A. Silva, F. Monticone, G. Castaldi, V. Galdi, A. Alù, N. Engheta, *Science* **2014**, *343*, 160.
[165] C. D. Giovampaola, N. Engheta, *Nat. Mater.* **2014**, *13*, 1115.
[166] T. Chang, J. U. Kim, S. K. Kang, H. Kim, D. K. Kim, Y.-H. Lee, J. Shin, *Nat. Commun.* **2016**, *7*, 12661.
[167] E. Yablonovitch, *Phys. Rev. Lett.* **1987**, *58*, 2059.
[168] S. John, *Phys. Rev. Lett.* **1987**, *58*, 2486.
[169] E. Yablonovitch, T. J. Gmitter, K. M. Leung, *Phys. Rev. Lett.* **1991**, *67*, 2295.
[170] J. D. Joannopoulos, P. R. Villeneuve, S. Fan, *Nature* **1997**, *386*, 143.
[171] H. Cao, J. Y. Xu, D. Z. Zhang, S.-H. Chang, S. T. Ho, E. W. Seelig, X. Liu, R. P. H. Chang, *Phys. Rev. Lett.* **2000**, *84*, 5584.
[172] H. Yin, B. Dong, X. Liu, T. Zhan, L. Shi, J. Zi, E. Yablonovitch, *Proc. Natl. Acad. Sci. USA* **2012**, *109*, 10798.
[173] L. Shi, Y. Zhang, B. Dong, T. Zhan, X. Liu, J. Zi, *Adv. Funct. Mater.* **2013**, *25*, 5314.
[174] B. Min, E. Ostby, V. Sorger, E. Ulin-Avila, L. Yang, X. Zhang, K. Vahala, *Nature* **2009**, *457*, 455.
[175] Y. Kim, S.-Y. Lee, J.-W. Ryu, I. Kim, J.-H. Han, H.-S. Tae, M. Choi, B. Min, *Nat. Photonics* **2016**, *10*, 647.
[176] M. Vieweg, T. Gissibl, S. Pricking, B. T. Kuhlmey, D. C. Wu, B. J. Eggleton, H. Giessen, *Opt. Express* **2010**, *18*, 25232.
[177] O. A. Schmidt, M. K. Garbos, T. G. Euser, P. St. J. Russell, *Phys. Rev. Lett.* **2012**, *109*, 024502.
[178] J.-M. Lim, S.-H. Kim, J.-H. Choi, S.-M. Yang, *Lab Chip* **2008**, *8*, 1580.
[179] Y. Yang, A. Q. Liu, L. K. Chin, X. M. Zhang, D. P. Tsai, C. L. Lin, C. Lu, G. P. Wang, N. I. Zheludev, *Nat. Commun.* **2012**, *3*, 651.
[180] M. Jablan, H. Buljan, M. Soljačic, *Phys. Rev. B* **2009**, *80*, 245435.
[181] D. K. Gramotnev, S. I. Bozhevolnyi, *Nat. Photonics* **2010**, *4*, 83.
[182] J. A. Schuller, E. S. Barnard, W. Cai, Y. C. Jun, J. S. White, M. L. Brongersma, *Nat. Mater.* **2010**, *9*, 193.
[183] D. N. Basov, M. M. Fogler, F. J. G. de Abajo, *Science* **2010**, *354*, 195.
[184] a) V. Myroshnychenko, J. Rodríguez-Fernández, I. Pastoriza-Santos, A. M. Funston, C. Novo, P. Mulvaney, L. M. Liz-Marzán, F. J. G. de Abajo, *Chem. Soc. Rev.* **2008**, *37*, 1792; b) W. Zhu, R. Esteban, A. G. Borisov, J. J. Baumberg, P. Nordlander, H. J. Lezec, J. Aizpurua, K. B. Crozier, *Nat. Commun.* **2016**, *7*, 11495; c) J. A. Scholl, A. García-Etxarri, A. L. Koh, J. A. Dionne, *Nano Lett.* **2013**, *13*, 564.
[185] A. R. Tao, S. Habas, P. Yang, *Small* **2008**, *4*, 310.
[186] Y. Xia, Y. Xiong, B. Lim, S. E. Skrabalak, *Angew. Chem. Int. Ed.* **2009**, *48*, 60.
[187] Y. Xia, K. D. Gilroy, H.-C. Peng, X. Xia, *Angew. Chem. Int. Ed.* **2017**, *56*, 60.
[188] R. Yan, P. Pausauskie, J. Huang, P. Yang, *Proc. Natl. Acad. Sci. USA* **2009**, *106*, 21045.
[189] T. Kang, W. Choi, I. Yoon, H. Lee, M.-K. Seo, Q-H. Park, B. Kim, *Nano Lett.* **2012**, *12*, 2331.
[190] X. Chen, H.-R. Park, M. Pelton, X. Piao, N. C. Lindquist, H. Im, Y. J. Kim, J. S. Ahn, K. J. Ahn, N. Park, D.-S. Kim, S.-H. Oh, *Nat. Commun.* **2013**, *4*, 2361.
[191] L. Weller, V. V. Thacker, L. O. Herrmann, E. A. Hemmig, A. Lombardi, U. F. Keyser, J. J. Baumberg, *ACS Photonics* **2016**, *3*, 1589.
[192] F. Monticone, A. Alù, *J. Mater. Chem. C* **2014**, *2*, 9059.
[193] X. Chen, T. M. Grzegorczyk, B.-I. Wu, J. Pacheco, J. A. Kong, *Phys. Rev. E* **2004**, *70*, 016608.
[194] D. R. Smith, D. C. Vier, Th. Koschny, C. M. Soukoulis, *Phys. Rev. E* **2005**, *71*, 036617.
[195] R. Merlin, *Proc. Natl. Acad. Sci. USA* **2009**, *106*, 1693.
[196] K. Chung, R. Kim, T. Chang, J. Shin, *Appl. Phys. Lett.* **2016**, *109*, 021114.
[197] M. Silveirinha, N. Engheta, *Phys. Rev. Lett.* **2006**, *97*, 157403.
[198] K. L. Young, M. R. Jones, J. Zhang, R. J. Macfarlane, R. Esquivel-Sirvent, R. J. Nap, J. Wu, G. C. Schatz, B. Lee, C. A. Mirkin, *Proc. Natl. Acad. Sci. USA* **2012**, *109*, 2240.
[199] Y. Tang, A. E. Cohen, *Phys. Rev. Lett.* **2010**, *104*, 163901.
[200] Y. Tang, A. E. Cohen, *Science* **2011**, *332*, 333.
[201] S. Yoo, Q.-H. Park, *Phys. Rev. Lett.* **2015**, *114*, 203003.
[202] D. Xia, Z. Ku, S. C. Lee, S. R. J. Brueck, *Adv. Mater.* **2011**, *23*, 147.
[203] J. W. Strutt, *Philos. Mag.* **1887**, *24*, 145.

[204] W. Liu, M. Tagawa, H. L. Xin, T. Wang, H. Emamy, H. Li, K. G. Yager, F. W. Starr, A. V. Tkachenko, O. Gang, *Science* **2016**, *351*, 582.
[205] E. Yablonovitch, *J. Opt. Soc. Am. B* **1993**, *10*, 283.
[206] E. R. Dufresne, H. Noh, V. Saranathan, S. G. J. Mochrie, H. Cao, R. O. Prum, *Soft Matter* **2009**, *5*, 1792.
[207] A. Marini, F. J. G. de Abajo, *Phys. Rev. Lett.* **2016**, *116*, 217401.
[208] N. C. Seeman, *J. Theor. Biol.* **1982**, *99*, 237.
[209] Q. Xu, M. R. Schlabach, G. J. Hannon, S. J. Elledge, *Proc. Natl. Acad. Sci. USA* **2009**, *106*, 2289.
[210] C. A. Mirkin, R. L. Letsinger, R. C. Mucic, J. J. Storhoff, *Nature* **1996**, *382*, 607.
[211] A. P. Alivisatos, K. P. Johnson, X. Peng, T. E. Wilson, C. J. Loweth, M. P. Bruchez Jr., P. G. Schultz, *Nature* **1996**, *382*, 609.
[212] E. Winfree, F. R. Liu, L. A. Wenzler, N. C. Seeman, *Nature* **1998**, *394*, 539.
[213] P. W. K. Rothemund, *Nature* **2006**, *440*, 297.
[214] S. M. Douglas, H. Dietz, T. Liedl, B. Högberg, F. Graf, W. M. Shih, *Nature* **2009**, *459*, 414.
[215] D. Nykypanchuk, M. M. Maye, D. van der Lelie, O. Gang, *Nature* **2008**, *451*, 549.
[216] S. Y. Park, A. K. R. Lytton-Jean, B. Lee, S. Weigand, G. C. Schatz, C. A. Mirkin, *Nature* **2008**, *451*, 553.
[217] M. R. Jones, R. J. Macfarlane, B. Lee, J. Zhang, K. L. Young, A. J. Senesi, C. A. Mirkin, *Nat. Mater.* **2010**, *9*, 913.
[218] E. Auyeong, J. I. Cutler, R. J. Macfarlane, M. R. Jones, J. Wu, G. Liu, K. Zhang, K. D. Osberg, C. A. Mirkin, *Nat. Nanotechnol.* **2012**, *7*, 24.
[219] F. Lu, K. G. Yager, Y. Zhang, H. Xin, O. Gang, *Nat. Commun.* **2015**, *6*, 6912.
[220] H. Dietz, S. M. Douglas, W. M. Shih, *Science* **2009**, *325*, 725.
[221] S. M. Douglas, I. Bachelet, G. M. Church, *Science* **2012**, *335*, 831.
[222] S. D. Perrault, W. M. Shih, *ACS Nano* **2014**, *8*, 5132.
[223] R. Schreiber, J. Do, E.-M. Roller, T. Zhang, V. J. Schüller, P. C. Nickels, J. Feldmann, T. Liedl, *Nat. Nanotechnol.* **2014**, *9*, 74.
[224] B. Yurke, A. J. Turberfield, A. P. Mills Jr., F. C. Simmel, J. L. Neumann, *Nature* **2000**, *406*, 605.
[225] Y. Xia, G. M. Whitesides, *Annu. Rev. Mater. Sci.* **1998**, *28*, 153.
[226] S. H. Lee, M. Choi, T.-T. Kim, S. Lee, M. Liu, X. Yin, H. K. Choi, S. S. Lee, C.-G. Choi, S.-Y. Choi, X. Zhang, B. Min, *Nat. Mater.* **2012**, *11*, 936.
[227] W. Lewandowski, M. Fruhnert, J. Mieczkowski, C. Rockstuhl, E. Górecka, *Nat. Commun.* **2014**, *6*, 6590.
[228] K. Matsubara, M. Watanabe, Y. Takeoka, *Angew. Chem. Int. Ed.* **2007**, *46*, 1688.
[229] J. Estefanell, J. Socorro, F. Tuya, M. Izquierdo, J. Roo, *Aquaculture* **2011**, *322*, 91.
[230] J. Estefanell, J. Roo, M. Izquierdo, J. Socorro, R. Guirao, *J. World Aquacult. Soc.* **2013**, *44*, 66.
[231] R. M. Kramer, W. J. Crookes-Goodson, R. R. Naik, *Nat. Mater.* **2007**, *6*, 533.
[232] L. Phan, W. G. Walkup, D. D. Ordinario, E. Karshalev, J.-M. Jocson, A. M. Burke, A. A. Gorodetsky, *Adv. Mater.* **2013**, *25*, 5621.
[233] C. Yu, Y. Li, X. Zhang, X. Huang, V. Malyarchuk, S. Wang, Y. Shi, L. Gao, Y. Su, Y. Zhang, H. Xu, R. T. Hanlon, Y. Huang, J. A. Rogers, *Proc. Natl. Acad. Sci. USA* **2014**, *111*, 12998.
[234] Q. Wang, G. R. Gossweiler, S. L. Craig, X. Zhao, *Nat. Commun.* **2014**, *5*, 4899.
[235] L. M. Mäthger, R. T. Hanlon, *Cell Tissue Res.* **2007**, *329*, 179.
[236] L. M. Mäthger, E. J. Denton, N. J. Marshall, R. T. Hanlon, *J. R. Soc., Interface* **2009**, *6*, S149.
[237] L. M. Mäthger, S. L. Senft, M. Gao, S. Karaveli, G. R. R. Bell, R. Zia, A. M. Kuzirian, P. B. Dennis, W. J. Crookes-Goodson, R. R. Naik, G. W. Kattawar, R. T. Hanlon, *Adv. Funct. Mater.* **2013**, *23*, 3980.
[238] G. R. R. Bell, L. M. Mäthger, M. Gao, S. L. Senft, A. M. Kuzirian, G. W. Kattawar, R. T. Hanlon, *Adv. Mater.* **2014**, *26*, 4352.
[239] A. C. N. Kingston, A. M. Kuzirian, R. T. Hanlon, T. W. Cronin, *J. Exp. Biol.* **2015**, *218*, 1596.
[240] R. A. Cloney, E. Florey, *Z. Zellforsch. Mikrosk. Anat.* **1968**, *89*, 250.
[241] R. T. Hanlon, K. M. Cooper, B. U. Budelmann, T. C. Pappas, *Cell Tissue Res.* **1990**, *259*, 3.
[242] E. Kreit, L. M. Mathger, R. T. Hanlon, P. B. Dennis, R. R. Naik, E. Forsythe, J. Heikenfeld, *J. R. Soc., Interface* **2012**, *10*, 20120601.
[243] E. J. Denton, *Philos. Trans. R. Soc., B* **1970**, *258*, 285.
[244] M. F. Land, *Prog. Biophys. Mol. Biol.* **1972**, *24*, 75.
[245] A. R. Parker, *J. Exp. Biol.* **1998**, *201*, 2343.
[246] M. Srinivasarao, *Chem. Rev.* **1999**, *99*, 1935.
[247] S. Kinoshita, *Structural Colors in the Realm of Nature*, World Scientific Publishing, Singapore **2008**.
[248] P. Vukusic, J. R. Sambles, *Nature* **2003**, *424*, 852.
[249] A. R. Parker, *Opt. Laser Technol.* **2011**, *43*, 323.
[250] M. Kreysing, R. Pusch, D. Haverkate, M. Landsberger, J. Engelmann, J. Ruiter, C. Mora-Ferrer, E. Ulbricht, J. Grosche, K. Franze, S. Streif, S. Schumacher, F. Makarov, J. Kacza, J. Guck, H. Wolburg, J. K. Bowmaker, G. von der Emde, S. Schuster, H.-J. Wagner, A. Reichenbach, M. Francke, *Science* **2012**, *336*, 1700.
[251] M. Kolle, U. Steiner, in *Encyclopedia of Nanotechnology* (Ed: B. Bhushan), Springer, Dordrecht, Netherlands **2012**, pp. 2514–2527.
[252] S. Vignolini, E. Moyroud, B. J. Glover, U. Steiner, *J. R. Soc., Interface* **2013**, *10*, 20130394.
[253] M. Grimann, T. Fuhrmann-Lieker, in *Organic and Hybrid Photonic Crystals* (Ed: D. Comoretto), Springer International Publishing, Cham, Switzerland **2015**, pp. 57–74.
[254] K. R. Thomas, M. Kolle, H. M. Whitney, B. J. Glover, U. Steiner, *J. R. Soc., Interface* **2010**, *7*, 1699.
[255] R. O. Prum, *J. Exp. Biol.* **2003**, *206*, 2409.
[256] R. O. Prum, *J. Exp. Biol.* **2004**, *207*, 2157.
[257] J. Teyssier, S. V. Saenko, D. van der Marel, M. C. Milinkovitch, *Nat. Commun.* **2015**, *6*, 6368.
[258] B. Kientz, S. Luke, P. Vukusic, R. Péteri, C. Beaudry, T. Renault, D. Simon, T. Mignot, E. Rosenfeld, *Sci. Rep.* **2016**, *6*, 19906.
[259] D. Gur, B. Leshem, M. Pierantoni, V. Farstey, D. Oron, S. Weiner, L. Addadi, *J. Am. Chem. Soc.* **2015**, *137*, 8408.
[260] J. Aizenberg, A. Tkachenko, S. Weiner, L. Addadi, G. Hendler, *Nature* **2001**, *412*, 819.
[261] L. Li, S. Kolle, J. C. Weaver, C. Ortiz, J. Aizenberg, M. Kolle, *Nat. Commun.* **2015**, *6*, 6322.
[262] L. Li, M. J. Connors, M. Kolle, G. T. England, D. I. Speiser, X. Xiao, J. Aizenberg, C. Ortiz, *Science* **2015**, *350*, 952.
[263] S. M. Doucet, M. G. Meadows, *J. R. Soc., Interface* **2009**, *6*, S115.
[264] N. I. Morehouse, R. L. Rutowski, A. E. D. Irwin, E. M. A. McPeek, *Am. Nat.* **2010**, *176*, 768.
[265] S. Johnsen, *Sci. Am.* **2000**, *282*, 80.
[266] P. C. Brady, K. A. Travis, T. Maginnis, M. E. Cummings, *Proc. Natl. Acad. Sci. USA* **2013**, *110*, 9764.
[267] S. Johnsen, *Annu. Rev. Mater. Sci.* **2014**, *6*, 369.
[268] R. H. Siddique, G. Gomard, H. Hölscher, *Nat. Commun.* **2015**, *6*, 6909.
[269] A. L. Holt, S. Vahidinia, Y. L. Gagnon, D. E. Morse, A. M. Sweeney, *J. R. Soc., Interface* **2014**, *11*, 20140678.
[270] M. Jacobs, M. Lopez-Garcia, O.-P. Phrathep, T. Lawson, R. Oulton, H. M. Whitney, *Nat. Plants* **2016**, *2*, 16162.
[271] J. P. Vigneron, M. Rassart, Z. Vértesy, K. Kertész, M. Sarrazin, L. P. Biró, D. Ertz, V. Lousse, *Phys. Rev. E* **2005**, *71*, 11906.
[272] N. N. Shi, C.-C. Tsai, F. Camino, G. D. Bernard, N. Yu, R. Wehner, *Science* **2015**, *349*, 298.
[273] C. J. Chandler, B. D. Wilts, S. Vignolini, J. Brodie, U. Steiner, P. J. Rudall, B. J. Glover, T. Gregory, R. H. Walker, *Sci. Rep.* **2015**, *5*, 11645.

[274] A. Bay, P. Cloetens, H. Suhonen, J. P. Vigneron, *Opt. Express* **2013**, *21*, 764.
[275] J. Wang, Y. Zhang, S. Wang, Y. Song, L. Jiang, *Acc. Chem. Res.* **2011**, *44*, 405.
[276] J. Zi, X. Yu, Y. Li, X. Hu, C. Xu, X. Wang, X. Liu, R. Fu, *Proc. Natl. Acad. Sci. USA* **2003**, *100*, 12576.
[277] S. Yoshioka, S. Kinoshita, *Proc. R. Soc. Lond. B* **2006**, *273*, 129.
[278] S. Vignolini, P. J. Rudall, A. V. Rowland, A. Reed, E. Moyroud, R. B. Faden, J. J. Baumberg, B. J. Glover, U. Steiner, *Proc. Natl. Acad. Sci. USA* **2012**, *109*, 15712.
[279] S. Kinoshita, S. Yoshioka, *ChemPhysChem* **2005**, *6*, 1442.
[280] J. W. C. Dunlop, P. Fratzl, *Annu. Rev. Mater. Res.* **2010**, *40*, 1.
[281] L. Li, C. Ortiz, *Adv. Mater.* **2013**, *25*, 2344.
[282] K. Liu, L. Jiang, *ACS Nano* **2011**, *5*, 6786.
[283] J. P. Vigneron, J. M. Pasteels, D. M. Windsor, Z. Vértesy, M. Rassart, T. Seldrum, J. Dumont, O. Deparis, V. Lousse, L. P. Biró, D. Ertz, V. Welch, *Phys. Rev. E* **2007**, *76*, 31907.
[284] L. F. Dougherty, S. Johnsen, R. L. Caldwell, N. J. Marshall, *J. R. Soc., Interface* **2014**, *11*, 20140407.
[285] D. Gur, B. A. Palmer, B. Leshem, D. Oron, P. Fratzl, S. Weiner, L. Addadi, *Angew. Chem. Int. Ed.* **2015**, *54*, 12426.
[286] P. Vukusic, D. Stavenga, *J. R. Soc., Interface* **2009**, *6*, S133.
[287] F. Xia, L. Jiang, *Adv. Mater.* **2008**, *20*, 2842.
[288] J. Aizenberg, P. Fratzl, *Adv. Mater.* **2009**, *21*, 387.
[289] K. Liu, L. Jiang, *Nano Today* **2011**, *6*, 155.
[290] A. Malshe, K. Rajurkar, A. Samant, H. N. Hansen, S. Bapat, W. Jiang, *CIRP Ann. – Manuf. Technol.* **2013**, *62*, 607.
[291] U. G. K. Wegst, H. Bai, E. Saiz, A. P. Tomsia, R. O. Ritchie, *Nat. Mater.* **2015**, *14*, 23.
[292] A. Lakhtakia, R. J. Martin-Palma, *Engineered Biomimicry*, Elsevier Inc., Amsterdam, The Netherlands **2013**.
[293] S. M. Luke, P. Vukusic, *Europhys. News* **2011**, *42*, 20.
[294] F. Liu, B. Dong, X. Liu, in *Optical Devices in Communication and Computation* (Ed: P. Xi), InTech, Croatia **2012**.
[295] V. C. Coffey, *Opt. Photonics News* **2015**, *26*, 30.
[296] G. Kaufmann, NOVA – Kings of Camouflage, TV Broadcast PBS, http://www.pbs.org/wgbh/nova/nature/kings-of-camouflage.html (accessed: July 2011).
[297] L. Phan, R. Kautz, E. M. Leung, K. L. Naughton, Y. Van Dyke, A. A. Gorodetsky, *Chem. Mater.* **2016**, *28*, 6804.
[298] L. F. Deravi, A. P. Magyar, S. P. Sheehy, G. R. R. Bell, L. M. Mathger, S. L. Senft, T. J. Wardill, W. S. Lane, A. M. Kuzirian, R. T. Hanlon, E. L. Hu, K. K. Parker, *J. R. Soc., Interface* **2014**, *11*, 20130942.
[299] H.-H. Chou, A. Nguyen, A. Chortos, J. W. F. To, C. Lu, J. Mei, T. Kurosawa, W.-G. Bae, J. B.-H. Tok, Z. Bao, *Nat. Commun.* **2015**, *6*, 8011.
[300] E. Florey, M. E. Kriebel, *Z. Vgl. Physiol.* **1969**, *65*, 98.
[301] J. J. Walish, Y. Kang, R. A. Mickiewicz, E. L. Thomas, *Adv. Mater.* **2009**, *21*, 3078.
[302] R. A. Potyrailo, H. Ghiradella, A. Vertiatchikh, K. Dovidenko, J. R. Cournoyer, E. Olson, *Nat. Photonics* **2007**, *1*, 123.
[303] R. A. Potyrailo, R. K. Bonam, J. G. Hartley, T. A. Starkey, P. Vukusic, M. Vasudev, T. Bunning, R. R. Naik, Z. Tang, M. A. Palacios, M. Larsen, L. A. Le Tarte, J. C. Grande, S. Zhong, T. Deng, *Nat. Commun.* **2015**, *6*, 7959.
[304] S. Yoshioka, T. Nakano, Y. Nozue, S. Kinoshita, *J. R. Soc., Interface* **2008**, *5*, 457.
[305] C. Pouya, D. G. Stavenga, P. Vukusic, *Opt. Express* **2011**, *19*, 11355.
[306] A. Saito, Y. Miyamura, M. Nakajima, Y. Ishikawa, K. Sogo, Y. Kuwahara, Y. Hirai, *J. Vac. Sci. Technol., B: Nanotechnol. Microelectron.: Mater., Process., Meas., Phenom.* **2006**, *24*, 3248.
[307] J. Huang, X. Wang, Z. L. Wang, *Nano Lett.* **2006**, *6*, 2325.
[308] J. W. Galusha, M. R. Jorgensen, M. H. Bartl, *Adv. Mater.* **2010**, *22*, 107.
[309] M. Kolle, P. M. Salgard-Cunha, M. R. J. Scherer, F. Huang, P. Vukusic, S. Mahajan, J. J. Baumberg, U. Steiner, *Nat. Nanotechnol.* **2010**, *5*, 511.
[310] M. R. Jorgensen, M. H. Bartl, *J. Mater. Chem.* **2011**, *21*, 10583.
[311] K. Chung, S. Yu, C.-J. Heo, J. W. Shim, S.-M. Yang, M. G. Han, H.-S. Lee, Y. Jin, S. Y. Lee, N. Park, J. H. Shin, *Adv. Mater.* **2012**, *24*, 2375.
[312] J. P. Vernon, N. Hobbs, Y. Cai, A. Lethbridge, P. Vukusic, D. D. Deheyn, K. H. Sandhage, *J. Mater. Chem.* **2012**, *22*, 10435.
[313] A. E. Seago, P. Brady, J.-P. Vigneron, T. D. Schultz, *J. R. Soc., Interface* **2009**, *6*, S165.
[314] P. Vukusic, J. R. Sambles, C. R. Lawrence, *Nature* **2000**, *404*, 457.
[315] Z. Wang, J. Zhang, J. Xie, C. Li, Y. Li, S. Liang, Z. Tian, T. Wang, H. Zhang, H. Li, W. Xu, B. Yang, *Adv. Funct. Mater.* **2010**, *20*, 3784.
[316] Q. Yang, S. Zhu, W. Peng, C. Yin, W. Wang, J. Gu, W. Zhang, J. Ma, T. Deng, C. Feng, D. Zhang, *ACS Nano* **2013**, *7*, 4911.
[317] D. G. Stavenga, S. Foletti, G. Palasantzas, K. Arikawa, *Proc. R. Soc. Lond. Ser. B* **2006**, *273*, 661.
[318] A. R. Parker, R. C. McPhedran, D. R. McKenzie, L. C. Botten, N. A. Nicorovici, *Nature* **2001**, *409*, 36.
[319] J. P. Vigneron, P. Simonis, A. Aiello, A. Bay, D. M. Windsor, J.-F. Colomer, M. Rassart, *Phys. Rev. E* **2010**, *82*, 21903.
[320] W.-L. Min, B. Jiang, P. Jiang, *Adv. Mater.* **2008**, *20*, 3914.
[321] S. Chattopadhyay, L. Chen, in *Optical Biomimetics: Materials and Applications*, (Ed: M. C. J. Large), Woodhead Pub., Portland, ORG, USA, **2012**, pp. 108–140.
[322] G. England, M. Kolle, P. Kim, M. Khan, P. Muñoz, E. Mazur, J. Aizenberg, *Proc. Natl. Acad. Sci. USA* **2014**, *111*, 15630.
[323] J. Hou, H. Zhang, Q. Yang, M. Li, Y. Song, L. Jiang, *Angew. Chem. Int. Ed.* **2014**, *53*, 5791.
[324] V. Welch, V. Lousse, O. Deparis, A. Parker, J. P. Vigneron, *Phys. Rev. E* **2007**, *75*, 41919.
[325] K. Michielsen, D. G. Stavenga, *J. R. Soc., Interface* **2008**, *5*, 85.
[326] C. I. Aguirre, E. Reguera, A. Stein, *Adv. Funct. Mater.* **2010**, *20*, 2565.
[327] M. D. Turner, G. E. Schröder-Turk, M. Gu, *Opt. Express* **2011**, *19*, 10001.
[328] L. Mishchenko, B. Hatton, M. Kolle, J. Aizenberg, *Small* **2012**, *8*, 1904.
[329] A. Kawamura, M. Kohri, G. Morimoto, Y. Nannichi, T. Taniguchi, K. Kishikawa, *Sci. Rep.* **2016**, *6*, 33984.
[330] Y. Takeoka, S. Yoshioka, A. Takano, S. Arai, K. Nueangnoraj, H. Nishihara, M. Teshima, Y. Ohtsuka, T. Seki, *Angew. Chem. Int. Ed.* **2013**, *52*, 7261.
[331] Y. Takeoka, S. Yoshioka, M. Teshima, A. Takano, M. Harun-Ur-Rashid, T. Seki, *Sci. Rep.* **2013**, *3*, 2371.
[332] M. Kohri, Y. Nannichi, T. Taniguchi, K. Kishikawa, *J. Mater. Chem. C* **2015**, *3*, 720.
[333] P. Vukusic, B. Hallam, J. Noyes, *Science* **2007**, *315*, 348.
[334] S. M. Luke, B. T. Hallam, P. Vukusic, *Appl. Opt.* **2010**, *49*, 4246.
[335] M. Burresi, L. Cortese, L. Pattelli, M. Kolle, P. Vukusic, D. S. Wiersma, U. Steiner, S. Vignolini, *Sci. Rep.* **2014**, *4*, 6075.
[336] A. Ghoshal, E. Eck, D. E. Morse, *Optica* **2016**, *3*, 108.
[337] P. Vukusic, J. R. Sambles, C. R. Lawrence, *Proc. R. Soc. Lond. Ser. B.* **2004**, *271*, S237.
[338] M. D. Shawkey, *J. Exp. Biol.* **2006**, *209*, 1245.
[339] A. Bay, N. André, M. Sarrazin, A. Belarouci, V. Aimez, L. A. Francis, J. P. Vigneron, *Opt. Express* **2013**, *21*, A179.
[340] M.-S. Choi, T. Yamazaki, I. Yamazaki, T. Aida, *Angew. Chem. Int. Ed.* **2004**, *43*, 150.
[341] G. McDermott, S. M. Prince, A. A. Freer, A. M. Hawthornthwaite-Lawless, M. Z. Papiz, R. J. Cogdell, N. W. Isaacs, *Nature* **1995**, *374*, 517.
[342] L. Li, C. Ortiz, *Adv. Funct. Mater.* **2015**, *25*, 3463.

[343] H.-B. Yao, H.-Y. Fang, Z.-H. Tan, L.-H. Wu, S.-H. Yu, *Angew. Chem. Int. Ed.* **2010**, *49*, 2140.
[344] A. G. Dumanli, H. M. van der Kooij, G. Kamita, E. Reisner, J. J. Baumberg, U. Steiner, S. Vignolini, *ACS Appl. Mater. Interfaces* **2014**, *6*, 12302.
[345] L. Phan, D. D. Ordinario, E. Karshalev, W. G. Walkup IV, M. A. Shenk, A. A. Gorodetsky, *J. Mater. Chem. C* **2015**, *3*, 6493.
[346] S. Vignolini, T. Gregory, M. Kolle, A. Lethbridge, E. Moyroud, U. Steiner, B. J. Glover, P. Vukusic, P. J. Rudall, *J. R. Soc., Interface* **2016**, *13*, 20160645.
[347] B. D. Wilts, H. M. Whitney, B. J. Glover, U. Steiner, S. Vignolini, *Mater. Today Proc.* **2014**, *1*, 177.
[348] S. N. Fernandes, Y. Geng, S. Vignolini, B. J. Glover, A. C. Trindade, J. P. Canejo, P. L. Almeida, P. Brogueira, M. H. Godinho, *Macromol. Chem. Phys.* **2013**, *214*, 25.
[349] A. G. Dumanli, G. Kamita, J. Landman, H. van der Kooij, B. J. Glover, J. J. Baumberg, U. Steiner, S. Vignolini, *Adv. Opt. Mater.* **2014**, *2*, 646.
[350] F. G. Omenetto, D. L. Kaplan, *Science* **2010**, *329*, 528.
[351] M. B. Applegate, M. A. Brenckle, B. Marelli, H. Tao, D. L. Kaplan, F. G. Omenetto, *Opt. Photonics News* **2014**, *25*, 30.
[352] S. Kujala, A. Mannila, L. Karvonen, K. Kieu, Z. Sun, *Sci. Rep.* **2016**, *6*, 22358.
[353] N. Huby, V. Vié, A. Renault, S. Beaufils, T. Lefèvre, F. Paquet-Mercier, M. Pézolet, B. Bêche, *Appl. Phys. Lett.* **2013**, *102*, 123702.
[354] J. N. Monks, B. Yan, N. Hawkins, F. Vollrath, Z. Wang, *Nano Lett.* **2016**, *16*, 5842.
[355] K. A. Burke, M. A. Brenckle, D. L. Kaplan, F. G. Omenetto, *ACS Appl. Mater. Interfaces* **2016**, *8*, 16218.
[356] R. L. Rutowski, J. M. Macedonia, N. Morehouse, L. Taylor-Taft, *Proc. R. Soc. Lond. Ser. B* **2005**, *272*, 2329.
[357] M. D. Shawkey, N. I. Morehouse, P. Vukusic, *J. R. Soc., Interface* **2009**, *6*, S221.
[358] B. D. Wilts, T. M. Trzeciak, P. Vukusic, D. G. Stavenga, *J. Exp. Biol.* **2012**, *215*, 796.
[359] O. L. Pursiainen, J. J. Baumberg, H. Winkler, B. Viel, P. Spahn, T. Ruhl, *Opt. Express* **2007**, *15*, 9553.
[360] S. Kondo, R. Asai, *Nature* **1995**, *376*, 765.
[361] S. Kondo, T. Miura, *Science* **2010**, *329*, 1616.
[362] A. Dinwiddie, R. Null, M. Pizzano, L. Chuong, A. L. Krup, H. Ee Tan, N. H. Patel, *Dev. Biol.* **2014**, *392*, 404.
[363] A. R. Tao, D. G. DeMartini, M. Izumi, A. M. Sweeney, A. L. Holt, D. E. Morse, *Biomaterials* **2010**, *31*, 793.
[364] D. G. DeMartini, M. Izumi, A. T. Weaver, E. Pandolfi, D. E. Morse, *J. Biol. Chem.* **2015**, *290*, 15238.
[365] R. Levenson, C. Bracken, N. Bush, D. E. Morse, *J. Biol. Chem.* **2016**, *291*, 4058.
[366] K. L. Naughton, L. Phan, E. M. Leung, R. Kautz, Q. Lin, Y. Van Dyke, B. Marmiroli, B. Sartori, A. Arvai, S. Li, M. E. Pique, M. Naeim, J. P. Kerr, M. J. Aquino, V. A. Roberts, E. D. Getzoff, C. Zhu, S. Bernstorff, A. A. Gorodetsky, *Adv. Mater.* **2016**, *28*, 8405.
[367] R. O. Prum, R. H. Torres, S. Williamson, J. Dyck, *Nature* **1998**, *396*, 28.
[368] D. G. Stavenga, J. Tinbergen, H. L. Leertouwer, B. D. Wilts, *J. Exp. Biol.* **2011**, *214*, 3960.
[369] G. M. Whitesides, B. Grzybowski, *Science* **2002**, *295*, 2418.
[370] Á. G. Marín, H. Gelderblom, A. Susarrey-Arce, A. van Houselt, L. Lefferts, J. G. E. Gardeniers, D. Lohse, J. H. Snoeijer, *Proc. Natl. Acad. Sci. USA* **2012**, *109*, 16455.
[371] S. Yang, X. Dai, B. B. Stogin, T.-S. Wong, *Proc. Natl. Acad. Sci. USA* **2016**, *113*, 268.
[372] W. L. Noorduin, A. Grinthal, L. Mahadevan, J. Aizenberg, *Science* **2013**, *340*, 832.
[373] M. Iwata, Y. Ohno, J. M. Otaki, *PLoS One* **2014**, *9*, e89500.
[374] Y. Ohno, J. M. Otaki, *PLoS One* **2015**, *10*, e0128332.
[375] N. Kröger, N. Poulsen, *Annu. Rev. Genet.* **2008**, *42*, 83.
[376] L. De Stefano, P. Maddalena, L. Moretti, I. Rea, I. Rendina, E. De Tommasi, V. Mocella, M. De Stefano, *Superlattices Microstruct.* **2009**, *46*, 84.
[377] L. De Stefano, L. Rotiroti, M. De Stefano, A. Lamberti, S. Lettieri, A. Setaro, P. Maddalena, *Biosens. Bioelectron.* **2009**, *24*, 1580.
[378] D. Zhang, Y. Wang, J. Cai, J. Pan, X. Jiang, Y. Jiang, *Chin. Sci. Bull.* **2012**, *57*, 3836.
[379] E. De Tommasi, I. Rea, L. De Stefano, P. Dardano, G. Di Caprio, M. A. Ferrara, G. Coppola, *Proc. SPIE* **2013**, *8792*, 87920O.
[380] Y. Su, N. Lundholm, S. M. M. Friis, M. Ellegaard, *Nano Res.* **2015**, *8*, 2363.
[381] A. D. Pris, Y. Utturkar, C. Surman, W. G. Morris, A. Vert, S. Zalyubovskiy, T. Deng, H. T. Ghiradella, R. A. Potyrailo, *Nat. Photonics* **2012**, *6*, 195.
[382] Q. Li, Q. Zeng, L. Shi, X. Zhang, K.-Q. Zhang, *J. Mater. Chem. C* **2016**, *4*, 1752.